

**SUPPORT-ENHANCED THERMAL OLIGOMERIZATION OF
ETHYLENE TO LIQUID FUEL HYDROCARBONS**

by

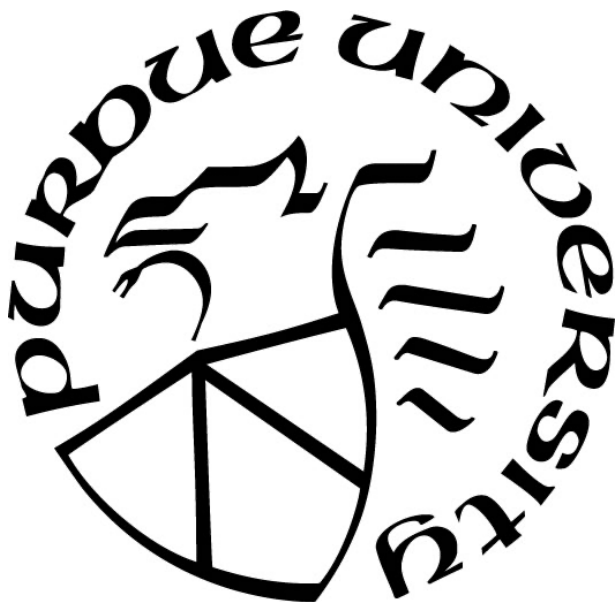
Matthew A. Conrad

A Dissertation

Submitted to the Faculty of Purdue University

In Partial Fulfillment of the Requirements for the degree of

Doctor of Philosophy



Davidson School of Chemical Engineering

West Lafayette, Indiana

August 2022

**THE PURDUE UNIVERSITY GRADUATE SCHOOL
STATEMENT OF COMMITTEE APPROVAL**

Dr. Jeffrey T. Miller, Chair

School of Chemical Engineering

Dr. Jeffrey Greeley

School of Chemical Engineering

Dr. Rajamani Gounder

School of Chemical Engineering

Dr. Jason Hicks

Department of Chemical and Biomolecular Engineering, University of Notre Dame

Approved by:

Dr. John Morgan

Dedicated to my family and friends

ACKNOWLEDGMENTS

The past four years at Purdue University have been a transformative experience for me in which I have faced and overcome many challenges. It would not have been possible without the support of several key individuals.

First and foremost, my advisor and mentor Jeff Miller has been instrumental in providing me with continual guidance throughout the years, while also giving me the freedom to grow tremendously as a researcher and problem-solver. I am also deeply grateful for my committee members, Jeff Greeley, Raj Gounder, and Jason Hicks for providing invaluable technical and thought-provoking questions about my research. Additionally, my time here would not have been possible without funding from CISTAR and support from the Davidson School of Chemical Engineering.

I also owe my gratitude to my group members, past and present, for training me, collaborating with me, and engaging in the numerous conversations after a long day in the lab. The same can be said for all the visiting scholars, undergraduates, and fellow classmates I've had the privilege of working alongside.

Finally, I would like to express my sincere gratitude to my parents, siblings, friends, and girlfriend for their unending support throughout my time as a Ph.D. student, and for whatever adventures lie ahead.

TABLE OF CONTENTS

LIST OF TABLES	8
LIST OF FIGURES	9
ABSTRACT	11
1. BACKGROUND.....	12
2. INSIGHTS INTO THE CHEMISTRY OF THE HOMOGENEOUS THERMAL OLIGOMERIZATION OF ETHYLENE TO LIQUID-FUEL RANGE HYDROCARBONS	13
2.1 Introduction	13
2.2 Experimental Methods	16
2.2.1 Atmospheric Pressure Olefin Oligomerization	16
2.2.2 High Pressure Olefin Oligomerization.....	17
2.2.3 Thermal Reactions of 1-Hexene at Atmospheric Pressure	18
2.2.4 Computational Methods.....	18
2.3 Results	19
2.3.1 High Ethylene Conversion at Elevated Temperature and Pressure	19
2.3.2 Effects of Temperature, Pressure, and Conversion on MW Distribution	19
2.3.3 Isomer Distributions of C ₄₊ Products.....	22
2.3.4 MW Distributions at Very Low Ethylene Conversions	24
2.3.5 Measured Kinetics of the Thermal Reactions of Ethylene	25
2.3.6 DFT of Proposed Initiation Reactions	27
2.3.7 Comparison of the Thermal Reactions of Other Olefins	33
2.4 Discussion	37
2.4.1 Product Distributions	37
2.4.2 Kinetics	39
2.4.3 Reaction Pathway.....	39
2.4.4 Comparison with Propylene and 1-Hexene	42
2.5 Conclusion.....	44
2.6 References	44
3. HIGH TEMPERATURE CONVERSION OF ETHYLENE TO LIQUID HYDROCARBONS USING γ -ALUMINA	52

3.1	Introduction	52
3.2	Experimental Methods	54
3.2.1	Materials	54
3.2.2	Atmospheric Pressure Olefin Oligomerization	54
3.2.3	High Pressure Ethylene Oligomerization.....	55
3.2.4	Thermal Reactions of 1-Hexene at Atmospheric Pressure	55
3.3	Results	56
3.3.1	Ethylene Reaction Rates and Products with High-Surface Area Supports.....	56
3.3.2	Product Distribution at High Ethylene Conversion with Al ₂ O ₃	60
3.3.3	Comparison of Products with Al ₂ O ₃ vs the Thermal Reaction at Low Pressure and Conversion	61
3.3.4	MW and Isomer Distributions versus Conversion.....	62
3.3.5	Selectivity versus Temperature.....	65
3.3.6	Selectivity versus Pressure.....	66
3.3.7	Reaction of Propylene with Al ₂ O ₃	67
3.3.8	Reaction of 1-Hexene with Al ₂ O ₃	69
3.4	Discussion	72
3.4.1	Effect of High Surface Area Supports on Rates, Kinetics, and Products	72
Silica		73
Alumina.....		73
3.4.2	Insights from the Products of C ₂ H ₄ with Al ₂ O ₃ versus Thermally	74
MW Distribution.....		74
Isomerization of C ₄ , C ₅ , and C ₆		74
H-Transfer.....		75
3.4.3	Insights from the Contrasting Products Formed by C ₃ H ₆ versus C ₂ H ₄ with Al ₂ O ₃	76
MW Distribution.....		76
Isomerization of C ₄ , C ₅ , and C ₆		76
H-Transfer.....		77
3.5	Conclusion.....	78
3.6	References.....	79
4.	FUTURE DIRECTIONS.....	85

APPENDIX A. SUPPORTING INFORMATION FOR CHAPTER 2.....	87
APPENDIX B. SUPPORTING INFORMATION FOR CHAPTER 3	93
PUBLICATIONS	104

LIST OF TABLES

Table 1. C ₂ H ₄ Conversion in an Empty 30 cm ³ Stainless Steel Reactor at 465 °C	20
Table 2. 1-C ₆ H ₁₂ Conversion in an Empty Quartz Reactor from 1-20 kPa.....	36
Table 3. Comparison of Ethylene Conversion Rates at 340 °C and 42.0 – 43.5 bar C ₂ H ₄	56
Table 4. 1-C ₆ H ₁₂ Conversion with Al ₂ O ₃ and Thermally.....	70

LIST OF FIGURES

Figure 1. Product distributions of ethylene thermal reactions at high pressure. (a) 21.0 bar and ~ 7 % conversion, temperature varied from 432 to 449 °C. (b) 449 °C and ~ 6 % conversion, pressure varied from 14.0 to 21.0 bar. (c) 432 °C and 21.0 bar, conversion varied from 3.7 to 11.0 %	21
Figure 2. Product distributions at 1.5 bar C ₂ H ₄ from 410 to 490 °C at 0.1 - 0.2 % conversion. (a) By carbon number, (b) C ₄ distribution, (c) C ₅ distribution.	23
Figure 3. Product distributions for ethylene feed below 400 °C at low conversion. (a) 1.5 bar, quartz reactor with volume = 11 cm ³ . (b) 43.5 bar, stainless steel reactor with volume = 30 cm ³	25
Figure 4. The kinetics of ethylene thermal reactions. Rates were measured with X < 5.0 % with units of moles C ₂ H ₄ converted/cm ³ /s. (a) The reaction order at 449 °C from 1.0 to 18.0 bar. (b) The Arrhenius plot at 1.5, 21.0 and 43.5 bar from about 340 to 500 °C	26
Figure 5. Free energy profiles for four ethylene bimolecular initiation reactions.....	27
Figure 6. Free energy profile for homolytic ring cleavage of cyclobutane.	28
Figure 7. Free energy profile for cyclobutene formation of homolytic ring cleavage.	29
Figure 8. Free energy profile for the addition of ethylene to tetramethylene.....	30
Figure 9. Free energy profile for the addition of ethylene to 2-butene 1,4-diradical.	30
Figure 10. Free energy profile for conversion of hexamethylene to 1-hexene.....	31
Figure 11. Free energy profile for hydrogen atom abstraction from one hexamethylene molecule to another.	32
Figure 12. Free energy profile for hydrogen atom abstraction from 1-hexene to a 2-hexene 1,6-diradical.	32
Figure 13. Free energy profile for the generation of a 2-hexene 1,4-diradical and ethane from 1-butene and ethylene.	33
Figure 14. Product distribution at 0.42 % conversion of pure propylene reacted at 1.5 bar and 400 °C. (a) By carbon number, (b) C ₄ distribution, (c) C ₅ distribution.	34
Figure 15. The kinetics of propylene thermal reactions. Rates were measured X < 1.0 % with units of moles C ₃ H ₆ converted/cm ³ /s. (a) The reaction order from 0.8 to 6.0 bar. Rates were normalized by the Arrhenius term exp(-E _a /RT) using the observed E _a of 125 kJ/mol. (b) The Arrhenius plot measured from 400 to 500 °C. Rate constants are the rate normalized by the observed 1.0 reaction order.....	35
Figure 16. Product distribution of non-C ₆ products at 0.1 % yield to non-C ₆ of 1-hexene reacted at 370 and 420 °C (a) By carbon number, (b) C ₄ distribution, (c) C ₅ distribution.	37
Figure 17. Beta-scission reaction of a mid-chain radical to yield an end-chain radical and a terminal alkene.....	41

Figure 18. General scheme for the two-phase thermal oligomerization of ethylene.....	42
Figure 19. Kinetics of C ₂ H ₄ reactions with different high surface area supports. Arrhenius plot from 300 to 410 °C at (a) 1.5 bar and (b) 42 - 43.5 bar C ₂ H ₄ . The thermal reactions of C ₂ H ₄ from 300 to 410 °C are shown in open squares.....	57
Figure 20. Products of ethylene conversion in the presence of SiO ₂ compared to the thermal reaction at 360 °C, 43.0-43.5 bar. The conversions thermally and with SiO ₂ were 0.58 and 0.96 %, respectively. (a) The products based on carbon number distribution.....	58
Figure 21. Products of ethylene conversion in the presence of alumina compared to the thermal reaction at 385 °C, 27.5 bar. The conversions thermally and with alumina were 11.9 and 16.9 %, respectively. (a) The products based on carbon number distribution.....	59
Figure 22. Products with Al ₂ O ₃ at 23 bar C ₂ H ₄ , 360 °C, from 1-70 % conversion.....	61
Figure 23. Products with Al ₂ O ₃ vs the thermal reaction at 1.5 bar C ₂ H ₄ , 400 °C, and 0.1 % conversion. (a) Carbon number distribution, (b) C ₄ distribution, (c) C ₅ distribution.....	63
Figure 24. Products with Al ₂ O ₃ versus conversion below 20 % at 1.5 bar C ₂ H ₄ , 360 °C. (a) Carbon number distribution, (b) C ₄ distribution, (c) C ₅ distribution.	64
Figure 25. Selectivity of Major Products with Al ₂ O ₃ at 300 vs 360 °C at 23 bar of C ₂ H ₄ below 20 % conversion.....	65
Figure 26. Selectivity of Major Products at 1.5 vs 23 bar of C ₂ H ₄ at 360 °C below 20 % conversion.	67
Figure 27. Kinetics of C ₃ H ₆ reactions with Al ₂ O ₃ . Arrhenius plot from 260 to 300 °C of 1.5 bar C ₃ H ₆ . X < 10 % The thermal reaction of C ₃ H ₆ from 400 to 500 °C are shown in open triangles for comparison.	68
Figure 28. Products of C ₃ H ₆ with Al ₂ O ₃ at 2.0 % conversion 260 °C and 1.5 bar.....	69
Figure 29. Products with Al ₂ O ₃ with 5 kPa 1-hexene fed at 260 °C	71

ABSTRACT

Thermal, non-catalytic conversion of light olefins ($C_2^=$ - $C_4^=$) was originally utilized in the production of motor fuels at several U.S. refineries in the 1920-30's. However, the resulting fuels had relatively low-octane number and required harsh operating conditions ($T > 450\text{ }^\circ\text{C}$, $P > 50\text{ bar}$), ultimately leading to its succession by solid acid catalytic processes. Despite the early utilization of the thermal reaction, relatively little is known about the reaction products, kinetics, and initiation pathway under liquid-producing conditions.

In this thesis, thermal ethylene conversion was investigated near the industrial operating conditions, i.e, at temperatures between 320 and 500 $^\circ\text{C}$ and ethylene pressures from 1.5 to 43.5 bar. Non-oligomer products such as propylene and/or higher odd carbon products were observed at all reaction temperatures, pressures, and reaction extents. Methane and ethane were minor products ($< 1\%$ each), even at ethylene conversions as high as 74 %. The isomer distributions revealed a preference for linear, terminal C_4 and C_5 . The reaction order was found to be 2nd order with a temperature dependent activation energy ranging from 165 to 244 kJ/mol. The importance of diradical species in generating free radicals during a two-phase initiation process was proposed. The reaction chemistry for ethylene, which has only strong, vinyl C-H bonds starkly contrasted propylene, which possesses weaker allylic C-H bonds and showed preference for dimeric C_6 products over C_2 - C_8 non-oligomers.

Extending this work further, the thermal oligomerization of ethylene was enhanced using high surface area supports such as silica and alumina. Both supports resulted in order of magnitude rate increases compared to the gas phase reaction, however the ethylene conversion rate with alumina was superior to silica by a factor of between 100 and 1,000. Additionally, the alumina evidently confers a catalytic function, resulting in altered product distributions, notably an increase in branched products such as isobutene and isopentenes. The oligomerization chemistry with alumina appears to reflect the involvement of Lewis acid sites rather than traditional Brønsted acid or transition metal catalysis, which operate via carbenium ion and metal-alkyl intermediates, respectively.

1. BACKGROUND

The U.S. shale gas boom has resulted in an abundance of residual ethane and propane that accompany the methane which is pipelined for electricity generation. Due to infrastructure constraints, the ethane and propane in remote shale locations cannot be processed and is essentially stranded at the well-head. Due to environmental concerns, flaring of these gases is not acceptable either. A two-step process of alkane dehydrogenation followed by oligomerization of the resulting light olefins could be a viable way to utilize ethane and propane if the oligomerization step directly produces a fungible fuel. State-of-the-art oligomerization catalysts utilize either transition metal complexes or acidic catalysts, however both have drawbacks limiting their utility for converting ethylene and propylene at small scale. Homogeneous transition metal catalysts require activators, co-catalysts, and separations, whereas acid catalysts typically suffer from deactivation, requiring frequent regeneration. An oligomerization process with little deactivation or coking issues is the thermal, gas phase oligomerization process, which was applied in several refineries in the 1920's. Unfortunately, the thermal reaction has a relatively low rate at regular catalytic operating parameters and requires higher temperatures and pressures (near 450 °C and > 50 bar). Additionally, the product distribution made by the thermal process tends to have a poor octane rating compared to acidic catalysts.

Studies of the thermal reactions of olefins above atmospheric pressure largely stopped after 1950. Thus, detailed product distributions and kinetics above 1 bar have not been clearly delineated, which has limited the interpretation of the reaction pathway, and thus no modeling of the reaction pathway has been reported. The advantage of understanding the reaction pathway is the possibility of engineering a catalyst that might enable a thermal radical oligomerization pathway at milder conditions, and/or with better product selectivity.

The goals of this thesis are therefore twofold: (1) to develop new insights into the chemistry of the thermal oligomerization of ethylene and (2) to study the influence of high surface area supports on controlling the rate and product distribution of the thermal conversion of ethylene to liquid fuel range hydrocarbons.

2. INSIGHTS INTO THE CHEMISTRY OF THE HOMOGENEOUS THERMAL OLIGOMERIZATION OF ETHYLENE TO LIQUID-FUEL RANGE HYDROCARBONS

2.1 Introduction

The U.S. shale gas boom has incentivized the on-site valorization of the residual ethane and propane which are of little value on their own.^{1,2} A two-step process of alkane dehydrogenation followed by oligomerization of the resulting light olefins could be viable if the oligomerization step directly produces a fungible fuel.³ Current oligomerization processes utilize either homogeneous transition metal complexes or solid Brønsted acid catalysts.⁴⁻¹⁹ Homogeneous transition metal catalysts²⁰⁻²⁹ can be tailored to make dimers or trimers selectively, or in the case of the Shell Higher Olefins Process, a distribution of C₄-C₂₀ linear olefins.^{23,24,30} However, these processes require activators, co-catalysts, and separation units. Heterogeneous nickel ion catalysts avoid these requirements but are overall less productive, favor dimerization, and deactivate at temperatures above 250 °C.^{7,31,32} Acidic catalysts such as solid phosphoric acid (SPA)³³⁻³⁷ and zeolites, namely H-ZSM-5,³⁸⁻⁴⁷ produce motor fuels from C₃-C₄ feedstocks; however, they tend to deactivate over time and must be regenerated.

The earliest processes for converting cracked refinery olefins were purely thermal methods dating back to the 1920's.⁴⁸⁻⁵⁸ While the thermal reactions of olefins has been studied at atmospheric pressure since the late 1790's,⁵⁹⁻⁷⁰ the high pressure reactions were pioneered by the work of Ipatieff in 1911.^{71,72} These high pressure processes generally converted C₂⁼ - C₄⁼ feedstocks at 450-500 °C and 50-70 bar into a liquid with a research octane number (RON) of 96 and motor octane number (MON) of 78.^{56,57} At higher temperatures such as 650 – 700 °C, a highly aromatic distillate with MON of roughly 100 was demonstrated.⁵⁶ In terms of productivity, Sullivan et al. achieved a liquid yield of 20.6 wt % during a contact time of 4.1 minutes from pure C₂H₄ at 34 bar and 453 °C in a 520 cm³ reaction bomb.⁵⁵

The thermal route was not widely implemented due to the discovery of the CatPoly process using SPA by Ipatieff and coworkers at UOP, which produced higher-octane gasoline at lower temperatures and pressures.⁴⁸ Studies of the thermal reactions of olefins above atmospheric pressure largely stopped after 1950. Thus, detailed product distributions and kinetics above 1 bar

have not been clearly delineated, which has limited the interpretation of the reaction pathway, and thus no modeling of the reaction pathway has been reported.

The most recent adjacent studies since 1950 take place either at lower temperatures and higher pressures in the thermal polymerization to polyethylene^{73–79} or at higher temperatures and lower pressures in ethylene pyrolysis from 500 to 650 °C and 1.3 to 79 kPa in which cracking processes dominate, leading to many light gas products.^{80–102} At these conditions, there is agreement across studies that propylene and ethane are major products from pure ethylene along with butenes, methane, propane, butane, butadiene, and small amounts of cyclopentene, cyclohexene, benzene, and toluene.^{82–84,91,93} Cyclobutane has also been reported.¹⁰³ Due to the low pressures in those studies, there is very little information about the dynamic effects of temperature, pressure, and conversion on the molecular-weight distribution at conditions leading to liquid fuel range products. Furthermore, the detailed C₄₊ isomer distributions are not known. Kinetic analyses in these studies agree on a second order ethylene pressure dependence, however the activation energy for ethylene conversion has varied from 145 to 181 kJ/mol across studies.^{82–84,91,92,96,104–106} Additionally, another recurring observation among studies is an initial induction period in which the rate is lower, followed by a rapid increase. This suggests the presence of a complex initiation pathway; however, no explanation given has been supported with computational evidence.

The lack of rigorous quantum chemical simulations has led to differing opinions on the initiation mechanism to generate free radicals from ethylene, which, unlike the higher olefins, does not contain any allylic C-H bonds. Heterogeneous initiation by reactor wall effects has been ruled out by multiple studies, which found no rate enhancement by increasing the reactor surface area.^{91,93,107,108} Buback suggested that the thermal polymerization of ethylene below 250 °C at about 2,500 bar initiates via a diradical intermediate arising from the collision of two ethylene monomers, i.e. tetramethylene.⁷⁶ The diradical initiation has been proposed in several other cases.^{78,84,109} Halstead and Quinn concluded that ethylene pyrolysis above 500 °C was controlled by the secondary decomposition of 1-butene.⁹³ That is, 1-butene forms initially from two ethylene via an undescribed molecular reaction and subsequently decomposes to methyl and allyl radicals which serve as the free radical chain initiators. In contrast, at similar conditions Boyd et al. asserted that the thermal reactions of ethylene initiate via a bimolecular H-transfer reaction to form vinyl and ethyl radicals, based on the claim that ethane was the only product observed during an induction period of several minutes.⁹¹

The various reaction chemistries and initiation mechanisms proposed in literature for ethylene pyrolysis make accurate kinetic modeling challenging in the application to liquid fuel production. The goal of this study, therefore, is to better understand the detailed product distributions and kinetics of the thermal reactions of ethylene at conditions conducive to producing liquid fuels – above atmospheric pressure and below pyrolytic (i.e. coking) temperatures (ca. 500 °C). New insights into the reaction chemistry may help to advance the understanding of the key reaction steps and intermediates. With this aim in mind, the following four questions are posed as a broad research framework:

- (1) *What are the detailed product distributions?* Notably, how does the molecular-weight distribution change as a function of temperature, pressure, and reaction conversion? What is the molecular-weight distribution at low conversion? What is the nature of the C₄₊ isomer distributions?
- (2) *What are the observed kinetic parameters*, i.e., the overall activation energy and reaction order for ethylene consumption?
- (3) *How do free radicals arise during the thermal initiation reactions of pure ethylene?* What are the free energy barriers for possible initiation mechanisms? What are possible reactions which might lead to the propagating radical chains following initiation?
- (4) *Do the thermal reactions of olefins which contain allylic C-H bonds, such as propylene and 1-hexene, behave like ethylene?* Do the C₄ and C₅ product distributions share the same isomer distributions? Are the activation energy and reaction order the same? How do the overall olefin conversion rates compare?

A combination of experiments and theory were performed to address these questions. First, a benchmark experiment was conducted near the industrial operating conditions at 465 °C and 31.5 bar with a pure ethylene feed to determine the general molecular-weight distribution and productivity at high ethylene conversion. Second, the influence of temperature, pressure, and conversion were measured from 432 - 449 °C, 14.0 - 21.0 bar, and 0 to 11 % conversion. The products at conversions below 0.1 % were measured from 340 to 380 °C at 1.5 bar and from 290 to 360 °C at 43.5 bar. Next, the isomer distributions for C₄₊ products were elucidated near 0.1 % conversion at 1.5 bar from 410 - 490 °C. Subsequently, the kinetics of ethylene consumption were measured below 5 % conversion from 340 °C to 500 °C at pressures ranging from 1.5 to 43.5 bar. The third question was answered by employing DFT to determine the free energy barriers for four

initiation reactions previously discussed in literature, but never rigorously calculated. The four elementary initiation reactions were the bimolecular reactions of ethylene to form either cyclobutane, 1-butene, tetramethylene, or vinyl and ethyl radicals. Secondary initiation steps involving cyclobutane cracking, cis-hydrogenation, diradical addition to ethylene, and H-transfer were then evaluated for each of the cases, where relevant.

Traditional oligomerization reactions produce even carbon chains from ethylene, i.e., butenes, hexenes, octenes, etc. However, non-oligomer products such as propylene, pentenes, etc. were observed in significant amounts in addition to the true oligomers under all experimental conditions. Moreover, olefins other than ethylene also contain allylic C-H bonds which might lead to more facile initiation reactions. Therefore, the thermal reactions of propylene were also tested to understand its products and kinetics from 400 to 500 °C and 0.8 to 6.0 bar. Since C₆ are the first common oligomers when comparing ethylene and propylene oligomerization, 1-hexene was reacted from 370 – 420 °C at 1-20 kPa to understand its reaction chemistry. Specifically, the 1-hexene cracking rate and products were measured to gauge its relative contribution to the formation of non-oligomer products from ethylene.

2.2 Experimental Methods

2.2.1 Atmospheric Pressure Olefin Oligomerization

A quartz tube (10.5 mm ID, 1.1 mm thickness) approximately 14” in total length was loaded into a clamshell furnace with insulation enclosing a heated reaction zone 5.7” in length (see Figure A.1). A thermal-well placed down the axial length of the tube allowed the temperature profile to be measured at 1” intervals. A length-averaged temperature was then calculated for each temperature setpoint. The reactor was then heated to the desired setpoint and olefin flow rate. For each data point, the product gas flow rate was verified using a bubble film flowmeter. Ultra-high purity ethylene or propylene was purchased from Indiana Oxygen and used in all experiments.

Products were analyzed using a Hewlett Packard 6890 Series Gas Chromatograph with an Agilent HP-AL/S column (25 m in length, 0.32 mm ID, and 8 μm film thickness) and flame ionization detector. To detect higher molecular weight products up to C₈, the reactor discharge lines were traced with heat tape and set to 150 °C during the experiments. The conversion and product distribution were calculated on a molar basis, assuming a closed carbon balance since no

significant carbon deposition was observed over the course of experiments. In experiments from 400 to 500 °C, the rates were measured at different flow rates to determine if the conversion increased proportionally with average residence time (see Figures A.2-a and A.5), which was the case.

2.2.2 High Pressure Olefin Oligomerization

To understand the product distributions and rates at higher olefin concentrations and conversions, ethylene was tested at pressures up to 43.5 bar, and propylene up to 6.0 bar. A 316 stainless steel tube (3/8" ID, 1/8" thickness) 2 feet in length, with VCR fittings at the inlet and outlet to seal the system was used. The reactor setup was in a ventilated fume hood as a safety precaution, and a pressure relief valve rated for 650 psi was installed at the top of the reactor. The insulation allowed a thermal reaction zone of about 16.5" which corresponded to a volume of ca. 30 cm³. A thermal-well placed down the length of the tube allowed the temperature profile to be measured at 2" intervals (see Figure A.1). A length-averaged temperature was then calculated for each temperature setpoint. The reactor was first pressurized to check for leaks and then the reactor was heated to the desired setpoint temperature in flowing N₂ and allowed to stabilize for 4 hr to purge oxygen from the system. Pure C₂H₄ or C₃H₆ was then flowed through the reactor. Ultra-high purity ethylene or propylene, purchased from Indiana Oxygen, were used in all experiments.

Products were analyzed using a Hewlett Packard 7890 Series Gas Chromatograph with an Agilent HP-1 column (25 m in length, 0.32 mm ID, and 8 μm film thickness) and flame ionization detector. To detect higher molecular weight products up to C₁₀, the reactor discharge lines were traced with heat tape and set to 175 °C during the experiment. The conversion and product distribution were calculated on a molar basis. A mass flow controller calibration curve was made, and so comparison of the product flow rate to the flow rate with no conversion enabled an estimation of the conversion. For differential conditions ($X < 10\%$), the product flow rate did not deviate from the expected flow rate. Additionally, very little carbon was observed over 5 days of continuous testing, thus, a 100% carbon balance was assumed in the calculations. For $X > 10\%$, the molar volumes of each carbon number group (e.g. 1-hexene for C₆ products) were obtained from Yaw's Handbook¹¹⁰ and the C₂H₄ conversion was estimated from the product volume flow rate. Products above C₅ were assumed to be saturated in the product stream at room temperature and atmospheric pressure where the bubble flowmeter was operated. In experiments above 400 °C,

the rates were measured at different flow rates to determine if the conversion increased proportionally with average residence time (see Figure A.2-b).

2.2.3 Thermal Reactions of 1-Hexene at Atmospheric Pressure

1-Hexene (> 99 %) was purchased from Sigma-Aldrich and N₂ was used as a carrier gas. Approximately 5-10 mL of 1-hexene were loaded into a roughly 100 mL stainless steel vessel, installed via Swagelok fittings, between the N₂ mass flow controller and the reactor. The 1-hexene concentration was varied from about 1-20 % in N₂ at a total system pressure of about 1 bar. The reactor system was purged for 3 hours with 100 sccm N₂ after sealing to purge any dissolved O₂ in the 1-hexene storage vessel. The reactor effluent was fed into a gas chromatography unit equipped with a flame ionization detector. Molar selectivity of non-C₆ products were reported in addition to the conversion of 1-hexene. Before the furnace was turned on, the 1-hexene was fed into the reactor at room temperature to verify no reaction due to contaminants, as well as to obtain a baseline of impurities present as received. The 1-hexene was found to be > 99 % pure.

2.2.4 Computational Methods

Density functional theory calculations were carried out to investigate ethylene oligomerization reactions. All calculations were conducted in the gas-phase using the M062X meta-hybrid functional with the Def2-TZVP basis set of Alrichs and co-workers. The UltraFine integration grid and default optimization convergence criteria were used throughout. Dispersion was included in the form of Grimme's D3 empirical dispersion correction without any damping scheme. The correctness of each transition state was confirmed by calculation of intrinsic reaction coordinates to connect transition states to appropriate minima.

Contributions to the enthalpy of the system from frequency modes below 100 cm⁻¹ were adjusted using the quasi-harmonic (QH) correction of Head-Gordon. Contributions to the entropy from the same small vibrational modes were adjusted using the QH method of Grimme. Both methods were used as provided in the GoodVibes software. GoodVibes was also used to scale all vibrational frequencies by a factor of 0.971, as recommended by Truhlar et al. All thermodynamic values are reported at 1 atmosphere of pressure and at 25 °C. All minima were confirmed to have

zero imaginary frequency modes, while transition states calculations showed exactly 1 negative frequency mode.

2.3 Results

2.3.1 High Ethylene Conversion at Elevated Temperature and Pressure

As discussed in the introduction, at pressures above 1 atm, the thermal conversion of ethylene to liquid hydrocarbons occurs above about 300 °C. Given the absence of recent studies of ethylene reactions at super-atmospheric conditions, high conversion experiments were conducted in a continuous flow stainless-steel tube reactor to determine the ethylene conversion rates and product distributions as a benchmark.

Ethylene conversions from 21 to 74 % were obtained at 465 °C from 15.0 to 31.5 bar with a feed flow rate of 156 sccm in a 30 cm³ stainless-steel tube flow reactor (see Table 1). The resulting C₅₊ yield ranged from 11 to 49 %. From the product analysis of ethylene reacted at 465 °C, four observations are apparent:

1. Non-oligomers, such as propylene, pentenes, heptenes, etc., comprised 50-55 % of the products.
2. 1-butene was 70-75 % of the C₄ isomers, with very little isobutene or isobutane detected (< 1 %).
3. The gas products were highly olefinic in nature, e.g., the mole ratios of propane to propylene and butane to butenes were less than about 0.1.
4. Little methane or ethane (< 1 % each) were produced.

Next, the products were studied systematically over a range of temperature, pressures, and conversion.

2.3.2 Effects of Temperature, Pressure, and Conversion on MW Distribution

To understand the dependence of product distribution on changes in temperature, a series of experiments were conducted from 432 to 449 °C at 21.0 bar and ca. 7 % ethylene conversion (Figure 1-a). Despite being at lower pressure, temperature, and conversion than the data in Table 1, the overall product distributions share many of the same features, with methane and ethane selectivity less than 1 mole % each, and many odd and even carbon products from C₃ to C₉. C₁₀

products, which were less than 5 mole % of the products in the benchmark experiment at 74 % ethylene conversion, were only detected in trace amounts at these conditions. Clearly, the selectivity to propylene and butenes increases as temperature increases, accompanied by similar decreases in C₆ to C₉. Meanwhile, the C₅ products remain around 20 mole % at each temperature.

Table 1. C₂H₄ Conversion in an Empty 30 cm³ Stainless Steel Reactor at 465 °C

P (bar)	15.0		25.0		31.5	
Flow _{feed} (sccm)	156		156		156	
GHSV (hr ⁻¹)	28		17		13	
Conversion (%)	21		56		74	
Selectivity (Carbon %)						
Methane	0.1		0.2		0.4	
Ethane	0.7		0.4		0.8	
Propane	0.2		0.6		1.4	
Propylene	20.8		15.6		12.4	
C ₄ [#]	<u>26.5</u>	(% of C ₄)	<u>24.4</u>	(% of C ₄)	<u>18.3</u>	(% of C ₄)
n-butane	0.4	(1.6 %)	1.0	(4.2 %)	2.2	(7.9 %)
1-butene	20.0	(75.5 %)	18.2	(74.4 %)	12.4	(72.0 %)
trans-2-butene	3.7	(14.1 %)	3.2	(13.1 %)	2.2	(12.2 %)
cis-2-butene	2.3	(8.8 %)	2.1	(8.4 %)	1.4	(7.9 %)
C ₅	19.5		20.1		15.1	
C ₆	13.4		15.4		13.6	
C ₇	10.6		13.2		13.3	
C ₈	5.3		7.9		11.4	
C ₉₊	2.9		2.2		13.3	
C ₅₊	51.7		58.7		66.7	
Yield to C ₅₊ (%)	11		33		49	
Rate of C ₂ H ₄ consumption (mol/cm ³ /s) x 10 ⁶	1.8		4.9		6.2	
Rate of C ₅₊ production (mol/cm ³ /s) x 10 ⁶	0.4		1.1		1.1	
#Isobutene, isobutane, and butadiene were only present in trace amounts (< 1 % each of C ₄)						

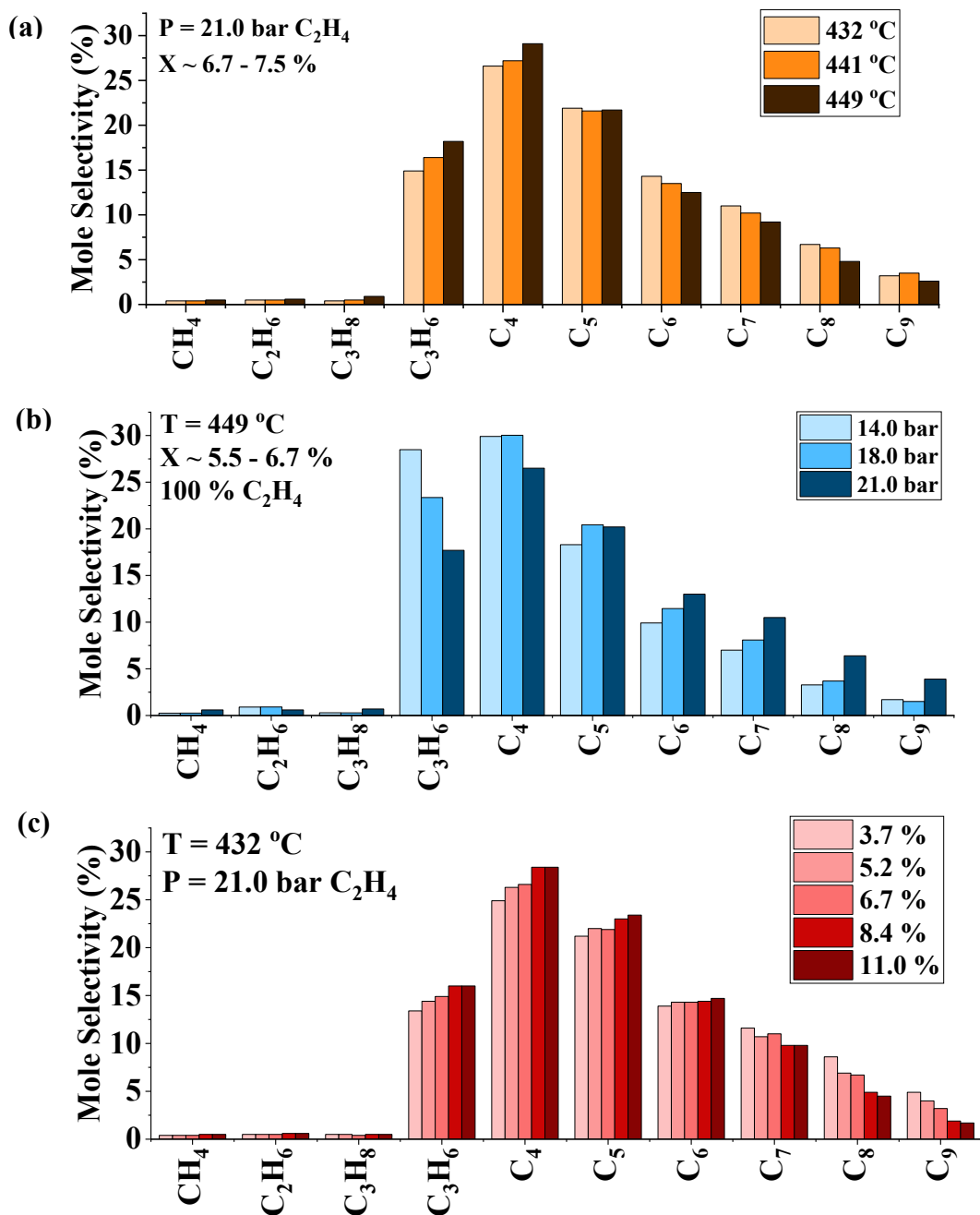


Figure 1. Product distributions of ethylene thermal reactions at high pressure. (a) 21.0 bar and ~ 7 % conversion, temperature varied from 432 to 449 °C. (b) 449 °C and ~ 6 % conversion, pressure varied from 14.0 to 21.0 bar. (c) 432 °C and 21.0 bar, conversion varied from 3.7 to 11.0 %.

To probe the effect of pressure, experiments were conducted from 14.0 to 21.0 bar at 449 °C and ~ 6 % ethylene conversion (Figure 1-b). Changes in the reaction pressure have noticeable effects on the selectivity to propylene, C₄, and C₆ to C₉ products. As the pressure increases,

selectivity to propylene and C₄ decreases commensurately with increases in C₅ to C₉. Thus, the influence of pressure appears to be opposite of the influence of increasing temperature on the C₃ to C₉ molecular weight distribution.

The effect of ethylene conversion on the product distribution was also investigated. At 21.0 bar and 432 °C, the data in Figure 1-c demonstrate two key trends: (1) an increase in C₃ to C₆ fractions and (2) a corresponding relative decrease in C₇ to C₉ fractions as the conversion increased from 3.7 to 11.0 %. While the relative amount of C₇ to C₉ decreased compared to C₃ through C₆ with increasing conversion, the net molar production rate of C₇ to C₉ did not appear to decrease, indicating that the change in selectivity is due to increased overall C₃ to C₆ production, and not decomposition of C₇ to C₉.

2.3.3 Isomer Distributions of C₄₊ Products

In the next series of experiments, the products were studied at 1.5 bar and ca. 0.1-0.2 % conversion from 410 to 490 °C with an emphasis on understanding the C₄, C₅, and C₆ isomer distributions. The C₄ distribution (Figure 2-b) shows the high prevalence for linear butenes (> 80 %), along with small amounts of butadiene, n-butane, and an unidentified C₄. Isobutene is a very minor product, comprising less than 1 % of all the C₄. The identity of the other C₄ was not confirmed but the retention time points towards either a cyclic C₄ or isobutane. Isobutane seems unlikely because formation of an isobutyl radical would require methyl shift reactions, which are uncommon in radical reactions.¹¹¹ Additionally, the isomer ratios were affected by the temperature. The ratio of 1-butene to 2-butenes increased from 2.7 at 410 °C to 12.2 at 490 °C. However, the ratio of linear butenes to isobutene remained greater than 130 at all three temperatures. Furthermore, butadiene increased over the temperature range from 2 to 7 %. The other C₄ similarly increased from less than 0.1 % at 410 °C to 8 % at 490 °C.

The C₅ distribution (Figure 2-c) also shows high selectivity to linear pentenes. However, while the C₅ products are more than 65 % linear, they display relatively more iso-olefins compared to the C₄ isomers. The branching is especially more significant at 410 °C, in which isopentenes were 27.8 % of C₅. This observation is consistent with the finding at 360 °C and 43.5 bar that the C₅ products consisted of some skeletal and/or cyclic isomers. N-pentane is the least abundant C₅ detected (2 mole %), while isopentane was not detected. The C₅ isomers showed a temperature dependence for both the ratio of linear to branched C₅ as well as the ratio of 1-pentene to 2-pentenes.

The ratio of linear to branched C₅ olefins increased from 2.4 at 410 °C to 8.9 at 490 °C. Likewise, the ratio of 1-pentene to 2-pentenes increased from 1.7 at 410 °C to 5.3 at 490 °C. The other C₅ isomer was observed to increase from 4 to 21 % of C₅ from 410 to 490 °C. This other C₅ isomer was not determined, but each of the n-pentenes, isopentenes, and saturated C₅ were identified, implying it must be either a multiply unsaturated open chain C₅ or a cyclic C₅ isomer.

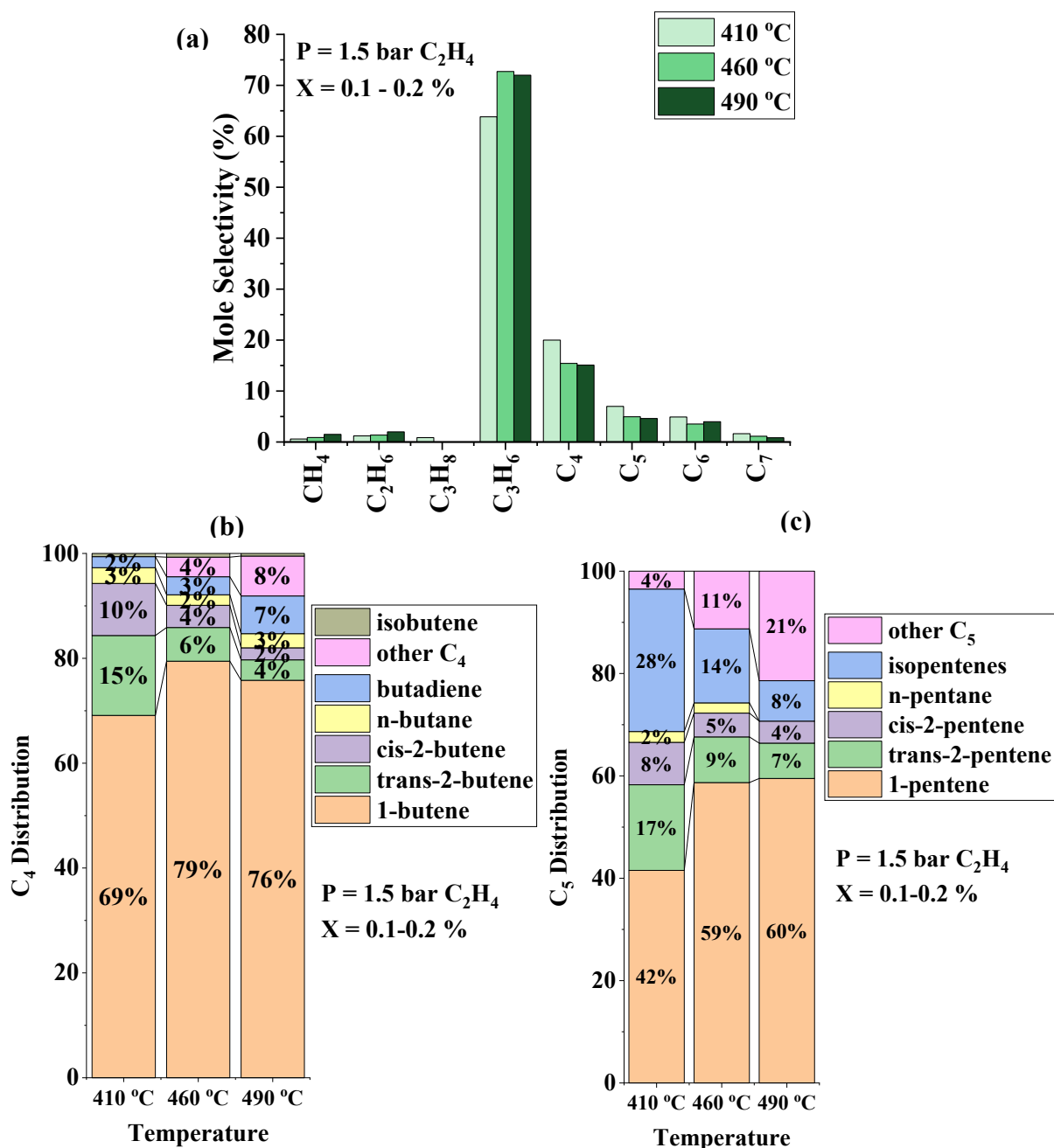


Figure 2. Product distributions at 1.5 bar C₂H₄ from 410 to 490 °C at 0.1 - 0.2 % conversion. (a) By carbon number, (b) C₄ distribution, (c) C₅ distribution.

From the C₆ distribution, the presence of at least 10 isomers is apparent at each temperature. While most C₆ isomer identities were not assigned, the 1-hexene retention time is known from 1-hexene feed experiments. The GC data show that 1-hexene comprises less than 5 % of C₆ at each of the temperatures. This result also agrees with the data at 360 °C and 43.5 bar, which provided evidence that no individual C₆ isomer accounted for more than 50 % of the C₆ products. Thus, the trend of high selectivity to terminal olefin is limited to C₄ and C₅ products.

2.3.4 MW Distributions at Very Low Ethylene Conversions

Pure ethylene was also reacted at 1.5 bar to determine the initial product distributions (See Figure 3-a) at very low conversion. The lowest measurable conversion was 0.00041 % at 340 °C. Propylene and 1-butene were the only products detected. At 380 °C and 0.0073 % conversion, C₅ and C₆ products were detected, however propylene was the most selective product in each case. These results are somewhat surprising considering that propylene is a non-oligomer product. That is, it requires both C-C formation and C-C scission for each propylene molecule formed starting from ethylene.

Ethylene was also reacted at 43.5 bar (Figure 3-b). As low as 290 °C at the lowest measurable conversion, the only products detected were 1-butene, C₅, and C₆ products. Propylene and C₈₊ products become detectable at 340 °C. At 360 °C and 0.58 % conversion, there are products of each carbon number from C₃ to C₁₀, with the selectivity of each group decreasing from C₆ > C₄ ~ C₈ ~ C₅ > C₇ > C₉ > C₃. The GC chromatogram shows the quantity of distinct isomers in each carbon number group (see Figure A.3). C₄ consists of about 80 % 1-butene and 20 % 2-butenes. There is an unassigned product between the C₄ and C₅ fractions. The last butene isomer, *cis*-2-butene, has a boiling point of 4 °C, whereas 3-methyl-1-butene and 1-pentene boil at 20 and 30 °C, respectively. On the other hand, cyclobutane boils at 12.5 °C. This, however, cannot be confirmed without a cyclobutane reference, but would be consistent with Quick et al.'s observation that cyclobutane is formed in ethylene thermal reactions.¹⁰³ The C₅ fraction contains at least 4 isomers, about 60 % of which is 1-pentene. Since there are only 3 possible linear pentene isomers, the data suggest that some cyclic and/or branched C₅ isomers are produced. C₆ appears to have 7 or more isomers. There are 5 possible linear C₆ isomers, so the occurrence of 7 or more isomers implies the presence of cyclic and/or branched C₆ isomers. The C₇ product group increases to at least 11 isomers (with 5 possible linear C₇ isomers), which appear highly distributed. Both C₈ and C₉

appear to each have even more distinct isomers. Furthermore, there is no evidence for significant amounts of saturated or doubly unsaturated products at 360 °C.

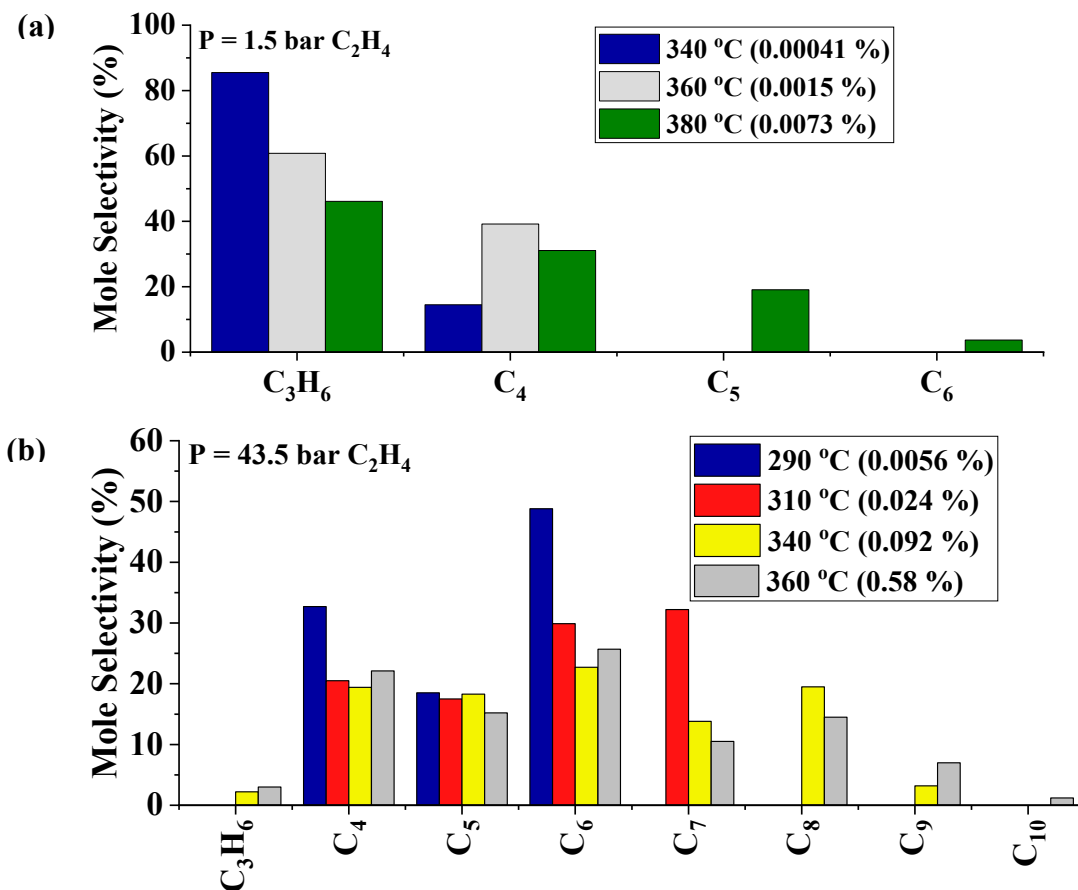


Figure 3. Product distributions for ethylene feed below 400 °C at low conversion. (a) 1.5 bar, quartz reactor with volume = 11 cm³. (b) 43.5 bar, stainless steel reactor with volume = 30 cm³.

2.3.5 Measured Kinetics of the Thermal Reactions of Ethylene

To further understand the behavior of the thermal reactions of ethylene, the reaction order and activation energies were measured across a range of temperature and pressures. Ethylene was studied from 336 to 500 °C from 1.0 to 43.5 bar. The reaction order for ethylene was determined to be 2.1 with pressure varied from 1.0 to 18.0 bar (see Figure 4-a). This 2nd order dependence suggests that the initiation mechanism is bimolecular. The Arrhenius analysis reveals a functional relationship between the activation energy and temperature. The result is the appearance of two distinct regions: a linear region below about 410 °C and a quasi-linear region above 410 °C which

decreases slightly in slope with increasing temperature up to about 500 °C. The values for the low and high temperature regions are 244 and 165 kJ/mol, respectively (Figure A.4). In either case, the activation energy is quite large, which is consistent with a non-catalytic gas phase reaction.

In radical chain reactions, the activation energy is a function of the initiation and propagation reactions. Propagation reactions in oligomerization, e.g. olefin addition or beta-scission, are relatively well-known; however, the initiation steps for this reaction are not clear. In the next section, four initiation reactions were modeled to propose a reaction pathway leading to free radicals which may be used to rationalize the observed kinetics.

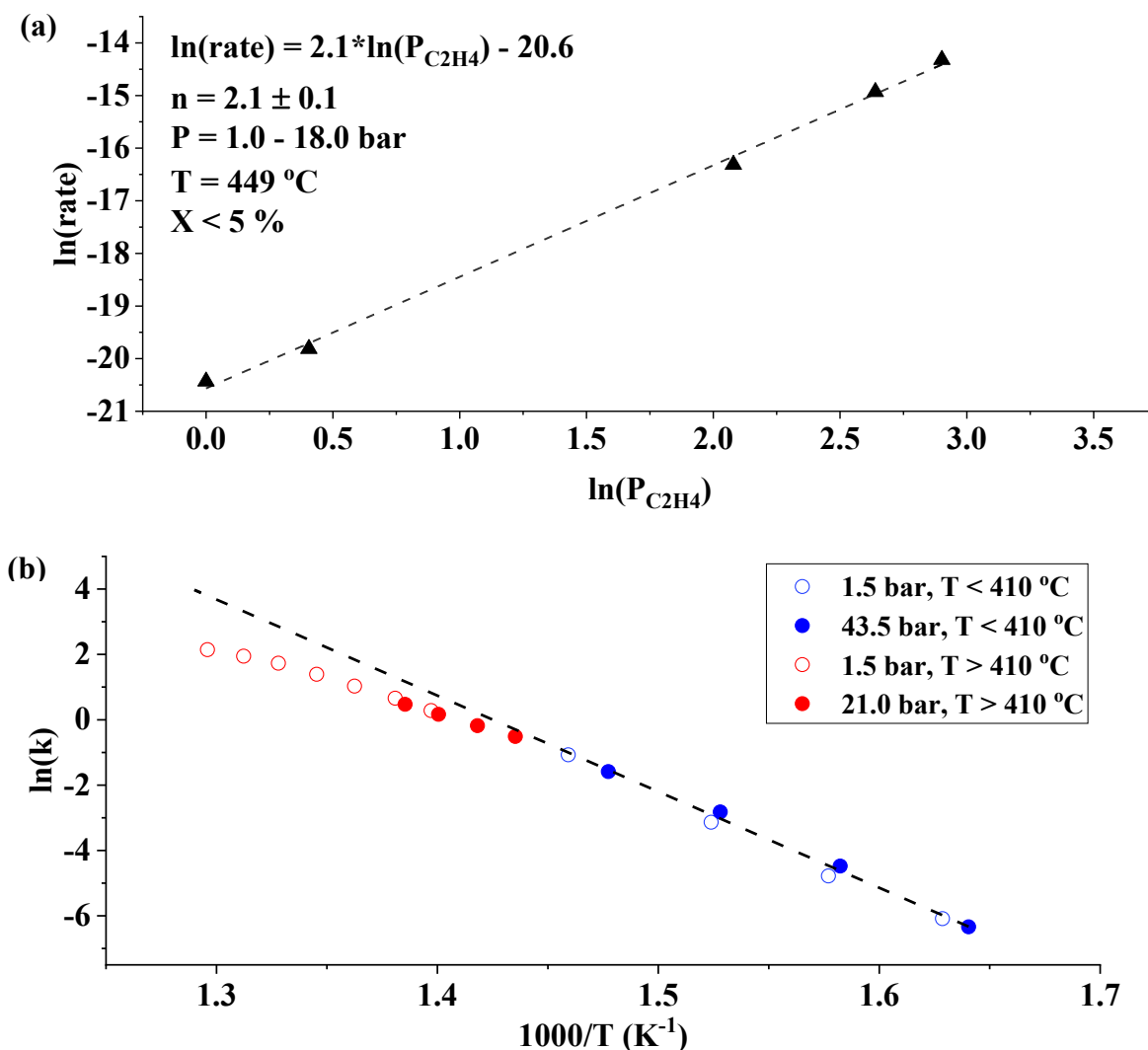


Figure 4. The kinetics of ethylene thermal reactions. Rates were measured with $X < 5.0 \%$ with units of moles C_2H_4 converted/ cm^3/s . (a) The reaction order at 449 °C from 1.0 to 18.0 bar. (b) The Arrhenius plot at 1.5, 21.0 and 43.5 bar from about 340 to 500 °C

2.3.6 DFT of Proposed Initiation Reactions

To ascertain the mechanism of initiation for ethylene oligomerization, four bimolecular ethylene reactions were modelled for comparison. The relative free energies for each pathway are shown in Figure 5, alongside the products of each reaction. The first pathway (blue) concerns the formation of cyclobutane through a 2+2 cycloaddition reaction. This single step reaction occurs through a highly distorted, asymmetric transition state with a large 78.8 kcal mol⁻¹ free energy barrier.

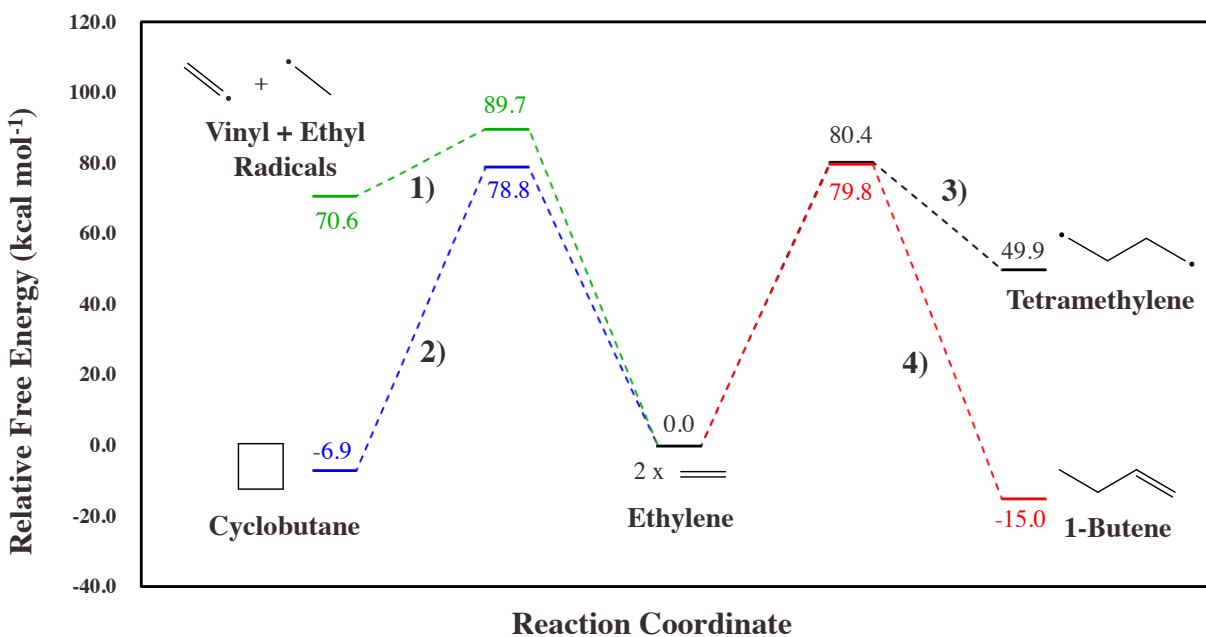


Figure 5. Free energy profiles for four ethylene bimolecular initiation reactions.

Tetramethylene, as shown in black in Figure 5, forms somewhat analogously to a standard ethylene polymerization reaction, differing in that one ethylene molecule must undergo cleavage of one C-C bond to yield a reactive dimethylene intermediate, which then attacks the other ethylene molecule. The activation barrier of 80.4 kcal mol⁻¹ for this reaction is almost identical to the cyclobutane formation, however, tetramethylene formation is considerably more endergonic due to the double-radical nature of the product formed. 1-butene formation, shown in red, occurs through a four-centered transition state wherein a hydrogen atom from one ethylene molecule is donated to the other and the remaining vinyl moiety of the first ethylene attacks the unsaturated carbon of the second molecule. Once again, this reaction proceeds through a barrier height that is

almost identical to the previous two at $79.8 \text{ kcal mol}^{-1}$. Unsurprisingly, the formation of 1-butene is more exergonic than cyclobutane owing to the increased degrees of freedom in the former and the ring-strain in the latter. The final initiation reaction, shown in green, is a simple hydrogen atom transfer from one ethylene molecule to another. This reaction, with a significant activation free energy of $89.7 \text{ kcal mol}^{-1}$, yields a vinyl and an ethyl radical. This reaction is highly endergonic, exhibiting a free energy of formation of $70.6 \text{ kcal mol}^{-1}$.

Cyclobutane Cracking Reactions.

We identified two routes for the decomposition of cyclobutane, the first of which is shown in Figure 6 alongside the free energy profile for the reaction. Formation of tetramethylene involves homolytic dissociation of a C-C bond in cyclobutane to yield a planar tetramethylene diradical. The barrier for this homolytic dissociation was calculated to be $57.1 \text{ kcal mol}^{-1}$. Following dissociation, the tetramethylene intermediate converts to an open-book like geometry with a C_1-C_4 dihedral angle of 60° . Rotation about the central C-C bond yields a slightly lower energy, more linear structure with a C_1-C_4 dihedral of 175° .

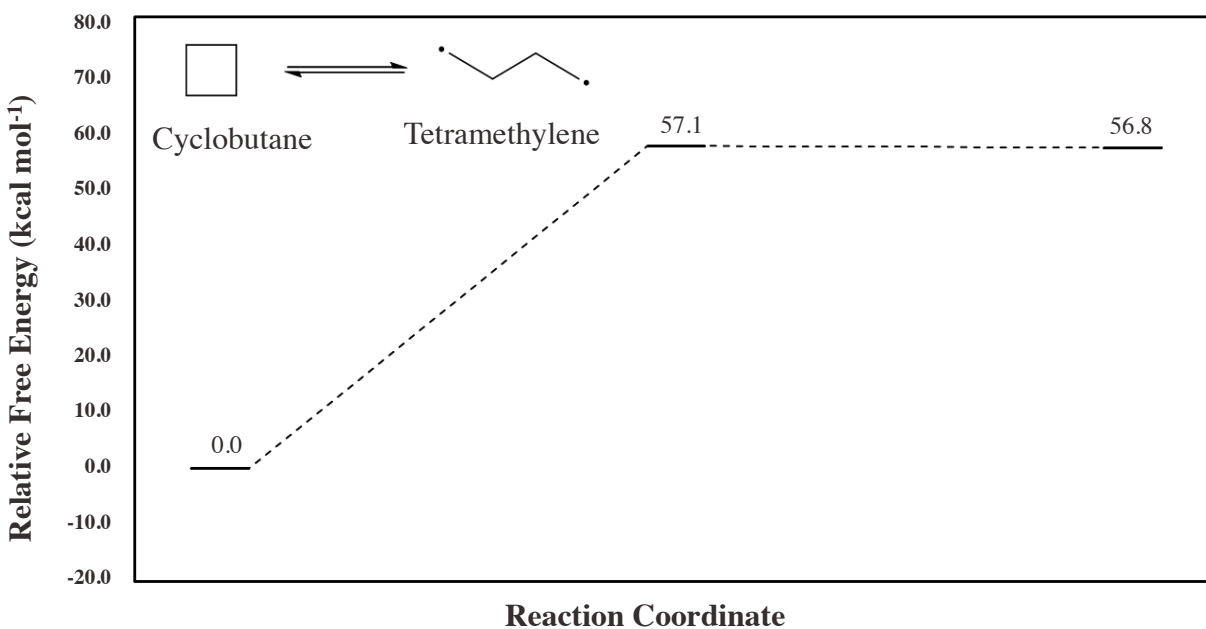


Figure 6. Free energy profile for homolytic ring cleavage of cyclobutane.

The second mechanism, shown in Figure 7, begins with the hydrogenation of ethylene by cyclobutane to yield cyclobutene and ethane. This cis-hydrogenation proceeds via a single symmetric transition state in which both hydrogen atoms transfer simultaneously from the

cyclobutane to the ethylene. This reaction has a barrier height of 56.4 kcal mol⁻¹ and exhibits a minimal change in the overall free energy.

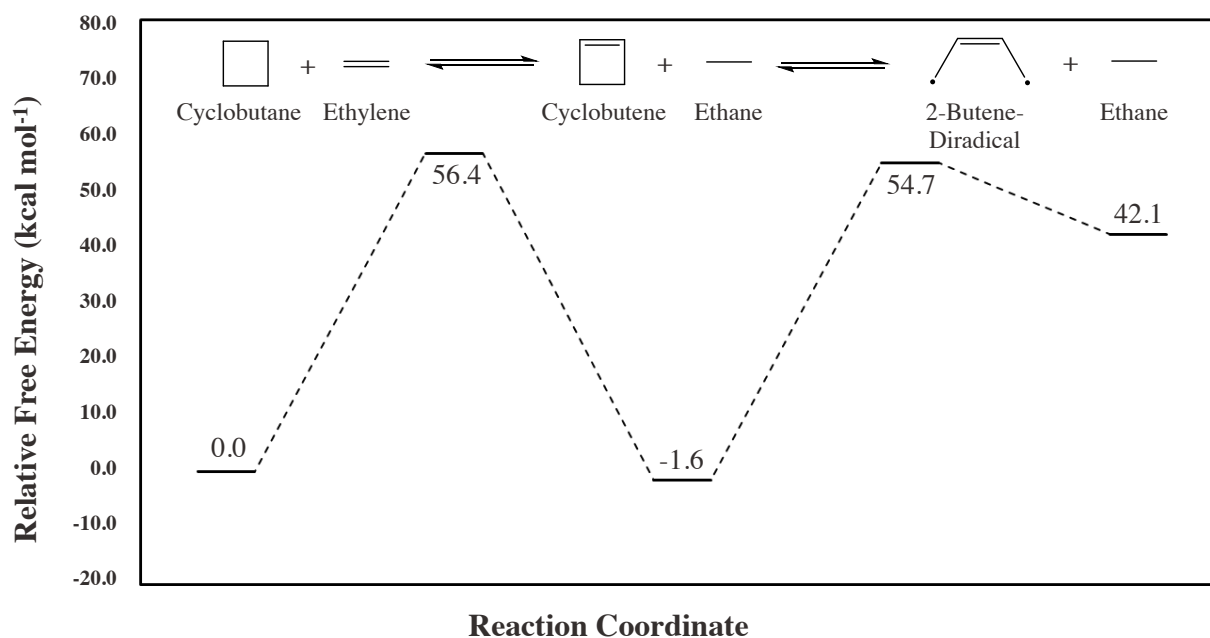


Figure 7. Free energy profile for cyclobutene formation of homolytic ring cleavage.

Cleavage of the bond between the two saturated carbons of cyclobutene yields a 2-butene 1,4-diradical and subsequent rotation of the terminal CH₂ groups yields a more stable planar structure. The free energy barrier for the homolytic ring-opening of cyclobutene is 56.3 kcal mol⁻¹, while rotation to the planar structure leads to a reduction in free energy of 12.6 kcal mol⁻¹.

Diradical Chain Growth Reactions

Both diradical species produced from the decomposition of cyclobutane can engage in free radical polymerization reactions with ethylene. Tetramethylene can react with ethylene to yield hexamethylene, as shown in Figure 8, while the 2-butene 1,4-diradical species can react with ethylene to give a 2-hexene 1,6-diradical, which is shown in Figure 9. Addition of ethylene to either diradical occurs through a sub-20 kcal mol⁻¹ barrier. Both pathways are also endergonic, with 2-hexene 1,4-diradical formation being slightly more free energy releasing than that of hexamethylene.

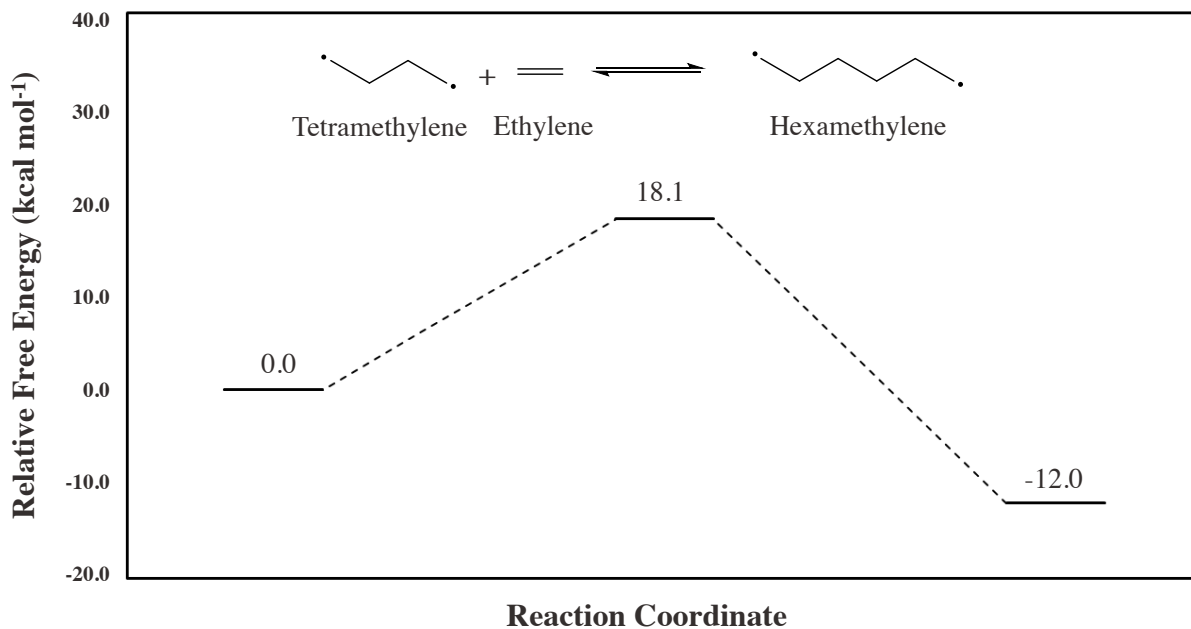


Figure 8. Free energy profile for the addition of ethylene to tetramethylene.

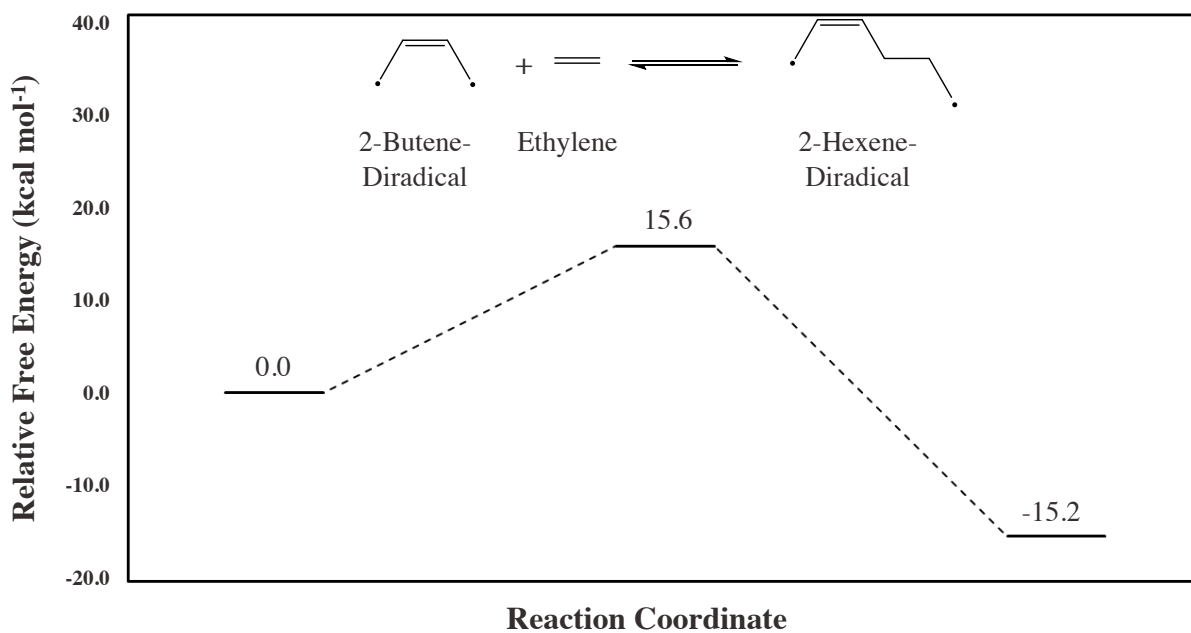


Figure 9. Free energy profile for the addition of ethylene to 2-butene 1,4-diradical.

Hexamethylene Conversion

One potential fate for the hexamethylene that is produced from the reaction of tetramethylene and ethylene is conversion to 1-hexene, as shown in Figure 10. This reaction proceeds via an intermolecular hydrogen atom transfer, similar in nature to a retro-ene reaction. This single step pathway has a small activation free energy of 18.1 kcal mol⁻¹ and is considerably exergonic, owing to the satiation of the two radical centers.

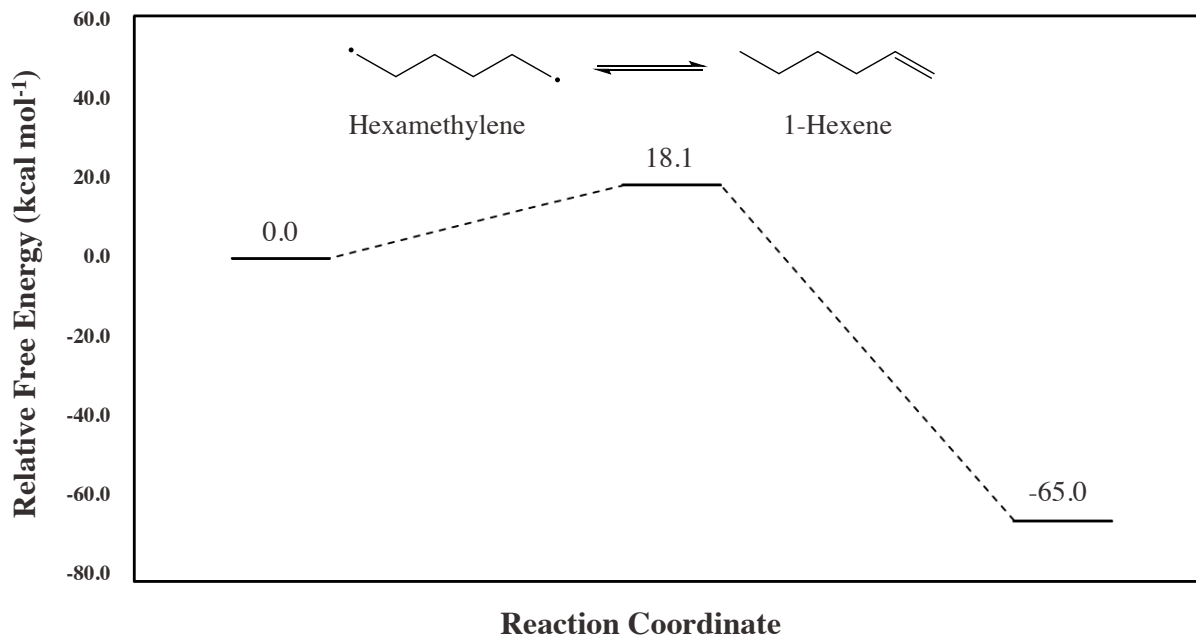


Figure 10. Free energy profile for conversion of hexamethylene to 1-hexene.

Hydrogen Atom Abstraction Reactions

While numerous hydrogen abstraction reactions can occur between the diradical species generated in the earlier pathways, we have chosen two possible mechanisms to focus on here. These two pathways are shown in Figures 11 and 12, alongside their respective free energy profiles. The first pathway, shown in Figure 11, is the transfer of a hydrogen atom from one 1-hexamethylene molecule to another, yielding a 1-hexane radical and a 1-hexene radical. Formation of the two single-radical species is highly exergonic, releasing -65.6 kcal mol⁻¹ in free energy, and requires a modest activation free energy of 22.7 kcal mol⁻¹.

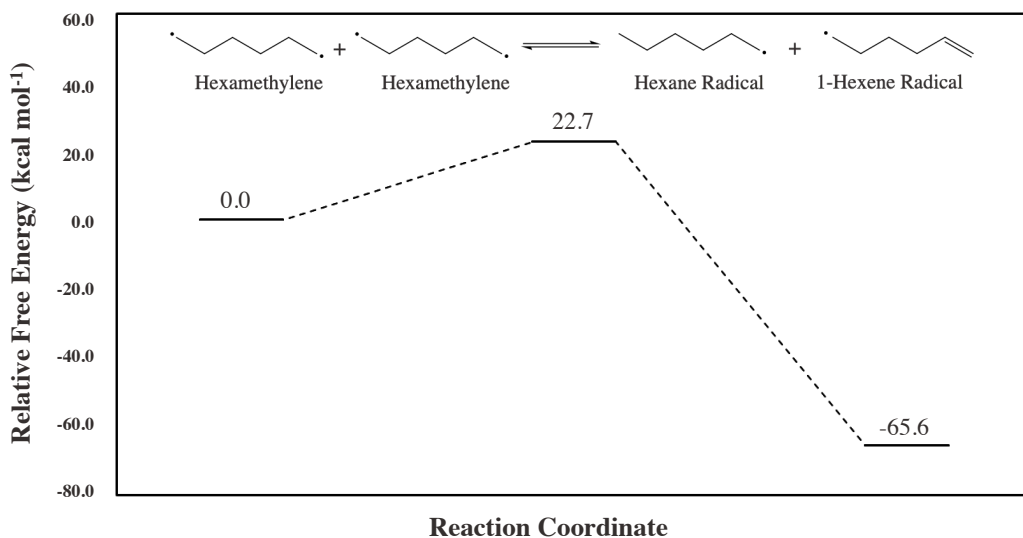


Figure 11. Free energy profile for hydrogen atom abstraction from one hexamethylene molecule to another.

The second pathway, which is provided in Figure 12, involves abstraction of an allylic hydrogen of 1-hexene to an end-chain carbon of a 2-hexene diradical. This reaction has a relatively small barrier height of 19.0 kcal mol⁻¹, but is significantly less exergonic than the hydrogen atom transfer reaction between two hexamethylene molecules shown previously.

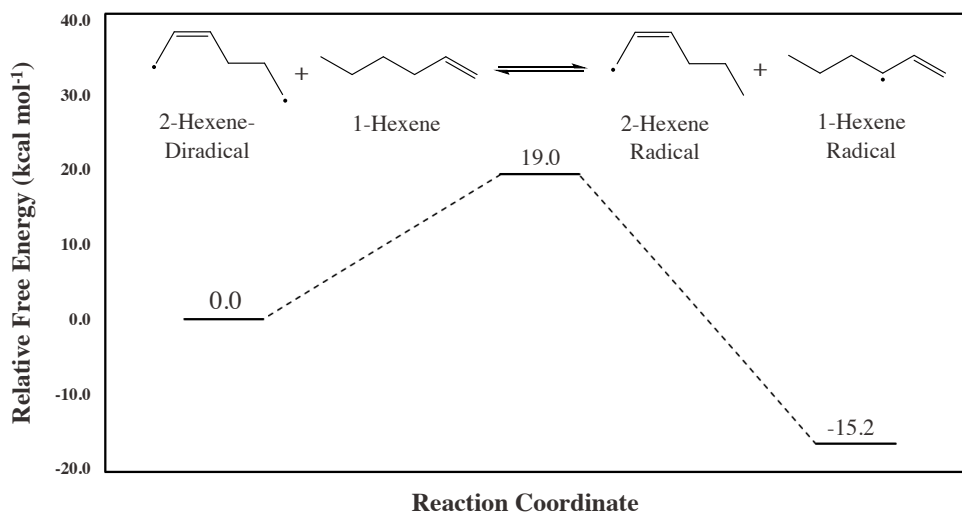


Figure 12. Free energy profile for hydrogen atom abstraction from 1-hexene to a 2-hexene 1,6-diradical.

Diradical Formation from 1-Butene

The final pathway modelled in this work is shown in Figure 13. It is a two-step reaction, the first step of which is the formation of butadiene and ethane from 1-butene and ethylene. This cis-hydrogenation is analogous to the one presented earlier in this work for cyclobutane and, unsurprisingly, has a similar free energy barrier of 54.6 kcal mol⁻¹ and reaction energy of -2.9 kcal mol⁻¹. The newly formed butadiene can then convert to a resonance stabilized diradical form, wherein the C2-C3 carbon bond has the most double bond character and the terminal carbons are the radical centers. The free energy required for this process is 53.0 kcal mol⁻¹, lower than any other radical generating reaction step reported in this work.

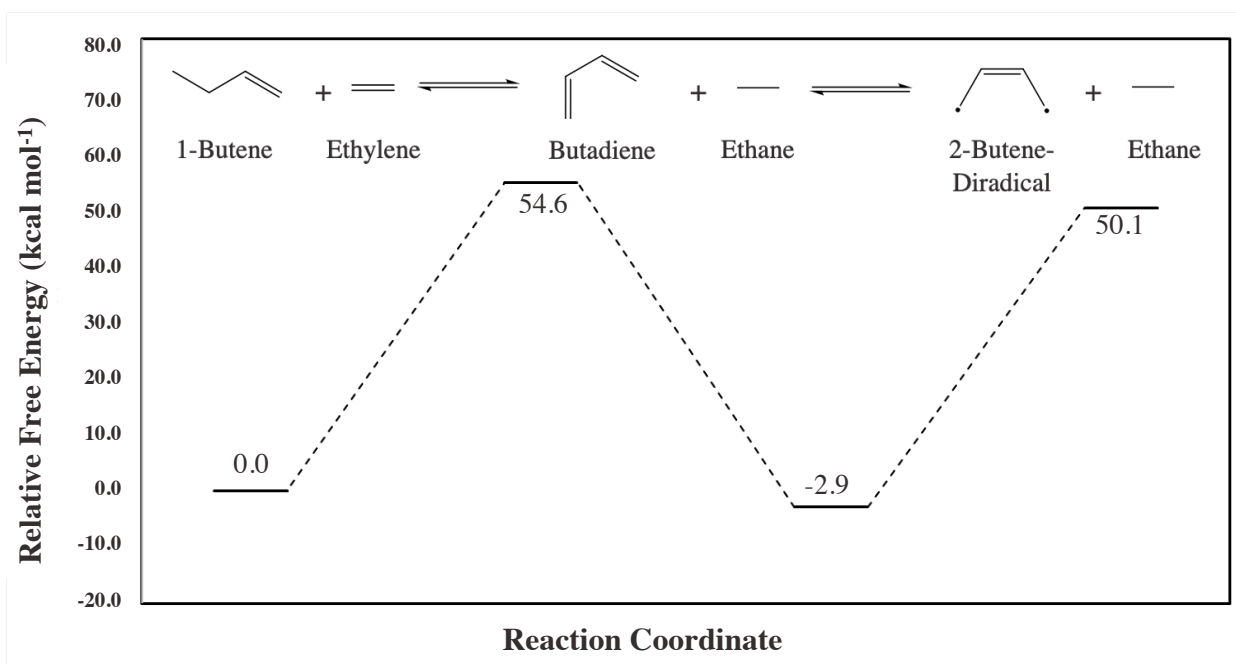


Figure 13. Free energy profile for the generation of a 2-hexene 1,4-diradical and ethane from 1-butene and ethylene.

2.3.7 Comparison of the Thermal Reactions of Other Olefins

Propylene.

The molecular-weight distribution of the propylene reaction at 400 °C, Figure 14-a, shows a marked difference between the products of propylene compared with ethylene. By carbon number, the C₆ dimer is the major product (ca. 70 %). Non-oligomer products were observed also (< 30 %), but in much smaller amounts compared to ethylene. C₂, C₄, C₅, C₇, and C₈ products were detected in similar amounts (about 3 – 8 mole % each). Methane and ethane were present in minor

amounts (less than 2 mole % each). Isobutene was 28 % and 1-butene only 16 % of the C₄. The C₅ products contained small amounts of 1-pentene (8 %). There were at least 15 distinct C₆ species present at 400 °C. 1-Hexene is about 10 % of the C₆, whereas several other isomers were present in larger amounts. There are 7 possible branched C₆H₁₂ isomers and therefore 12 maximum expected open-chain olefin isomers. The presence of 15 isomers implies the presence of dienes, saturated C₆, and/or cyclic isomers in addition to iso-hexenes and n-hexenes.

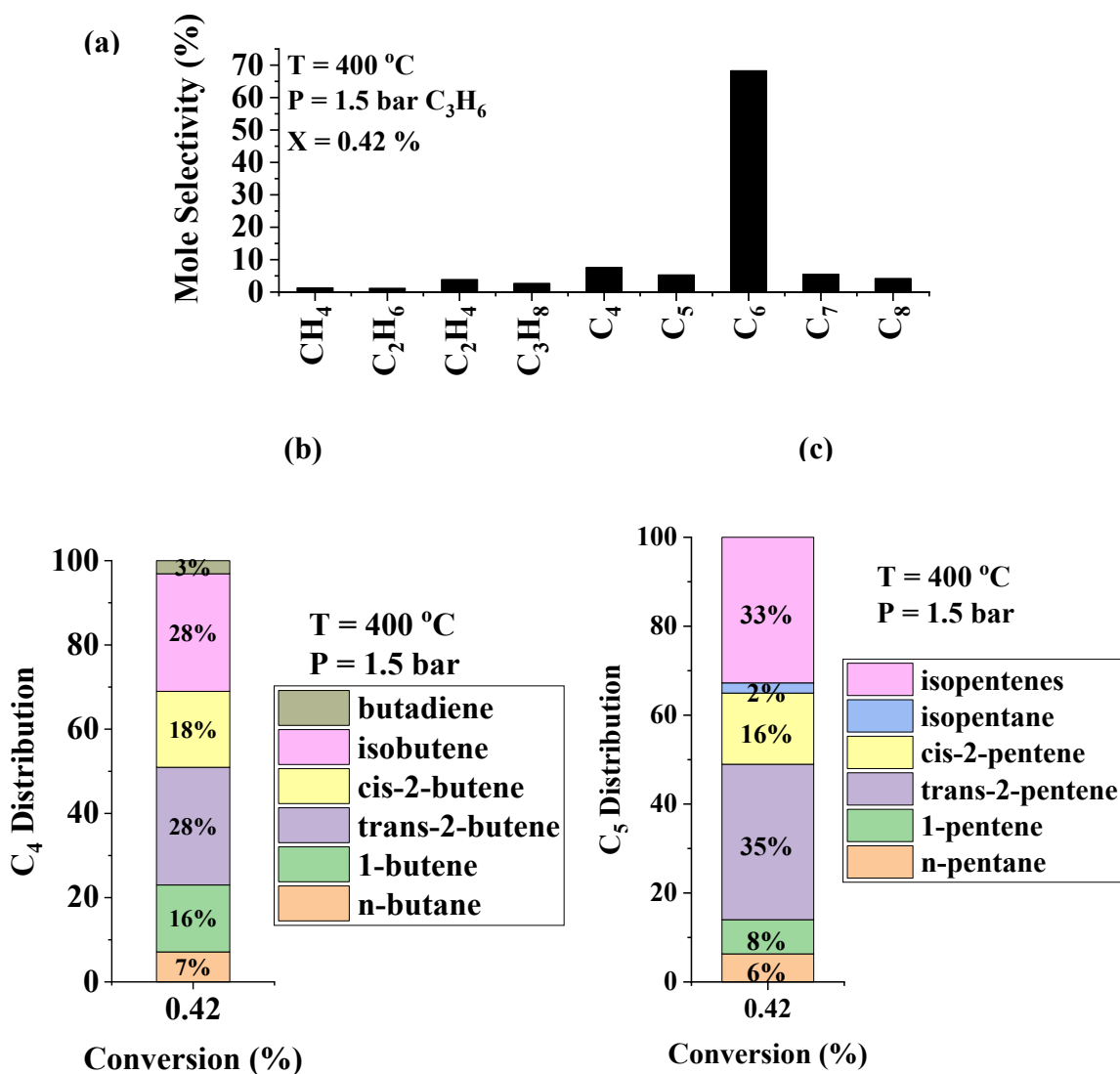


Figure 14. Product distribution at 0.42 % conversion of pure propylene reacted at 1.5 bar and 400 °C. (a) By carbon number, (b) C₄ distribution, (c) C₅ distribution.

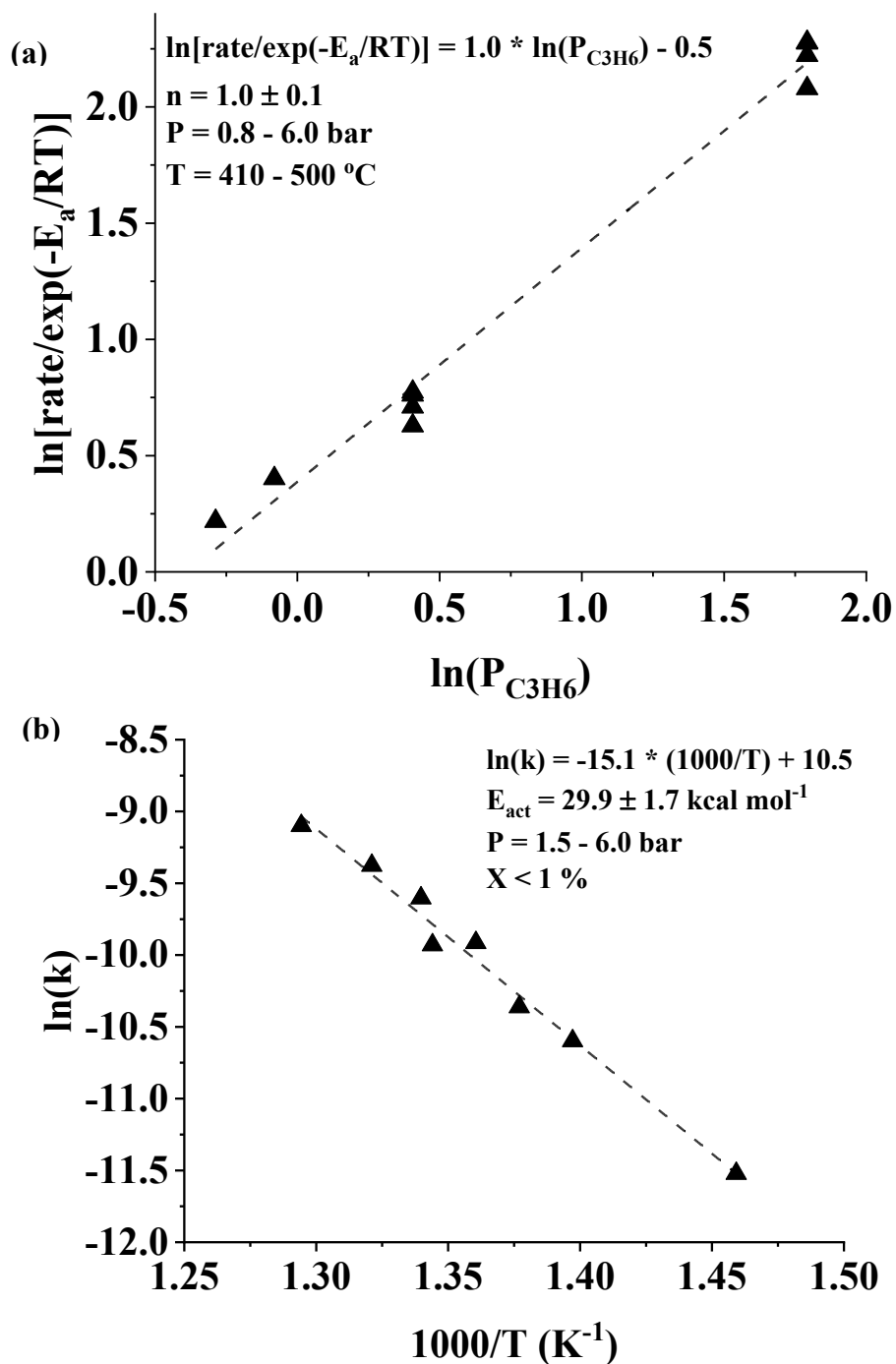


Figure 15. The kinetics of propylene thermal reactions. Rates were measured $X < 1.0 \%$ with units of moles C_3H_6 converted/ cm^3/s . (a) The reaction order from 0.8 to 6.0 bar. Rates were normalized by the Arrhenius term $\exp(-E_a/RT)$ using the observed E_a of 125 kJ/mol. (b) The Arrhenius plot measured from 400 to 500 $^\circ\text{C}$. Rate constants are the rate normalized by the observed 1.0 reaction order.

The reaction order for propylene was found to be first order from 0.8 to 6.0 bar, with an activation energy of roughly 125 kJ/mol from 400 to 500 °C (see Figure 15). Thus, the kinetics of propylene compared to ethylene thermal reactions are quite distinguished, like their different product behaviors, suggesting a different reaction pathway.

1-Hexene.

The experimental results for 1-hexene are shown in Table 2. At 260 °C, no detectable conversion of 1-hexene occurred. At 370 °C, 22.0 % of the 1-hexene was converted. 99.5 % of the products were 7 or more C₆ isomers, and the other 0.5 % were C₂-C₈ olefins. No methane, ethane or higher paraffins were detected. At 400 °C and 86.0 % 1-hexene conversion, 99.0% of the products were 12 or more distinct C₆ isomers (Figure A.8). The remaining 1.0 % of products were C₂ – C₈ olefins, with a very small amount of methane and ethane (< 1 mole % each). At 420 °C and 38.9 % conversion there is some methane and ethane (about 2.5 mole % each) in addition to the other non-C₆ olefin products (see Figure 16-a). The C₄ and C₅ products from 1-hexene cracking consist of linear and branched isomers. At 370 °C, 29 % of the C₄ was isobutene, and 38 % was 1-butene (Figure 16-b). 1-Pentene was only 26 % of C₅, and about 28 % were isopentenes (Figure 16-c). The appearance of about 5 % total methane and ethane at 420 °C is accompanied by butadiene, 13 % of the C₄, which was not detected at 370 °C.

Table 2.1-C₆H₁₂ Conversion in an Empty Quartz Reactor from 1-20 kPa

Average Temperature (°C)	260	370	420	400	400
1-Hexene Pressure (kPa)	~ 5	~ 10	~ 5	~ 1	~ 20
Insulated Reactor Volume (cm ³)	11	11	11	25	25
Flow of N ₂ feed (sccm)	5	100	100	100	20
Conversion (%)	Tr	22.0	38.9	88.4	86.0
Yield to C ₆ isomers (carbon %)		21.9	38.8	88.2	85.1
Number of C ₆ isomer peaks		> 7	> 7	> 12	> 12
Yield to non-C ₆ isomers (carbon %)		0.1	0.1	0.2	0.9
Rate of 1-hexene isomerization (mol/cm ³ /s) x 10 ⁹		320	220	67	210
Rate of 1-hexene cracking (mol/cm ³ /s) x 10 ⁹		1.6	0.6	0.1	2.2
Ratio of isomerization to cracking		200x	370x	460x	100x

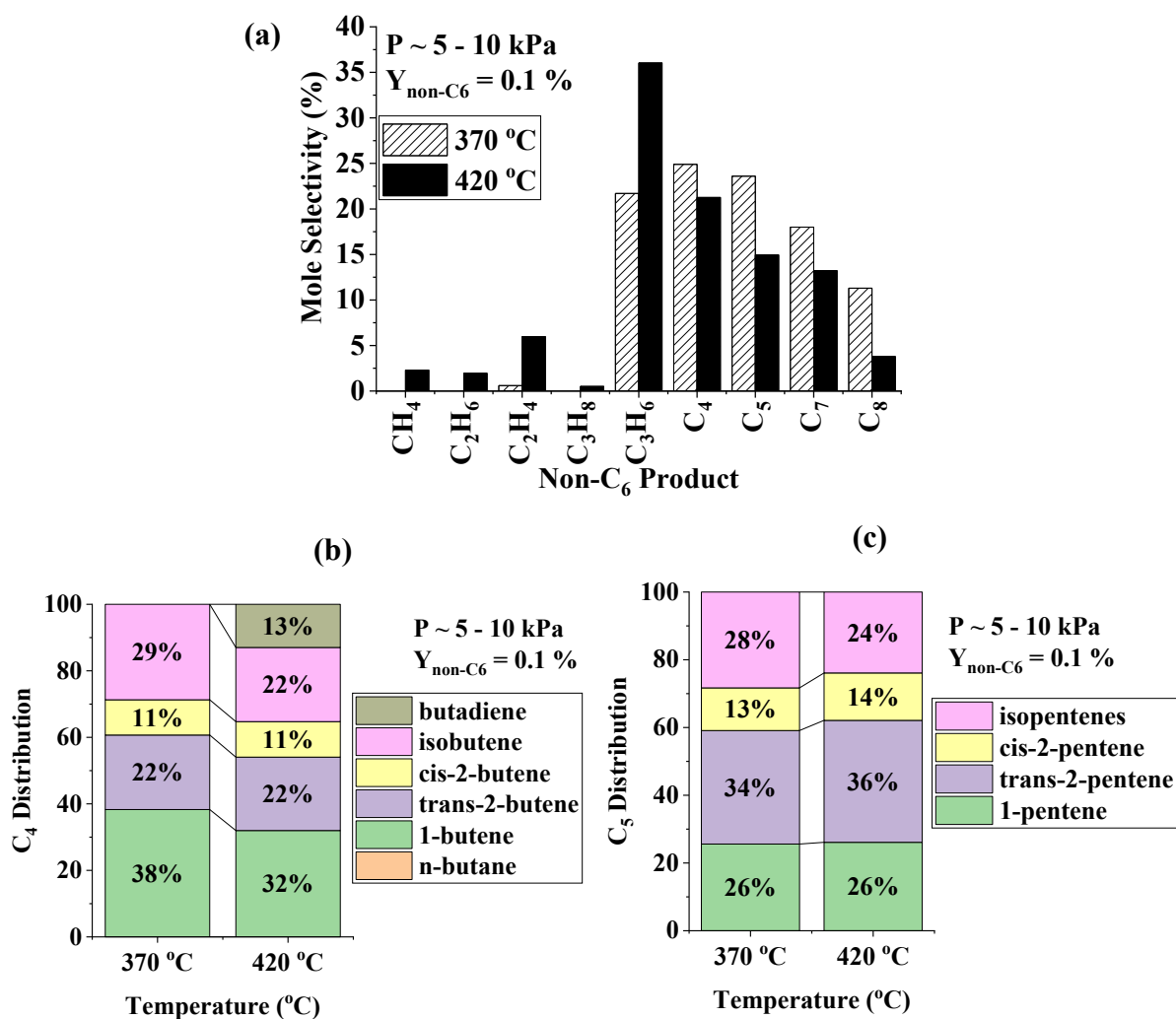


Figure 16. Product distribution of non-C₆ products at 0.1 % yield to non-C₆ of 1-hexene reacted at 370 and 420 °C (a) By carbon number, (b) C₄ distribution, (c) C₅ distribution.

2.4 Discussion

2.4.1 Product Distributions

Detailed molecular weight distributions for the thermal oligomerization of ethylene have not been reported above atmospheric pressure. The effects of temperature, pressure, and conversion were evaluated from 14.0 to 21.0 bar and 432 to 449 °C with conversions between 3.7 and 11.0 %. The effects of temperature and pressure affect the product distribution in an opposing manner. Lower temperature and higher pressure promote the formation of longer chain products (C₆₊),

whereas higher temperature and lower pressure result in more short chain olefins such as propylene and 1-butene. As the reaction progresses from 3.7 to 11.0 % conversion, more C₃ to C₆ are produced compared to C₇₊. It is important to note that even though the relative molar selectivity to C₇ to C₉ becomes less, the overall molar production rates of C₇ to C₉ do not appear to decrease. Thus, the shift towards higher C₃ to C₆ selectivity is due to greater production from the reactions of the remaining ethylene as opposed to the decomposition of stable C₇ to C₉ products. These molecular-weight distribution trends are thus a reflection of the propagation steps, in which C-C bond formation, leading to higher olefins such as C₆₊, competes with C-C scission, leading to lighter olefins such as C₃H₆ and C₄.

The occurrence of non-oligomer products such as propylene, pentenes, etc. has been reported in previous reports above 500 °C at low pressure.^{91–93,96} However, product distributions at high pressures below 500 °C were all conducted at significant conversions above 10 %.^{52,55,56,72} This study has provided evidence that non-oligomers are present even at very low conversions (see Figure 3). Furthermore, the results suggest that at 43.5 bar and 290 °C, for example, propylene is not necessarily the first non-oligomer formed. At 43.5 bar and low conversion, the growth pattern no longer resembles 1-carbon chain growth. Knowledge of this result demonstrates that the chain growth is not addition of single carbon species, as in the Fischer-Tropsch reaction,¹¹² but that the competing C-C bond formation and scission propagation reactions lead to scrambling of the molecular-weight distribution very rapidly.

This study also brings to light new information about the C₄, C₅, and C₆ products. The high preference for terminal C₄ and C₅ compared to internal double bonds and branched olefins is evident. This outcome is distinct from Brønsted acid-catalyzed oligomerization, which preferentially produces internal and branched olefins, due to the higher stability of tertiary and secondary carbenium ions compared to primary carbenium ions.⁴² The stability of radicals follows the same trend, i.e., tertiary are the most stable, and primary, the least.¹¹³ Therefore, the fact that branched C₄ and C₅ olefins are minor products is evidence of a reaction pathway in which there is low preference to forming tertiary radicals. The ratios of 1-butene to 2-butenes, 1-pentene to 2-pentenes, and n-pentenes to isopentenes all increased from 410 to 490 °C. Thus, another conclusion is that temperature influences the propagation reactions in a way that leads to a stronger preference for linear, terminal C₄ and C₅ olefins at 490 °C compared to 410 °C at 1.5 bar.

The C₆ isomers deviate substantially from the C₄ and C₅ isomer distributions, which showed strong preference to 1-butene and 1-pentene, respectively. In contrast, no individual C₆ isomer accounted for more than half of the total C₆. In fact, at 490 °C, the 1-hexene appears to be less than 5 % of all C₆, a marked difference compared to C₄ and C₅. The same observation can be made for the C₇ to C₉ isomers at 43.5 bar and 360 °C. More isomers are present for C₆₊ than are accounted for by the theoretical number of linear olefins, indicating that skeletal isomerization and/or cyclization is occurring. The ability of n-alkyl radicals to undergo 1,4 and 1,5 hydrogen-transfer reactions resulting in more stable secondary radicals is well known,^{114–118} and gives rise to highly branched polyethylene in the radical polymerization of ethylene.^{119,120} Thus, in conjunction with the thermal isomerization of 1-hexene demonstrated in this study, at least two pathways exist that can lead to the observed numbers of isomers for C₆₊ products.

2.4.2 Kinetics

In addition to the products, the kinetics of ethylene reactions were also investigated. The previous kinetic measurements above atmospheric pressure estimated the rates from reactor pressure changes at conversions greater than 10 %.¹⁰⁴ In the present study, the kinetic measurements were determined from conversions below 5.0 % in a continuous flow reactor. The reaction order of 2.1 obtained here agrees well with those previous studies.^{82,83,91,104,105} However, the activation energy was observed to be a function of temperature, a feature not previously reported in ethylene pyrolysis. Above 410 °C, the measured value, 165 kJ/mol, agrees with the values reported previously, but increased to 244 kJ/mol below 410 °C. The change in activation energy with temperature is an important finding, which highlights the fact that different reaction steps can become rate controlling as conditions change.

2.4.3 Reaction Pathway

Free radical chain reaction pathways are well-known to be characterized by initiation, propagation, and termination reactions. Propagation and termination steps for radical chemistry are well-studied,^{121,122} but the initiation step for this reaction has been under debate, lacking a rigorous energetics study.

There is strong evidence suggesting that the thermal oligomerization of ethylene proceeds first through a slow initiation stage, followed by a secondary faster period of oligomerization. Our computational results propose several possible mechanisms that can account for a slow initiation phase, as well as more facile oligomerization reactions that are accessible through the products formed during the initiation period.

While all four of the bimolecular reactions provided in Figure 5 require significant energy input to overcome their free energy barriers, it is clear to see that the hydrogen atom transfer reaction pathway (green) is considerably less favorable than the other possible routes. While the remaining three bimolecular reactions pathways exhibit similar energy requirements, the formation of cyclobutane and of 1-butene are notably more thermodynamically favorable than tetramethylene formation. Both pathways are also reasonably exergonic, thus promoting accumulation of cyclobutane and 1-butene in the early stages of the ethylene thermal oligomerization process. For these reasons, cyclobutane and 1-butene are further explored as potential intermediates in ethylene oligomerization reactions.

Both cyclobutane decomposition pathways in Figures 6 and 7 have comparable free energy barriers, however, the resonance stability of the 2-butene 1,4-diradical makes its formation the more thermodynamically favorable pathway. It is worth noting that formation of the 2-butene 1,4-diradical is a bimolecular reaction, requiring one mole of ethylene for each mole of cyclobutane reacted, and thus will exhibit greater pressure dependency than the unimolecular decomposition route that produces tetramethylene. Our proposed mechanism for the formation of cyclobutane also provides a source for the small concentrations of ethane consistently observed in our experimental results.

In Figures 8 and 9 we have explored the free-radical addition of ethylene to both tetramethylene and to the 2-butene 1,4-diradical, giving hexamethylene and a 2-hexene 1,6-diradical, respectively. While we have only reported the first step of the chain-growth reactions involving tetramethylene and 2-butene 1,4-diradical, it is reasonable to assume that rapid growth of biradical chains will occur through free-radical polymerization and that this chain-growth will proceed with similar energetic requirements.

The instability of diradical intermediates is demonstrated clearly by the facile conversion of hexamethylene to 1-hexene. As seen in Figure 10, this conversion is highly exergonic and proceeds

via a small free energy barrier. The 1-hexene produced from this reaction can participate in the reaction pathway outlined in Figure 12, producing a 2-hexene 1,6-diradical and ethane.

An alternative means of stabilizing the diradical intermediates is through hydrogen atom abstraction reactions between two diradical compounds. One example reaction, provided in Figure 11, is the abstraction of a hydrogen atom from the second carbon of one hexamethylene to the end chain radical site of another hexamethylene, yielding a hexane radical and a 1-hexene radical. The second example hydrogen atom abstraction reaction in this study is the reaction of 2-hexene 1,6-diradical and 1-hexene. Abstraction from the allylic site of 1-hexene was chosen owing to the resonance stabilization of the neighboring double bond. Similarly, the non-allylic radical site of the 2-hexene 1,6-diradical was saturated with the abstracted hydrogen atom as the radical position at the other end of the chain is resonance stabilized.

Regardless of the formation pathway, the four monoradical species generated from the hydrogen atom abstraction reactions can participate in free radical polymerization reactions with ethylene, rapidly generating oligomeric polyethylene type species. The length of the growing carbon chains is dictated by an interplay of polymerization and cracking reactions. Such reactions have been discussed at length elsewhere and their roles in the thermal chemistry of polyolefins are well understood. Of particular interest to this work are beta-scission reactions (see Figure 17), a mid-chain cleavage reaction that generates a smaller end-chain radical and a terminal alkene.



Figure 17. Beta-scission reaction of a mid-chain radical to yield an end-chain radical and a terminal alkene.

The rapid polymerization of ethylene and subsequent generation of unsaturated products through cracking reactions represents the end of the initiation phase. Up to this point, all pathways are dependent on the bimolecular reactions of ethylene to form the diradical species. These reactions have very high activation free energies and so consequently the concentration of all radical intermediates will remain low and the rate of oligomerization will be severely limited.

The terminal alkenes that are formed through beta-scission reactions are able to participate in a lower energy radical forming pathway that is shown in Figure 13. The dehydrogenation of 1-butene by ethylene gives butadiene and ethane. This is followed by formation of the 2-butene 1,4-

diradical generated in our earlier reactions. The free energy barrier for the first step is 54.6 kcal mol⁻¹ and for the second it is 53.0 kcal mol⁻¹. Both these values are significantly lower than any of the bimolecular ethylene reactions that were necessary for initial diradical formation. While not shown explicitly, we have observed that any unsaturated functionality within a chain is able to dehydrogenate another chain. We therefore posit that unsaturated chains of all observed lengths may be formed through these hydrogenation/dehydrogenation reactions.

Figure 18 provides a summary of the proposed oligomerization reaction pathways. The reactions that form part of the initiation pathways are shown with black arrows, while the secondary phase pathways are shown with green arrows. While not an exhaustive description of possible reactions, our computational study clearly supports a two-phase oligomerization of ethylene. High energy barrier bimolecular reactions of ethylene are required to generate the initial free radicals necessary for free radical oligomerization. Rapidly growing polyethylene chains are then subject to thermal cracking, yielding shorter chain free radicals and unsaturated terminal alkenes amongst other species. The formation of these terminal alkenes allows for the generation of free radicals through lower energy pathways when compared against the bimolecular ethylene reactions. This more facile formation of free radicals will promote ethylene oligomerization at a much higher rate than during the initiation phase.

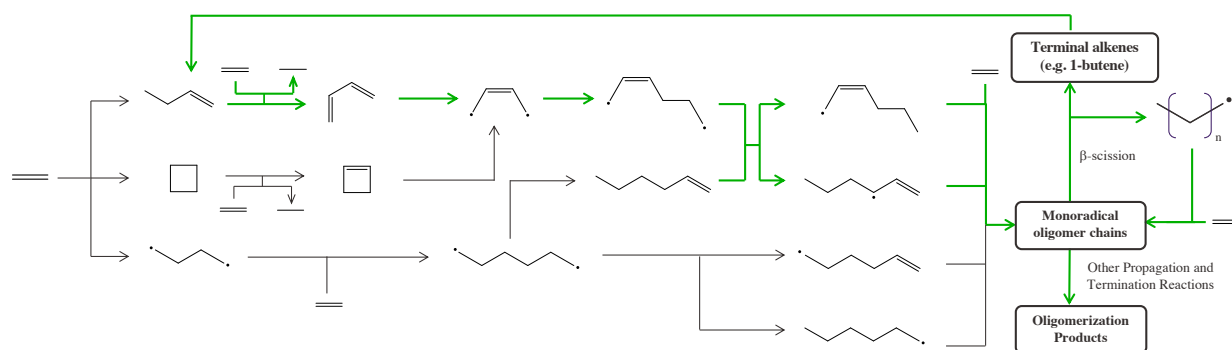


Figure 18. General scheme for the two-phase thermal oligomerization of ethylene.

2.4.4 Comparison with Propylene and 1-Hexene

In contrast to ethylene, the thermal reactions of propylene and 1-hexene revealed major product differences. At 400 °C, C₃H₆ results in mostly the C₆ oligomer, which is the opposite of ethylene,

shown to produce mostly propylene at the same conditions. Furthermore, propylene produces branched and linear C₄ and C₅, whereas ethylene makes mostly linear C₄ and C₅. Propylene also gives rise to large amounts (> 10 mole %) of methane at 500 °C (Figure S6), whereas ethylene does not. On the other hand, a similarity of both C₂H₄ and C₃H₆ reactions was the fact that 1-hexene was less than 10 % of all C₆, which also formed skeletal and/or cyclic isomers. For 1-hexene cracking, the C₄ and C₅ isomers resembled those of C₃H₆ much more closely than C₂H₄, with the presence of branched C₄ and C₅. Thus, in general propylene and 1-hexene tend to produce more isobutene and isopentenes, whereas ethylene favors n-butenes and n-pentenes.

The reaction kinetics further highlight the dissimilarity between ethylene and propylene thermal reactions. Propylene was 1st order with a lower activation energy of 125 kJ/mol from 410 to 500 °C. The lower activation energy is consistent with the observed higher rate of propylene conversion at 400 °C and 1.5 bar, but higher rate of ethylene conversion at 500 °C and 1.5 bar. Additionally, the 2nd order pressure dependence results in high ethylene conversion rates at higher ethylene pressures, but also a more severe drop-off in rate as the pressure decreases below atmospheric. This observation is consistent with conclusions by previous workers that ethylene is the easiest olefin to polymerize thermally at high pressures.^{9,55}

The nature of the C-H bond strengths in ethylene and propylene are quite different. Ethylene contains four vinyl C-H bonds, which have a homolytic bond dissociation energy (BDE) of about 463 kJ/mol.¹¹³ Propylene, on the other hand, possesses three allylic C-H bonds, which are much weaker (BDE = 372 kJ/mol) due to the resulting resonance stabilization that occurs for the allyl radical. Thus, the disparate chemical bond strengths of ethylene and propylene also suggest that their behavior in thermal reactions should be different, which is the case.

The extrapolated rates of 1-hexene cracking and isomerization at its experimentally observed concentration in the products, shown in Table A.1, demonstrate strong evidence that 1-hexene cracking is not responsible for the observed non-oligomer products. This result indicates that the molecular-weight distribution is controlled by the propagation reactions of reactive free radical intermediates rather than degradation of stable C₆ products. The relative isomerization rate, however, is at the same order of magnitude of the conversion rate of both ethylene and propylene to products and could be competitive with other routes of isomerization such as 1,4 and 1,5 hydrogen shifts.

2.5 Conclusion

In-depth study of the chemistry of the thermal reactions of ethylene has demonstrated several important characteristics. Below 500 °C and above atmospheric pressure, the reaction is 2nd order with a temperature dependent activation energy, spanning 165 to 244 kJ/mol. Non-oligomer products are formed under all conditions, but are not accompanied by formation of more than about 1 mole % each of methane and ethane. The C₄ and C₅ products are highly linear, with strong preference for the terminal olefin. The free radical oligomerization appears to initiate by a two-phase process typified by the formation of diradical intermediates. In the first phase, ethylene can react to form 1-butene or cyclobutane. Following several reaction steps such as cyclobutane cracking, ethylene addition, and hydrogen transfer, a 2nd initiation phase can occur with more facile free radical generation due to the presence of unsaturated products which can hydrogenate ethylene and form conjugated diradicals.

The thermal reactions of propylene are very different than ethylene, displaying 1st order kinetics with an activation energy of about 125 kJ/mol. The selectivity to non-oligomers is small compared the dimer C₆ product, and many branched C₄ and C₅ products result in contrast to ethylene. The C₆ products for both ethylene and propylene reactions, however, are highly distributed among many isomers including skeletal isomers and/or cyclic products. 1-Hexene is converted efficiently to other C₆ isomers in the almost complete absence of methane formation. Decomposition to C₂-C₈ olefins occurs at a rate about 2-3 orders of magnitude slower than isomerization. The formation of C₃H₆ from C₂H₄, which occurs at very low conversion, does not occur by cracking of 1-hexene, but instead as the result of a complex family of initiation and propagation steps of reactive radical polyethylene chains.

2.6 References

- (1) Bell, A. T.; Alger, M. M.; Flytzani-Stephanopoulos, M.; Gunnoe, T. B.; Lercher, J. A.; Stevens, J.; Alper, J.; Tran, C. *The Changing Landscape of Hydrocarbon Feedstocks for Chemical Production: Implications for Catalysis: Proceedings of a Workshop*; 1344369; 2016; p 1344369. <https://doi.org/10.2172/1344369>.
- (2) Nalley, S.; LaRose, A. *Annual Energy Outlook 2021*; Press Release; Washington, D.C., 2021.
- (3) Ridha, T.; Li, Y.; Gençer, E.; Siirola, J.; Miller, J.; Ribeiro, F.; Agrawal, R. Valorization of Shale Gas Condensate to Liquid Hydrocarbons through Catalytic Dehydrogenation and Oligomerization. *Processes* **2018**, 6 (9), 139. <https://doi.org/10.3390/pr6090139>.

- (4) Nicholas, C. P. Applications of Light Olefin Oligomerization to the Production of Fuels and Chemicals. *Applied Catalysis A: General* **2017**, *543*, 82–97. <https://doi.org/10.1016/j.apcata.2017.06.011>.
- (5) Ghashghaee, M. Heterogeneous Catalysts for Gas-Phase Conversion of Ethylene to Higher Olefins. *Reviews in Chemical Engineering* **2018**, *34* (5), 595–655. <https://doi.org/10.1515/revce-2017-0003>.
- (6) Sydora, O. L. Selective Ethylene Oligomerization. *Organometallics* **2019**, *38* (5), 997–1010. <https://doi.org/10.1021/acs.organomet.8b00799>.
- (7) Olivier-Bourbigou, H.; Breuil, P. A. R.; Magna, L.; Michel, T.; Espada Pastor, M. F.; Delcroix, D. Nickel Catalyzed Olefin Oligomerization and Dimerization. *Chem. Rev.* **2020**, *120* (15), 7919–7983. <https://doi.org/10.1021/acs.chemrev.0c00076>.
- (8) Mehlberg, R. L.; Pujadó, P. R.; Ward, D. J. Olefin Condensation. In *Handbook of Petroleum Processing*; Treese, S. A., Pujadó, P. R., Jones, D. S. J., Eds.; Springer International Publishing: Cham, 2015; pp 457–478. https://doi.org/10.1007/978-3-319-14529-7_6.
- (9) Schmerling, L.; Ipatieff, V. N. The Mechanism of the Polymerization of Alkenes. In *Advances in Catalysis*; Elsevier, 1950; Vol. 2, pp 21–80. [https://doi.org/10.1016/S0360-0564\(08\)60374-0](https://doi.org/10.1016/S0360-0564(08)60374-0).
- (10) Jones, E. K. Polymerization of Olefins from Cracked Gases. In *Advances in Catalysis*; Elsevier, 1956; Vol. 8, pp 219–238. [https://doi.org/10.1016/S0360-0564\(08\)60541-6](https://doi.org/10.1016/S0360-0564(08)60541-6).
- (11) Oblad, A. G.; Mills, G. A.; Heinemann, H. Polymerization of Olefins (to Liquid Polymers). In *Catalysis*; Reinhold Publishing Corporation, 1958; Vol. 6.
- (12) Pillai, S. M.; Ravindranathan, M.; Sivaram, S. Dimerization of Ethylene and Propylene Catalyzed by Transition-Metal Complexes. *Chem. Rev.* **1986**, *86* (2), 353–399. <https://doi.org/10.1021/cr00072a004>.
- (13) O'Connor, C. T.; Kojima, M. Alkene Oligomerization. *Catalysis Today* **1990**, *6* (3), 329–349. [https://doi.org/10.1016/0920-5861\(90\)85008-C](https://doi.org/10.1016/0920-5861(90)85008-C).
- (14) Skupinska, Jadwiga. Oligomerization of .Alpha.-Olefins to Higher Oligomers. *Chem. Rev.* **1991**, *91* (4), 613–648. <https://doi.org/10.1021/cr00004a007>.
- (15) Al-Jarallah, A. M.; Anabtawi, J. A.; Siddiqui, M. A. B.; Aitani, A. M.; Al-Sa'doun, A. W. Ethylene Dimerization and Oligomerization to Butene-1 and Linear α -Olefins. *Catalysis Today* **1992**, *14* (1), 1–121. [https://doi.org/10.1016/0920-5861\(92\)80128-A](https://doi.org/10.1016/0920-5861(92)80128-A).
- (16) Sanati, M.; Hörnell, C.; Järäs, S. G. The Oligomerization of Alkenes by Heterogeneous Catalysts. In *Catalysis*; Spivey, J. J., Ed.; Royal Society of Chemistry: Cambridge, 2007; Vol. 14, pp 236–288. <https://doi.org/10.1039/9781847553263-00236>.
- (17) Forestière, A.; Olivier-Bourbigou, H.; Saussine, L. Oligomerization of Monoolefins by Homogeneous Catalysts. *Oil & Gas Science and Technology - Rev. IFP* **2009**, *64* (6), 649–667. <https://doi.org/10.2516/ogst/2009027>.
- (18) McGuinness, D. S. Olefin Oligomerization via Metallacycles: Dimerization, Trimerization, Tetramerization, and Beyond. *Chem. Rev.* **2011**, *111* (3), 2321–2341. <https://doi.org/10.1021/cr100217q>.
- (19) Antunes, B. M.; Rodrigues, A. E.; Lin, Z.; Portugal, I.; Silva, C. M. Alkenes Oligomerization with Resin Catalysts. *Fuel Processing Technology* **2015**, *138*, 86–99. <https://doi.org/10.1016/j.fuproc.2015.04.031>.
- (20) Ziegler, K. Aluminium-organische Synthese im Bereich olefinischer Kohlenwasserstoffe. *Angew. Chem.* **1952**, *64* (12), 323–329. <https://doi.org/10.1002/ange.19520641202>.

- (21) Ziegler, K. Neuartig katalytische Umwandlungen von Olefinen. *Brennst. Chem.* **1952**, *33* (11), 193–224.
- (22) Bauer, R. S.; Chung, H.; Glockner, P. W.; Keim, W.; van Zwet, H. Ethylene Polymerization. 3635937, January 18, 1972.
- (23) Peuckert, M.; Keim, W. A New Nickel Complex for the Oligomerization of Ethylene. *Organometallics* **1983**, *2* (5), 594–597. <https://doi.org/10.1021/om00077a004>.
- (24) Lutz, E. F. Shell Higher Olefins Process. *J. Chem. Educ.* **1986**, *63* (3), 202. <https://doi.org/10.1021/ed063p202>.
- (25) Shiraki, Y.; Kawano, S.; Takeuchi, K. Process For Preparing Linear A-Olefins. 4783573, November 8, 1988.
- (26) Andrews, J.; Bonnifay, P. The IFP Dimersol Process for Dimerization of Propylene into Isohexenes. In *ACS Symposium Series*; AMERICAN CHEMICAL SOCIETY, 1977; pp 328–340.
- (27) Al-Sherehy, F. A. IFP-SABIC Process for the Selective Ethylene Dimerization to Butene-1. In *Studies in Surface Science and Catalysis*; Elsevier, 1996; Vol. 100, pp 515–523. [https://doi.org/10.1016/S0167-2991\(96\)80052-8](https://doi.org/10.1016/S0167-2991(96)80052-8).
- (28) McGuinness, D. S.; Wasserscheid, P.; Keim, W.; Hu, C.; Englert, U.; Dixon, J. T.; Grove, C. Novel Cr-PNP Complexes as Catalysts for the Trimerisation of Ethylene. *Chem. Commun.* **2003**, No. 3, 334–335. <https://doi.org/10.1039/b210878j>.
- (29) Speiser, F.; Braunstein, P.; Saussine, L. Catalytic Ethylene Dimerization and Oligomerization: Recent Developments with Nickel Complexes Containing P, N-Chelating Ligands. *Acc. Chem. Res.* **2005**, *38* (10), 784–793. <https://doi.org/10.1021/ar050040d>.
- (30) Freitas, E. R.; Gum, C. R. CEP SHOP Process 1979.Pdf. *Chemical Engineering Progress*. 1979, pp 73–76.
- (31) Hogan, J. P.; Banks, R. L.; Lanning, W. C.; Clark, A. Polymerization of Light Olefins over Nickel Oxide–Silica–Alumina. *Ind. Eng. Chem.* **1955**, *47* (4), 752–757. <https://doi.org/10.1021/ie50544a032>.
- (32) Finiels, A.; Fajula, F.; Hulea, V. Nickel-Based Solid Catalysts for Ethylene Oligomerization – a Review. *Catal. Sci. Technol.* **2014**, *4* (8), 2412–2426. <https://doi.org/10.1039/C4CY00305E>.
- (33) Ipatieff, V. N. Catalytic Polymerization of Gaseous Olefins by Liquid Phosphoric Acid I. Propylene. *Ind. Eng. Chem.* **1935**, *27* (9), 1067–1069. <https://doi.org/10.1021/ie50309a024>.
- (34) Ipatieff, V. N.; Corson, B. B. Gasoline from Ethylene by Catalytic Polymerization. *Ind. Eng. Chem.* **1936**, *28* (7), 860–863. <https://doi.org/10.1021/ie50319a027>.
- (35) Ipatieff, V. N.; Pines, H. Polymerization of Ethylene Under High Pressures in the Presence of Phosphoric Acid. *Ind. Eng. Chem.* **1935**, *27* (11), 1364–1369. <https://doi.org/10.1021/ie50311a032>.
- (36) Ipatieff, V. N.; Pines, H. Propylene Polymerization: Under High Pressure and Temperature with and without Phosphoric Acid. *Ind. Eng. Chem.* **1936**, *28* (6), 684–686. <https://doi.org/10.1021/ie50318a018>.
- (37) Ipatieff, V. N.; Corson, B. B. II. Butylenes. *Ind. Eng. Chem.* **1935**, *27* (9), 1069–1071. <https://doi.org/10.1021/ie50309a025>.
- (38) Norton, C. J. Olefin Polymerization over Synthetic Molecular Sieves. *Ind. Eng. Chem. Proc. Des. Dev.* **1964**, *3* (3), 230–236. <https://doi.org/10.1021/i260011a009>.

- (39) *Intrazeolite Chemistry*; Stucky, G. D., Dwyer, F. G., Eds.; ACS Symposium Series; AMERICAN CHEMICAL SOCIETY: WASHINGTON, D.C., 1983; Vol. 218. <https://doi.org/10.1021/bk-1983-0218>.
- (40) Chen, N. Y.; Yan, T. Y. M2 Forming - a Process for Aromatization of Light Hydrocarbons. *Ind. Eng. Chem. Proc. Des. Dev.* **1986**, *25* (1), 151–155. <https://doi.org/10.1021/i200032a023>.
- (41) Tabak, S. A.; Krambeck, F. J.; Garwood, W. E. Conversion of Propylene and Butylene over ZSM-5 Catalyst. *AIChE J.* **1986**, *32* (9), 1526–1531. <https://doi.org/10.1002/aic.690320913>.
- (42) Quann, R. J.; Green, L. A.; Tabak, S. A.; Krambeck, F. J. Chemistry of Olefin Oligomerization over ZSM-5 Catalyst. *Ind. Eng. Chem. Res.* **1988**, *27* (4), 565–570. <https://doi.org/10.1021/ie00076a006>.
- (43) Chang, C. D. The New Zealand Gas-to-Gasoline Plant: An Engineering Tour de Force. *Catalysis Today* **1992**, *13* (1), 103–111. [https://doi.org/10.1016/0920-5861\(92\)80190-X](https://doi.org/10.1016/0920-5861(92)80190-X).
- (44) Lukyanov, D. B.; Gnep, N. S.; Guisnet, M. R. Kinetic Modeling of Ethene and Propene Aromatization over HZSM-5 and GaHZSM-5. *Ind. Eng. Chem. Res.* **1994**, *33* (2), 223–234. <https://doi.org/10.1021/ie00026a008>.
- (45) Dzikh, I. P.; Lopes, J. M.; Lemos, F.; Ramôa Ribeiro, F. Transformation of Light Alkenes over Templated and Non-Templated ZSM-5 Zeolites. *Applied Catalysis A: General* **1999**, *177* (2), 245–255. [https://doi.org/10.1016/S0926-860X\(98\)00272-5](https://doi.org/10.1016/S0926-860X(98)00272-5).
- (46) Amin, N. A. S.; Anggoro, D. D. Dealuminated ZSM-5 Zeolite Catalyst for Ethylene Oligomerization to Liquid Fuels. **2002**, *11* (1), 8.
- (47) Garwood, W. E. Conversion of C2-C10 Olefins to Higher Olefins over Synthetic Zeolite ZSM-5. In *Symposium on Advances in Zeolite Chemistry*; American Chemical Society: Las Vegas, NV, 1982; pp 563–575.
- (48) Egloff, G. POLYMER GASOLINE. *INDUSTRIAL AND ENGINEERING CHEMISTRY* **1936**, *28* (12), 7.
- (49) Egloff, G.; Wilson, E. Thermal Reactions of Gaseous Hydrocarbons. *Ind. Eng. Chem.* **1935**, *27* (8), 917–933. <https://doi.org/10.1021/ie50308a017>.
- (50) Dunstan, A. E. Fluid Fuels To-Day and to-Morrow. Second Jubilee Memorial Lecture. *J. Soc. Chem. Ind.* **1932**, *51* (41), 822–842. <https://doi.org/10.1002/jctb.5000514102>.
- (51) Dunstan, A. E.; Hague, E. N.; Wheeler, R. V. The Heat Treatment of Hydrocarbons with Special Reference to the Gaseous Hydrocarbons. Part II. *J. Soc. Chem. Ind.* **1932**, *51* (18), 131T-140T. <https://doi.org/10.1002/jctb.5000511807>.
- (52) Dunstan, A. E.; Hague, E. N.; Wheeler, R. V. Symposium on Hydrocarbon Decomposition Thermal Treatment of Gaseous Hydrocarbons I. Laboratory Scale Operation. *Ind. Eng. Chem.* **1934**, *26* (3), 307–314. <https://doi.org/10.1021/ie50291a019>.
- (53) Frolich, P. K.; Wiezevich, P. J. Symposium on the Chemistry of Gaseous Hydrocarbons Cracking and Polymerization of Low Molecular Weight Hydrocarbons. *Ind. Eng. Chem.* **1935**, *27* (9), 1055–1062. <https://doi.org/10.1021/ie50309a022>.
- (54) Tropsch, H.; Parrish, C. I.; Egloff, G. High-Temperature Pyrolysis of Gaseous Olefins. *Ind. Eng. Chem.* **1936**, *28* (5), 581–586. <https://doi.org/10.1021/ie50317a019>.
- (55) Sullivan, F. W.; Ruthruff, R. F.; Kuentzel, W. E. Pyrolysis and Polymerization of Gaseous Paraffins and Olefins. *Ind. Eng. Chem.* **1935**, *27* (9), 1072–1077. <https://doi.org/10.1021/ie50309a026>.

- (56) Wagner, C. R. Production of Gasoline by Polymerization of Olefins. *Ind. Eng. Chem.* **1935**, 27 (8), 933–936. <https://doi.org/10.1021/ie50308a018>.
- (57) Maschwitz, P. A.; Henderson, L. M. Polymerization of Hydrocarbon Gases to Motor Fuels. *PROGRESS IN PETROLEUM TECHNOLOGY* **1951**, 5. <https://doi.org/10.1021/ba-1951-0005>.
- (58) Asinger, F. THE WORKING UP OF LOWER, NORMALLY GASEOUS PARAFFINS AND MONO-OLEFINS TO GIVE CARBURETTOR FUELS. In *Mono-Olefins*; Elsevier, 1968; pp 414–505. <https://doi.org/10.1016/B978-0-08-011547-4.50008-2>.
- (59) Bondt; Deiman; van Troostwyk; Lauwerenburg. Sur trois espèces différentes de Gaz hydragène carboné, retirées de l'éther et de l'alcool par différents procédés. *Ann. Chim. Phys.* **1797**, 21, 48–71.
- (60) Extract of a Memoir Concerning Three Different Species of Carbonated Hydrogenous Gas, Obtained from Ether and Alcohol by Different Processes. *J. Nat. Phil.* **1797**, 1, 44–55.
- (61) Fourcroy; Hecht; Vauquelin. Versuche der Gesellschaft Amsterdammer Physiker über drei verschiedene Arten von kohlenhaltigem Wasserstoffgas, welche sich aus Alkohol und Aether entwickeln lassen. *Ann. Phys.* **1799**, 2 (2), 201–215. <https://doi.org/10.1002/andp.17990020207>.
- (62) Henry, W.; Dalton, J. XXVI. Experiments on Ammonia, and an Account of a New Method of Analyzing It, by Combustion with Oxygen and Other Gases; in a Letter to Humphry Davy, Esq. Sec. R. S. &c. from William Henry, M.D., F. R. S. V. P. of the Lit and Phil Society, and Physician to the Infirmary, at Manchester. *Phil. Trans. R. Soc.* **1809**, 99, 430–449. <https://doi.org/10.1098/rstl.1809.0028>.
- (63) Marchand. *J. fur. prakt. Chem.* **1839**, 26, 478.
- (64) Berthelot, M. Theorie des corps pyrogenes. *Bull. Soc. Chim.* **1865**, 6, 280–288.
- (65) Day, D. T. On the Changes Effected by Heat in the Constitution of Ethylene. *Am. Chem. J.* **1886**, 8 (3), 153–167.
- (66) Norton, L. M.; Noyes, A. A. On the Action of Heat upon Ethylene. *Am. Chem. J.* **1886**, 8 (1), 362–364.
- (67) Noyes, A. A. On the Action of Heat on Isobutylene. *Mass. Inst. Tech. Quarterly* **1888**, 1, 278–281.
- (68) Lewes, V. B. II. The Action of Heat upon Ethylene. *Proc. R. Soc. Lond.* **1894**, 55 (331–335), 90–107. <https://doi.org/10.1098/rspl.1894.0017>.
- (69) Bone, W. A.; Coward, H. F. CXVII.—The Thermal Decomposition of Hydrocarbons. Part I. [Methane, Ethane, Ethylene, and Acetylene.]. *J. Chem. Soc., Trans.* **1908**, 93 (0), 1197–1225. <https://doi.org/10.1039/CT9089301197>.
- (70) Malisoff, W.; Egloff, G. Ethylene. *J. Phys. Chem.* **1919**, 23 (2), 65–138. <https://doi.org/10.1021/j150191a001>.
- (71) Ipatieff, V. N. Каталитическая реакция при высоких давлениях и температурах влияние давления на ход катализа. *Zh. Russ. Fiz. Khim.* **1906**, 63–75.
- (72) Ipatieff, V. N. Polymerisation der Äthylen-Kohlenwasserstoffe bei hohen Temperaturen und Drucken. *Ber. Dtsch. Chem. Ges.* **1911**, 44 (3), 2978–2987. <https://doi.org/10.1002/cber.191104403146>.
- (73) Fawcett, E. W.; Gibson, R. O.; Perrin, M. W. POLYMERIZATION OF OLEFINS. 2,153,553, April 11, 1939.
- (74) Laird, R. K.; Morrell, A. G.; Seed, L. The Velocity of Ethylene Polymerization at High Pressures. *Discuss. Faraday Soc.* **1956**, 22, 126. <https://doi.org/10.1039/df9562200126>.

- (75) Woodbrey, J. C.; Ehrlich, Paul. The Free Radical, High Pressure Polymerization of Ethylene. II. The Evidence for Side Reactions from Polymer Structure and Number Average Molecular Weights. *J. Am. Chem. Soc.* **1963**, *85* (11), 1580–1584. <https://doi.org/10.1021/ja00894a008>.
- (76) Buback, M. The High Pressure Polymerization of Pure Ethylene. *Makromol. Chem.* **1980**, *181* (2), 373–382. <https://doi.org/10.1002/macp.1980.021810208>.
- (77) Buback, M. Spectroscopic Investigation of the High Pressure Ethylene Polymerization. *Zeitschrift für Naturforschung A* **1984**, *39* (4), 399–411. <https://doi.org/10.1515/zna-1984-0417>.
- (78) Scelta, D.; Ceppatelli, M.; Bini, R. Pressure Induced Polymerization of Fluid Ethylene. *The Journal of Chemical Physics* **2016**, *145* (16), 164504. <https://doi.org/10.1063/1.4966154>.
- (79) Citroni, M.; Ceppatelli, M.; Bini, R.; Schettino, V. High-Pressure Reactivity of Propene. *The Journal of Chemical Physics* **2005**, *123* (19), 194510. <https://doi.org/10.1063/1.2109947>.
- (80) Szwarc, M. The Kinetics of the Thermal Decomposition of Propylene. *The Journal of Chemical Physics* **1949**, *17* (3), 284–291. <https://doi.org/10.1063/1.1747240>.
- (81) Ingold, K. U.; Stubbs, F. J. 382. The Kinetics of the Thermal Decomposition of Olefins. Part I. Propylene. *J. Chem. Soc.* **1951**, 1749. <https://doi.org/10.1039/jr9510001749>.
- (82) Molera, M. J.; Stubbs, F. J. 75. The Kinetics of the Thermal Decomposition of Olefins. Part II. *J. Chem. Soc.* **1952**, 381. <https://doi.org/10.1039/jr9520000381>.
- (83) Silcocks, C. G. The Kinetics of the Thermal Decomposition and Polymerization of Ethane and Ethylene. *Proc. R. Soc. Lond. A* **1956**, *233* (1195), 465–479. <https://doi.org/10.1098/rspa.1956.0004>.
- (84) Dahlgren, G.; Douglas, J. E. Kinetics of the Thermal Reactions of Ethylene. *J. Am. Chem. Soc.* **1958**, *80* (19), 5108–5110. <https://doi.org/10.1021/ja01552a028>.
- (85) Laidler, K. J.; Wojciechowski, B. W. Kinetics of the Thermal Decomposition of Propylene, and of Propylene-Inhibited Hydrocarbon Decompositions. *Proc. R. Soc. Lond. A* **1960**, *259* (1297), 257–266. <https://doi.org/10.1098/rspa.1960.0222>.
- (86) Skinner, G. B.; Sokoloski, E. M. SHOCK TUBE EXPERIMENTS ON THE PYROLYSIS OF ETHYLENE. *J. Phys. Chem.* **1960**, *64* (8), 1028–1031. <https://doi.org/10.1021/j100837a015>.
- (87) Taniewski, M. Investigations on the Thermal Decomposition of Olefins. *Proc. R. Soc. Lond. A* **1962**, *265* (1323), 519–537. <https://doi.org/10.1098/rspa.1962.0040>.
- (88) Amano, A.; Uchiyama, M. Mechanism of the Pyrolysis of Propylene: The Formation of Allene. *J. Phys. Chem.* **1964**, *68* (5), 1133–1137. <https://doi.org/10.1021/j100787a028>.
- (89) Benson, S. W.; Haugen, G. R. Mechanisms for Some High-Temperature Gas-Phase Reactions of Ethylene, Acetylene, and Butadiene. *J. Phys. Chem.* **1967**, *71* (6), 1735–1746. <https://doi.org/10.1021/j100865a029>.
- (90) Kallend, A. S.; Purnell, J. H.; Shurlock, B. C. The Pyrolysis of Propylene. *Proc. R. Soc. Lond. A* **1967**, *300* (1460), 120–139. <https://doi.org/10.1098/rspa.1967.0161>.
- (91) Boyd, M. L.; Wu, T.-M.; Back, M. H. Kinetics of the Thermal Reactions of Ethylene. Part I. *Can. J. Chem.* **1968**, *46* (14), 2415–2426. <https://doi.org/10.1139/v68-394>.
- (92) Boyd, M. L.; Back, M. H. Kinetics of the Thermal Reactions of Ethylene. Part II. Ethylene–Ethane Mixtures. *Can. J. Chem.* **1968**, *46* (14), 2427–2433. <https://doi.org/10.1139/v68-395>.

- (93) Halstead, M. P.; Quinn, C. P. Pyrolysis of Ethylene. *Trans. Faraday Soc.* **1968**, *64*, 103. <https://doi.org/10.1039/tf9686400103>.
- (94) Kunugi, T.; Sakai, T.; Soma, K.; Sasaki, Y. Kinetics and Mechanism of Thermal Reaction of Ethylene. *Ind. Eng. Chem. Fund.* **1969**, *8* (3), 374–383. <https://doi.org/10.1021/i160031a002>.
- (95) Kunugi, T.; Sakai, T.; Soma, K.; Sasaki, Y. Thermal Reaction of Propylene. Kinetics. *Ind. Eng. Chem. Fund.* **1970**, *9* (3), 314–318. <https://doi.org/10.1021/i160035a002>.
- (96) Simon, M.; Back, M. H. Kinetics of the Thermal Reactions of Ethylene. *Can. J. Chem.* **1969**, *47* (2), 251–255. <https://doi.org/10.1139/v69-035>.
- (97) Back, M. H. Mechanism of the Bimolecular Reactions of Ethylene and Propylene. *Int. J. Chem. Kinet.* **1970**, *2* (5), 409–418. <https://doi.org/10.1002/kin.550020506>.
- (98) Simon, M.; Back, M. H. Kinetics of the Pyrolysis of Propylene. Part I. *Can. J. Chem.* **1970**, *48* (2), 317–325. <https://doi.org/10.1139/v70-048>.
- (99) Simon, M.; Back, M. H. Kinetics of the Pyrolysis of Propylene. Part II. *Can. J. Chem.* **1970**, *48* (21), 3313–3319. <https://doi.org/10.1139/v70-558>.
- (100) Back, M. H.; Martin, R. The Thermal Reactions of Ethylene at 500°C in the Presence and Absence of Small Quantities of Oxygen: THERMAL REACTIONS OF ETHYLENE. *Int. J. Chem. Kinet.* **1979**, *11* (7), 757–774. <https://doi.org/10.1002/kin.550110708>.
- (101) Ayranci, G.; Back, M. H. Kinetics of the Bimolecular Initiation Process in the Thermal Reactions of Ethylene. *Int. J. Chem. Kinet.* **1981**, *13* (9), 897–911. <https://doi.org/10.1002/kin.550130913>.
- (102) Ayranci, Güler. Kinetics of the Bimolecular Initiation Process in the Thermal Reactions of Ethylene., University of Ottawa, 1982.
- (103) Quick, L. M.; Knecht, D. A.; Back, M. H. Kinetics of the Formation of Cyclobutane from Ethylene. *Int. J. Chem. Kinet.* **1972**, *4* (1), 61–68. <https://doi.org/10.1002/kin.550040105>.
- (104) Pease, R. N. KINETICS OF THE POLYMERIZATION OF ETHYLENE AT PRESSURES ABOVE ONE ATMOSPHERE. *J. Am. Chem. Soc.* **1931**, *53* (2), 613–619. <https://doi.org/10.1021/ja01353a025>.
- (105) Storch, H. H. Kinetics of Ethylene Polymerization. *J. Am. Chem. Soc.* **1934**, *56* (2), 374–378. <https://doi.org/10.1021/ja01317a029>.
- (106) Storch, H. H. Kinetics of Ethylene Polymerization. II. *J. Am. Chem. Soc.* **1935**, *57* (12), 2598–2601. <https://doi.org/10.1021/ja01315a082>.
- (107) Pease, R. N. THE NON-CATALYTIC POLYMERIZATION AND HYDROGENATION OF ETHYLENE. *J. Am. Chem. Soc.* **1930**, *52* (3), 1158–1164. <https://doi.org/10.1021/ja01366a052>.
- (108) Douglas, J. E.; Rabinovitch, B. S.; Looney, F. S. Kinetics of the Thermal *Cis-Trans* Isomerization of Dideuteroethylene. *The Journal of Chemical Physics* **1955**, *23* (2), 315–323. <https://doi.org/10.1063/1.1741959>.
- (109) Hurd, C. D. Pyrolysis of Unsaturated Hydrocarbons. *Ind. Eng. Chem.* **1934**, *26* (1), 50–55. <https://doi.org/10.1021/ie50289a012>.
- (110) Yaws, C. L. Yaws' Critical Property Data for Chemical Engineers and Chemists.
- (111) Beckwith, A. L. J.; Ingold, K. U. Free-Radical Rearrangements. In *Organic Chemistry: A Series of Monographs*; Elsevier, 1980; Vol. 42, pp 161–310. <https://doi.org/10.1016/B978-0-12-481301-4.50010-3>.
- (112) Rofer-DePoorter, C. K. A Comprehensive Mechanism for the Fischer-Tropsch Synthesis. *Chem. Rev.* **1981**, *81* (5), 447–474. <https://doi.org/10.1021/cr00045a002>.

- (113) Loudon, G. Marc. *Organic Chemistry*, 5th ed.; Roberts and Co.: Greenwood Village, Colo, 2009.
- (114) Quinn, C. P. Isomerization of Primary N-Alkyl Radicals in the Pyrolysis of Ethane. *Trans. Faraday Soc.* **1963**, *59*, 2543. <https://doi.org/10.1039/tf9635902543>.
- (115) Viskolcz, B.; Lendvay, G.; Körtvélyesi, T.; Seres, L. Intramolecular H Atom Transfer Reactions in Alkyl Radicals and the Ring Strain Energy in the Transition Structure. *J. Am. Chem. Soc.* **1996**, *118* (12), 3006–3009. <https://doi.org/10.1021/ja951393i>.
- (116) Viskolcz, B.; Lendvay, G.; Seres, L. Ab Initio Barrier Heights and Branching Ratios of Isomerization Reactions of a Branched Alkyl Radical. *J. Phys. Chem. A* **1997**, *101* (38), 7119–7127. <https://doi.org/10.1021/jp970717h>.
- (117) Tsang, W.; Walker, J. A.; Manion, J. A. The Decomposition of Normal Hexyl Radicals. *Proceedings of the Combustion Institute* **2007**, *31* (1), 141–148. <https://doi.org/10.1016/j.proci.2006.07.069>.
- (118) Cheng, J.; Gao, Y.; Li, X.; You, X.; Zou, C. Reaction Kinetics of Hydrogen Shift Isomerization of 1-Hexyl Radicals. *Fuel* **2020**, *278*, 118221. <https://doi.org/10.1016/j.fuel.2020.118221>.
- (119) Roedel, M. J. The Molecular Structure of Polyethylene. I. Chain Branching in Polyethylene during Polymerization ¹. *J. Am. Chem. Soc.* **1953**, *75* (24), 6110–6112. <https://doi.org/10.1021/ja01120a005>.
- (120) Bryant, W. M. D.; Voter, R. C. The Molecular Structure of Polyethylene. II. Determination of Short Chain Branching ¹. *J. Am. Chem. Soc.* **1953**, *75* (24), 6113–6118. <https://doi.org/10.1021/ja01120a006>.
- (121) Elias, H.-G. Free-Radical Polymerization. In *Macromolecules*; Wiley-VCH Verlag GmbH: D-69451 Weinheim, Germany, 2014; pp 309–367. <https://doi.org/10.1002/9783527627219.ch10>.
- (122) Yamada, B.; Zetterlund, P. B. General Chemistry of Radical Polymerization. In *Handbook of Radical Polymerization*; Matyjaszewski, K., Davis, T. P., Eds.; John Wiley & Sons, Inc.: Hoboken, NJ, USA, 2002; pp 117–186. <https://doi.org/10.1002/0471220450.ch3>.

3. HIGH TEMPERATURE CONVERSION OF ETHYLENE TO LIQUID HYDROCARBONS USING γ -ALUMINA

3.1 Introduction

Oligomerization of ethylene and propylene is an important upgrading reaction, such as in the valorization of the ethane and propane in shale gas into motor fuels or the production of sustainable aviation fuels from bio-alcohol.¹⁻³ There are three broad classes of olefin oligomerization, deriving from the type of reactive intermediate formed: carbanion-like species (organometallic or supported metal catalysts),⁴⁻¹⁴ carbenium ions (acid catalysts),¹³⁻²¹ and free radicals (thermally induced).^{15,22-32} The first two have been studied extensively over the past half-century, whereas the latter, which was discovered first, has been given little consideration since the 1950's.

Carbanionic-like, alkyl chains are ubiquitous to metal-based oligomerization catalysts. These catalysts convert ethylene either into select oligomers (dimers, trimers, etc.) or non-selective (Schultz-Flory or Poisson) product distributions using a cationic form of one of the following: nickel,³³⁻³⁷ titanium,³⁸ chromium,^{39,40} aluminum,^{10,41} and zirconium,⁴² among several other less commonly used metals.⁴ These oligomers are central to the specialty chemicals industry but require additional transformations to become usable fuels. Furthermore, homogeneous processes require activators, co-catalysts, and separators, spurring interest in heterogeneous transition-metal catalysts as more efficient alternatives. These catalysts have not been commercialized, however, due to the comparatively lower productivity and/or catalyst deactivation.

Carbenium ion oligomerization is a common refinery operation to make motor fuels from cracked light olefins. The acidic catalysts can be liquid (e.g. H_3PO_4 , H_2SO_4 , HF) or solid phase (e.g. solid phosphoric acid (SPA), zeolites, resins). Since the liquid acids are corrosive and more hazardous, solid acid catalytic systems such as SPA and zeolites are preferred. Moreover, solid acid catalytic systems circumvent the need for expensive separations, but are hindered by deactivation due to coking, site loss, and pore blockage, requiring frequent regeneration.

The thermally induced free-radical conversion of light olefins to liquids was the first refinery oligomerization process^{26-28,43} yet did not experience widespread implementation due to the harsh temperatures required and relatively low octane rating compared to SPA.⁴⁴ The detailed products and kinetic behaviors were recently delineated for the gas phase, thermal radical reactions of ethylene, revealing that the C_4 and C_5 isomers by thermal oligomerization were mostly linear,

terminal olefins. The thermal reactions of ethylene are attractive to study further since very little coking occurs in an empty reactor even at 450 °C and the reaction pathway gives rise to non-oligomer (odd carbons) distributions under all conditions. In contrast to the metal-alkyl and carbenium ion pathways, which require catalysts, there is no precedent for catalyzing a free radical reaction using a solid material. Thus, if the reaction pathway could be controlled to some extent, then the productivity and/or product distribution might be greatly enhanced.

In this study, we hypothesized that high surface area supports might exert influence on the thermal reactions of ethylene, accelerating rates and/or altering the product distributions. The basis for this hypothesis stemmed from two hallmarks of traditional heterogeneous catalysis: (1) the adsorption properties of supports, resulting in higher surface concentrations than in the gas phase, and (2) the ability to form reactive surface intermediates. To test this hypothesis, an experimental approach was structured to answer the following two questions:

1. *Does filling the reactor volume with a high-surface area support affect ethylene conversion rates?* What are the apparent kinetics for ethylene thermal reactions in the presence of a support? Is the rate proportional only to surface area, or does the support composition matter too?
2. *Are the product distributions affected by the presence of a high-surface area support?* Are non-oligomer products such as propylene produced analogously to the gas phase, thermal reaction? Are the C₄, C₅, and C₆ products mostly linear or does branching occur as well?

To probe the effect of adding high-surface area supports, γ -Al₂O₃ and amorphous SiO₂ were initially screened by packing the entire thermal volume and reacting with ethylene. These solids both adsorb hydrocarbons⁴⁵⁻⁴⁷ but embody varying levels of known catalytic activity.^{48,49} Silica is comprised of weakly acidic silanol (Si-OH) surface sites, which are generally regarded as inert.

In contrast to silica, alumina has been the subject of numerous catalytic studies,⁵⁴⁻⁷⁰ many of which suggest that pure alumina does not have Brønsted acidity but does contain multiple types of strong and weak Lewis acid sites.⁷⁰⁻⁷³ Commercial processes using acidified aluminas almost exclusively rely on the addition of chloride or fluoride ions, which confer Brønsted acidity.⁷⁴⁻⁷⁷ Pure aluminas are generally less active but have been demonstrated to catalyze the following hydrocarbon reactions involving olefins or paraffins: alcohol dehydration,^{55,56,78,79} propane dehydrogenation,^{69,70} ethylene hydrogenation,^{60,61,64,80} olefin double bond and cis/trans isomerization,^{58,59,63,65,66} and H₂-D₂ exchange of olefins and paraffins.⁸⁰⁻⁸⁴ In chemisorption experiments, infrared spectroscopy has provided evidence that ethylene forms chemically bonded

intermediates at room temperature with alumina.⁸⁵ Silica, on the other hand, did not chemisorb ethylene.⁸⁶ Clearly, these two supports, while having similarly high surface areas, possess varying catalytic properties.

For both supports, C₂H₄ conversion rates were measured from 300 to 400 °C at 1.5 bar and 43 bar, from which comparisons can be made of the product distributions and apparent kinetics relative to the empty tube reaction. Since Al₂O₃ was found to be clearly the most active, detailed product distributions were measured to evaluate the effects of conversion, temperature, and pressure. In addition, propylene and 1-hexene were also reacted with Al₂O₃ to understand more about the product selectivity and possible secondary reaction pathways.

3.2 Experimental Methods

3.2.1 Materials

Alumina (Al₂O₃). High-purity Catalox Sba 200 γ -alumina was obtained from Sasol, having a reported average pore size of 4 -10 nm, surface area of 200 m²/g, and pore volume of 0.35-0.5 cm³/g. This alumina was in powder form with an average size of 45 microns.

Silica (SiO₂). High-purity grade (> 99%) amorphous silica (Davisil 636) was purchased from Sigma-Aldrich, having an average pore diameter of 6.0 nm, surface area of 480 m²/g, and pore volume of 0.75 cm³/g. The particle size distribution was 200-500 microns (35-60 mesh).

3.2.2 Atmospheric Pressure Olefin Oligomerization

A quartz tube (10.5 mm ID, 1.1 mm thickness) approximately 14” in total length was loaded into a clamshell furnace with insulation enclosing a 5-inch-long heated reaction zone. A thermal-well placed down the axial length of the tube allowed the temperature profile to be measured at 1” intervals. A length-averaged temperature was then calculated for each temperature setpoint. The reactor was then heated to the desired setpoint and ethylene flow rate. For each data point, the product gas flow rate was verified using a bubble film flowmeter. Ultra-high purity ethylene or propylene was purchased from Indiana Oxygen and used in all experiments.

Products were analyzed using a Hewlett Packard 6890 Series Gas Chromatograph with an Agilent HP-AL/S column (25 m in length, 0.32 mm ID, and 8 μ m film thickness) and flame ionization detector. To detect higher molecular weight products up to C₈, the reactor discharge lines were traced with heat tape and set

to 150 °C during the experiments. The conversion and product distribution were calculated on a molar basis, assuming a closed carbon balance since no significant carbon deposition was observed over the course of experiments.

3.2.3 High Pressure Ethylene Oligomerization

To understand the product distributions and rates at higher olefin concentrations and conversions, ethylene was tested at pressures up to 43.0 bar. A 316 stainless steel tube (3/8" ID, 1/8" thickness) 2 feet in length, with VCR fittings at the inlet and outlet to seal the system was used. The reactor setup was in a ventilated fume hood as a safety precaution, and a pressure relief valve rated for 650 psi was installed at the top of the reactor. The insulation allowed a thermal reaction zone of about 16.5" which corresponded to a volume of ca. 30 cm³. A thermal-well placed down the length of the tube allowed the temperature profile to be measured at 2" intervals. A length-averaged temperature was then calculated for each temperature setpoint. The reactor was first pressurized to check for leaks and then the reactor was heated to the desired setpoint temperature in flowing N₂ and allowed to stabilize for 4 hr to purge oxygen from the system. Pure C₂H₄ was then flowed through the reactor. Ultra-high purity ethylene, purchased from Indiana Oxygen, was used in all experiments.

Products were analyzed using a Hewlett Packard 7890 Series Gas Chromatograph with an Agilent HP-1 column (25 m in length, 0.32 mm ID, and 8 μm film thickness) and flame ionization detector. To detect higher molecular weight products up to C₁₀, the reactor discharge lines were traced with heat tape and set to 175 °C during the experiment. The conversion and product distribution were calculated on a molar basis, except at high conversions ($X > 20\%$), in which the mass selectivity was more convenient to calculate due to the condensation of considerable amounts of liquid products, which were collected in a glass vial maintained in an ice bath. Comparison of the liquid production rate and unreacted ethylene in the gas effluent to the feed mass flow rate enabled an estimation of the conversion. For lower conversions ($X < 20\%$), the product did not condense significantly. Additionally, little carbon deposition was observed over several days of testing, thus, a 100% carbon balance was assumed in the calculations.

3.2.4 Thermal Reactions of 1-Hexene at Atmospheric Pressure

1-Hexene (> 99 %) was purchased from Sigma-Aldrich and N₂ was used as a carrier gas. Approximately 5-10 mL of 1-hexene were loaded into a roughly 100 mL stainless steel vessel, installed via Swagelok fittings, between the N₂ mass flow controller and the reactor. The vessel was housed in an ice bath to control the 1-hexene vapor concentration. The reactor system was purged for 3 hours with 100 sccm N₂ after sealing to purge any dissolved O₂ in the 1-hexene storage vessel. The reactor effluent was fed into a gas

chromatography unit equipped with a flame ionization detector. Molar selectivity of non-C₆ products were reported in addition to the conversion of 1-hexene. Before the furnace was turned on, the 1-hexene was fed into the reactor at room temperature to verify no reaction due to contaminants, as well as to obtain a baseline of the 1-hexene purity.

3.3 Results

3.3.1 Ethylene Reaction Rates and Products with High-Surface Area Supports

The ethylene conversion rates were measured from 300 to 400 °C at conversions below 5 %. In each case, a higher ethylene conversion rate was observed by packing the reactor with high surface area support, evidenced at ca. 43 bar, shown in Table 3. Since the densities of the supports were different, each had a different weight loading. Furthermore, the thermal background conversion was subtracted from the rates of the supports. At 340 °C and 43 bar, the gas phase conversion was 0.082 % at a gas-hourly space velocity (GHSV) of 8.0 hr⁻¹, whereas with Al₂O₃, the conversion was 5.0 % at a GHSV of 81 hr⁻¹. With SiO₂, a GHSV of 5.4 hr⁻¹ resulted in 0.32 % ethylene conversion. Thus, the conversion rate was about 600 times higher in the presence of Al₂O₃ and only 2.6 times higher in the presence of SiO₂. The supports were also compared to each other by normalizing with the surface area (see Table B.1). The SiO₂ had the larger surface area per gram (480 m²/g) compared to Al₂O₃ (200 m²/g). However, the Al₂O₃ was about 270 times more reactive than SiO₂ per m² available. Therefore, the available surface area alone does not control the rate of ethylene conversion on these two high surface area materials.

Table 3. Comparison of Ethylene Conversion Rates at 340 °C and 42.0 – 43.5 bar C₂H₄

		GHSV (hr ⁻¹)	Conversion (%)	Rate per Surface Area vs SiO ₂	Rate per Volume vs Thermal
Thermal, Phase	Gas	8.0	0.082	-	1
SiO₂		5.4	0.32	1	2.6
Al₂O₃		81	5.0	270	620

Estimates for the reaction order were made from the rate measurements at 1.5 and 43 bar. At 340 °C, the orders for SiO₂ and Al₂O₃ were 1.4 and 1.1, respectively, compared to the gas phase order of 1.9 (Table B.2). The observed Arrhenius relationship revealed a lower apparent activation energy for each support compared to the empty reactor, which is about 244 kJ/mol at both 1.5 and

43.5 bar (Figure 19). At 1.5 bar, the apparent activation energies for SiO₂ and Al₂O₃ were 89 and 55 kJ/mol, respectively. At 43 bar, these values for SiO₂ and Al₂O₃ were 176 and 76, respectively. Thus, SiO₂ showed a 100 % higher activation energy at 43 bar, whereas the Al₂O₃ was 35 % higher. Clearly, the composition of the support plays a significant role in determining the overall rates and kinetics.

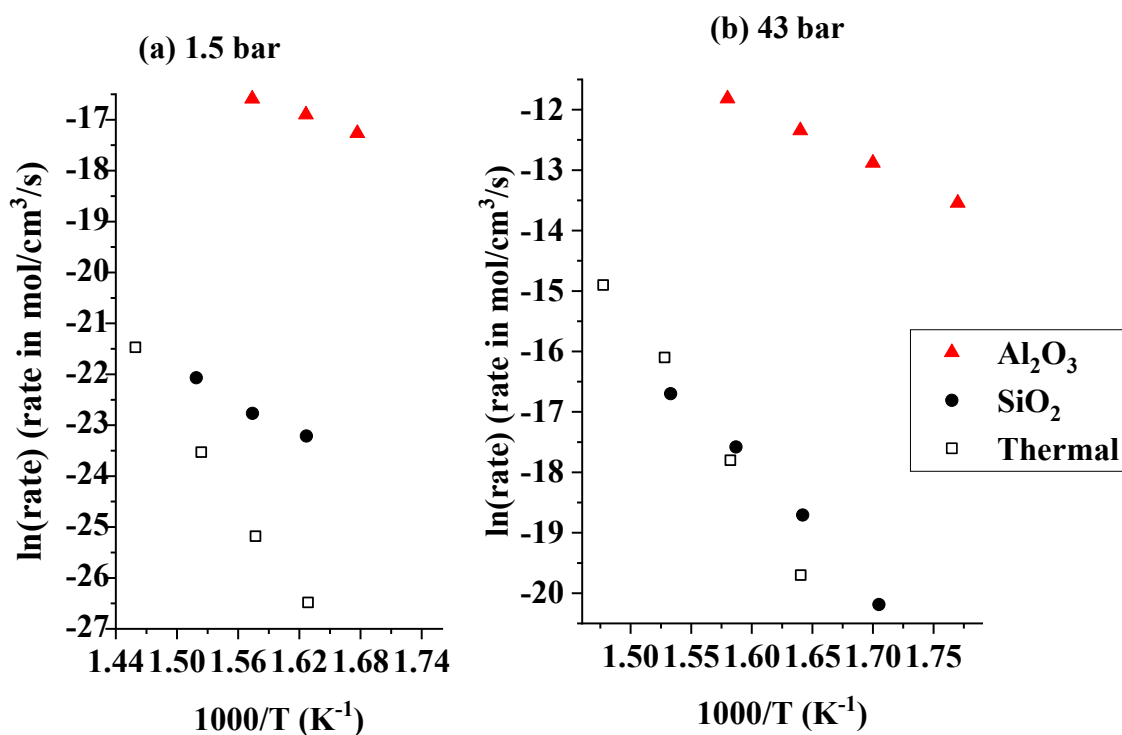


Figure 19. Kinetics of C₂H₄ reactions with different high surface area supports. Arrhenius plot from 300 to 410 °C at (a) 1.5 bar and (b) 42 - 43.5 bar C₂H₄. The thermal reactions of C₂H₄ from 300 to 410 °C are shown in open squares.

The products for ethylene conversion in the presence of SiO₂ and Al₂O₃ were also compared to the gas phase reaction at high pressure, and the two displayed unique behaviors. SiO₂ was reacted with ethylene at 360 °C and 43 bar, giving a conversion of 0.96 %. For comparison, thermally the conversion was 0.58 %. The carbon number distributions, shown in Figure 20, are very similar for SiO₂ and the gas phase reaction, with one noticeable difference, the selectivity to C₄ products were about twice as high with SiO₂. Given that the relative rate of ethylene reaction with SiO₂ is only about twice the thermal rate, the data suggest that the presence of SiO₂ gives rise to more C₄ products. The C₄ linear isomer distributions in Figure 18-b show that double bond isomerization occurs with SiO₂ compared to gas phase reaction, which produces about 80 % 1-

butene. With SiO₂, 1-butene is 44 % of C₄, with the remainder being mostly trans- and cis-2-butene. The amount of n-butane is very small (ca. 1 %) in both cases. Furthermore, there was no evidence of increased branched products such as isobutane or isobutene compared.

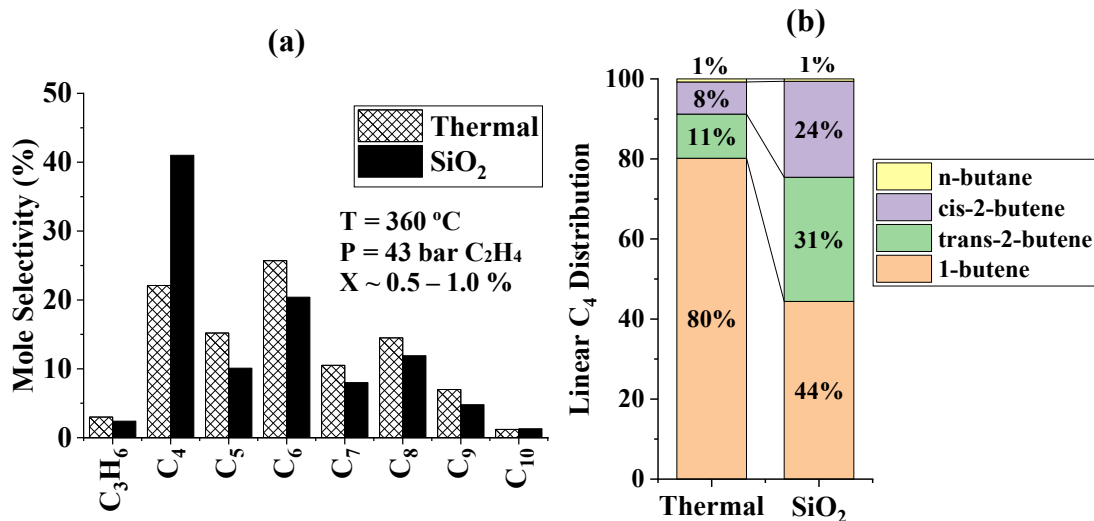


Figure 20. Products of ethylene conversion in the presence of SiO₂ compared to the thermal reaction at 360 °C, 43.0-43.5 bar. The conversions thermally and with SiO₂ were 0.58 and 0.96 %, respectively. (a) The products based on carbon number distribution.

Alumina gave rise to a unique product distribution. The products were compared to the thermal reaction at 385 °C and 27.5 bar around 15 % conversion. Since the rate with Al₂O₃ was much higher relative to SiO₂ compared to the thermal rate, the conversions at high pressure with a fully packed reactor of Al₂O₃ were too high to compare. Thus, in one experiment, only about 10 % of the reactor was filled (3 g of Al₂O₃). The thermal reaction rate was verified to be less than 10 % of the rate with 3 g of Al₂O₃, and the small thermal background conversion was subtracted from the products reported in Figure 21. Despite subtracting the thermal background, the carbon number distributions share many features, such as little methane production (< 2 %) and the presence of many non-oligomer products, resulting in analogous apparent single-carbon growth patterns. For example, the most abundant products with Al₂O₃ at these conditions is C₄ followed by propylene (35 and 25 %, respectively). The remaining higher MW products (C₅₊) decrease in order of increasing carbon number. The same is true for the thermal reaction, except that there is less propylene and more C₅ to C₉ products. Thermally, C₄ was the most abundant carbon number group (nearly 32 %) while propylene was just 11 %.

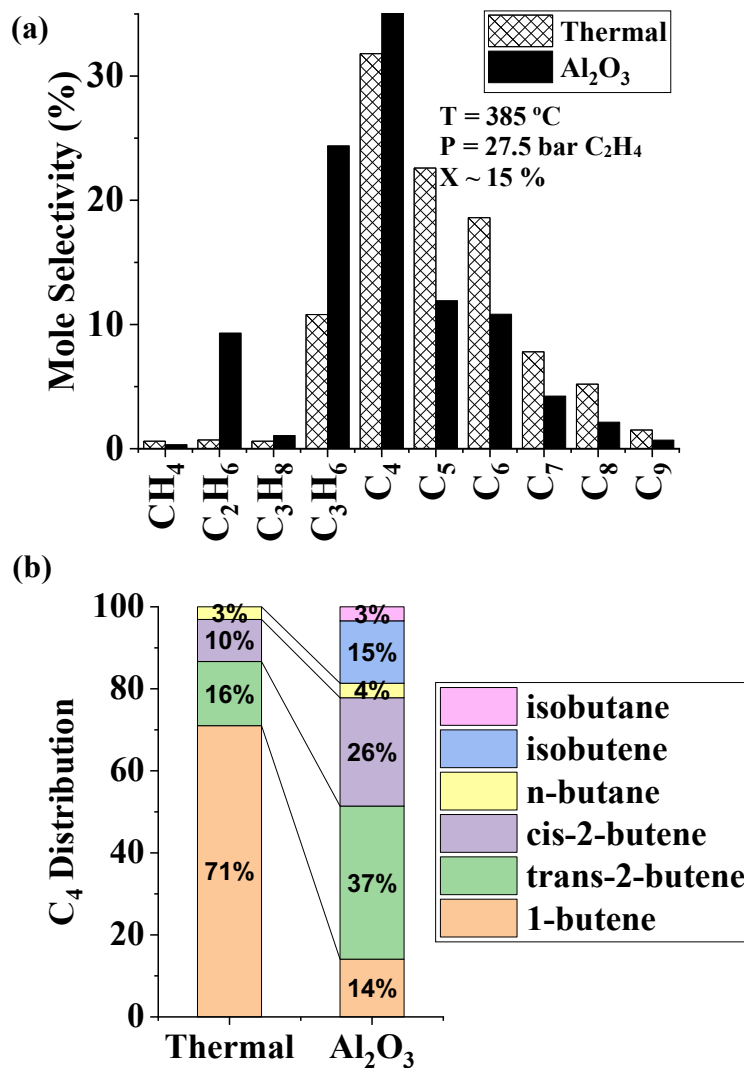


Figure 21. Products of ethylene conversion in the presence of alumina compared to the thermal reaction at 385 °C, 27.5 bar. The conversions thermally and with alumina were 11.9 and 16.9 %, respectively. (a) The products based on carbon number distribution

The two major differences observed here between Al_2O_3 and the gas phase reaction are the production of ethane and the C_4 distribution. With Al_2O_3 , there is about 9 % selectivity to ethane, whereas in the thermal reaction ethane is less than 1 % of the products. The C_4 distribution, shown in Figure 3-b, features the introduction of branched C_4 products, which were not observed thermally. Isobutene and isobutane were collectively 18 % of the C_4 , and 1-butene was only 14 %

of C₄. The remaining C₄ were 2-butenes (63 %). The gas phase reaction produced 1-butene with 71 % selectivity among C₄ isomers.

In summary, the comparative study of SiO₂ and Al₂O₃ demonstrated varying levels of ethylene rates compared to the thermal reaction, as well as product alterations. Al₂O₃ provided the best yield to desired products C₃₊ and introduced branched C₄ products. Therefore, Al₂O₃ was studied over a wider range of conditions to determine the effects of temperature, pressure, and conversion on the products with ethylene. Additionally, to gain further insights into the reactions of olefins with Al₂O₃, propylene and 1-hexene were reacted over Al₂O₃.

3.3.2 Product Distribution at High Ethylene Conversion with Al₂O₃

At 360 °C and 23 bar, by varying the space velocity, ethylene conversions from 1 to 70 % were obtained. At the same conditions, the purely thermal reaction was not significant. The higher activity with alumina is consistent with the measured kinetic rates at lower conversions since, as mentioned earlier, comparing the rates with alumina at high temperature and pressure resulted in about two orders of magnitude higher rate than thermally. The molecular-weight distributions as a function of conversion in Figure 22 demonstrate the high selectivity to C₅₊ products. During this experiment, a light-yellow liquid product was condensed into an in-line vial submerged in an ice bath. The weight-hourly space velocity (WHSV) required to obtain 70 % conversion was 0.1 hr⁻¹. Nonetheless, the high conversion remained stable for at least 24 hours. Approximately 1 cm³ of liquid hydrocarbons were condensed per hour during the 24 hour duration of the trial. At the end of the experiment, the Al₂O₃ in the center of the packed bed displayed a yellow-orange color, but was not black, suggesting coking was not significant at this temperature. In our previous study of the thermal reactions of ethylene, conversions near 70 % required temperatures greater than 450 °C, and the resulting carbon number distribution produced more light olefins such as propylene and 1-butene, and less C₅₊.

Figure 22 illustrates several noteworthy observations about the reaction pathway, with the major products being C₅₊, C₄, propylene, and ethane. Methane was less than about 1 % selective at each conversion. The ethane selectivity decreased steadily with increasing conversion, starting as high as 15 % at 2 % conversion, but becoming only about 5 % at 70 % conversion. Conversely, the C₅₊ production increased over the same conversion range from about 40 to 80 % of the products. The propylene and C₄ selectivity profiles appear to increase in the early stages of the reaction

(below 20 % conversion), however decrease steadily after reaching maximum selectivity values, signifying their importance in secondary reactions leading to C₅₊ liquids.

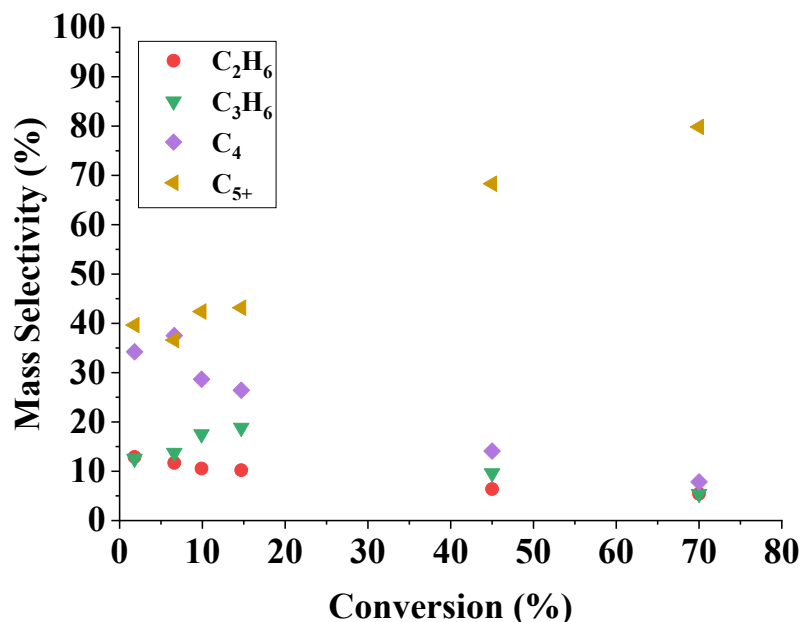


Figure 22. Products with Al₂O₃ at 23 bar C₂H₄, 360 °C, from 1-70 % conversion

As was seen earlier in Figure 21, the comparison of the product distribution with the gas phase reaction at similar conversion shared some product behavior, namely the presence of non-oligomer products. Since secondary reactions become important at higher conversions, i.e. above 1 %, an experiment was conducted to compare the reaction with alumina compared to the gas phase at the early stage of the reaction ($X < 1$ %).

3.3.3 Comparison of Products with Al₂O₃ vs the Thermal Reaction at Low Pressure and Conversion

Figure 23 shows that at 0.1 % conversion at 400 °C and 1.5 bar there is a completely different molecular-weight distribution due to Al₂O₃, despite also sharing several similarities with the gas phase reaction. To compare Al₂O₃ to the thermal reaction at 0.1 % conversion, 0.25 g of Al₂O₃ were loaded. The thermal conversion at the same flow rate was at least 50 times lower so that the products observed were only due to Al₂O₃. In a separate experiment, employing a much lower flow rate, 0.1 % conversion was achieved thermally for comparison. With Al₂O₃, the major

products were 60 % C₄ followed by 15 % C₃H₆ and 10 % ethane, in stark contrast to the gas phase which produces about 65 % propylene, 20 % C₄, and little ethane. Both the thermal reaction and Al₂O₃ produce less than 1.5 % methane at this temperature. Along with propylene, non-oligomer products such as C₅ and C₇ were present in comparable amounts to oligomers such as C₆ and C₈.

The C₄ isomer distribution further highlights the influence Al₂O₃ has on the reaction. The C₄ products were 68 % 2-butenes and only 25 % 1-butene, whereas for the gas phase reaction 1-butene was about 69 %. While the amount of isobutene produced is small (4 %), it is nonetheless relatively more than produced without Al₂O₃ (< 0.1 %). Butadiene is also produced to a small extent in both cases (near 2 %). No butane was observed with Al₂O₃, although about 3 % selectivity was seen thermally. The distribution of C₅ products with Al₂O₃ forms much less 1-pentene compared to double bond and skeletal isomers. With Al₂O₃, 1-pentene was 7 % of C₅, whereas isopentenes and 2-pentenes were 61 and 33 %, respectively. In contrast, without Al₂O₃, the C₅ were 42 % 1-pentene, 31 % isopentenes, and 25 % 2-pentenes. N-pentane was also only observed thermally, around 3 % of C₅.

3.3.4 MW and Isomer Distributions versus Conversion

The products were next studied to identify the effects of increasing conversion below 20 %, with an emphasis on tracking changes in the molecular-weight and isomer distributions. At 1.5 bar and 360 °C the conversion was varied from 2.7 to 15.6 %. The molecular weight distribution, in Figure 24-a, demonstrated several clear trends. Importantly, C₄ decreased from about 35 to 25 % whereas C₅ increased from 7 to 13 % and C₆ from 3 to 7 %. The propylene selectivity increased from 31 to about 40 %. The ethane selectivity decreased from 14 to 8 %. However, the propane selectivity increased from < 0.5 to 2 %.

The C₄ to C₆ isomer behavior offer several notable observations. The C₄ distribution, which is mostly 2-butenes (50-70 %), demonstrated a notable increase in branched isomers, with isobutene and isobutane increasing from 15 % to 24 % combined of C₄. Additionally, the ratio of isobutene to isobutane decreased from > 50 at 2.7 % conversion to 2.1 at 15.6 % due to increasing isobutane production. The C₅ isomers reveal similar trends to the C₄ isomers when the conversion increased from 2.7 to 15.6 %. The branched C₅, isopentane and isopentenes, together increased from 64 to 73 % of C₅. Meanwhile, the isopentenes to isopentane ratio decreased from > 50 to 4.5 due to increasing isopentane formation. The C₆ isomers are illustrated by the raw GC data in Figure B.7.

Clearly, there are at least 20 isomers present, which implies that many skeletal isomers must be present. Less than about 5 % of the C₆ is 1-hexene, which is comparable to the C₄ and C₅ isomer trends.

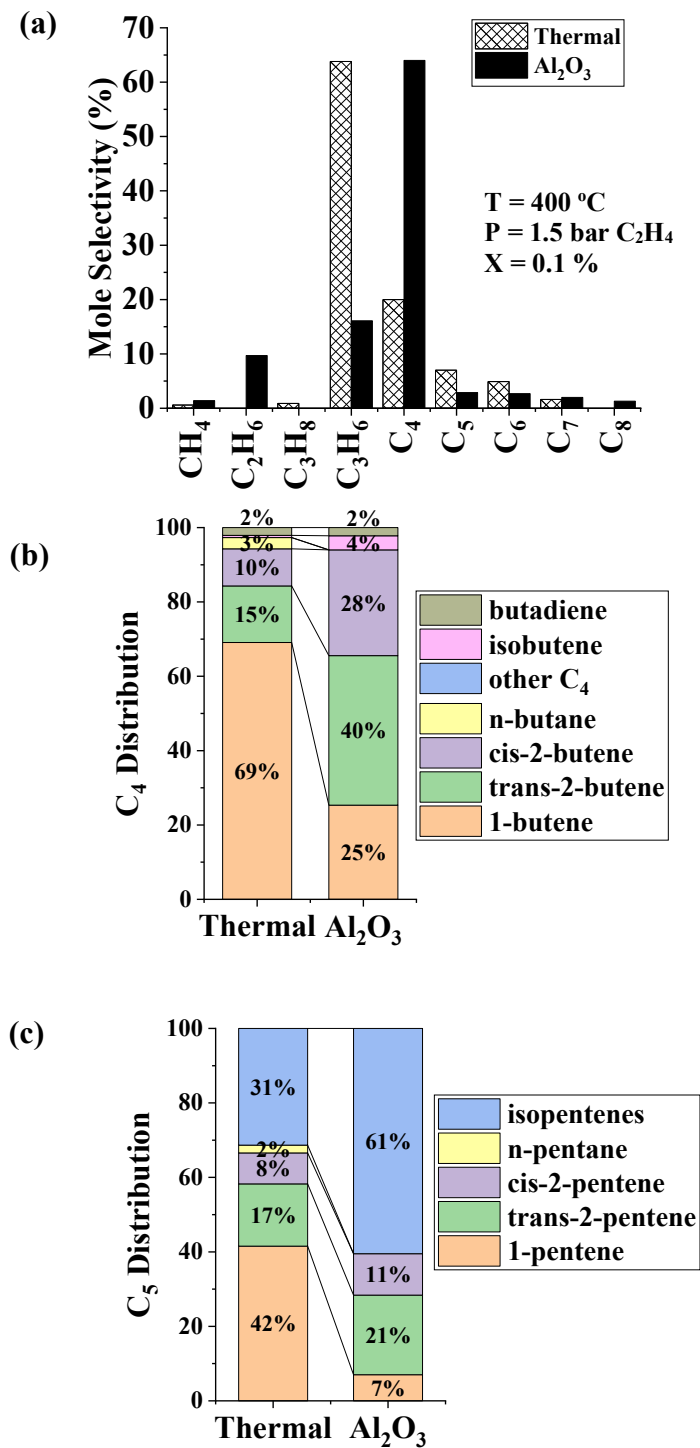


Figure 23. Products with Al₂O₃ vs the thermal reaction at 1.5 bar C₂H₄, 400 °C, and 0.1 % conversion. (a) Carbon number distribution, (b) C₄ distribution, (c) C₅ distribution.

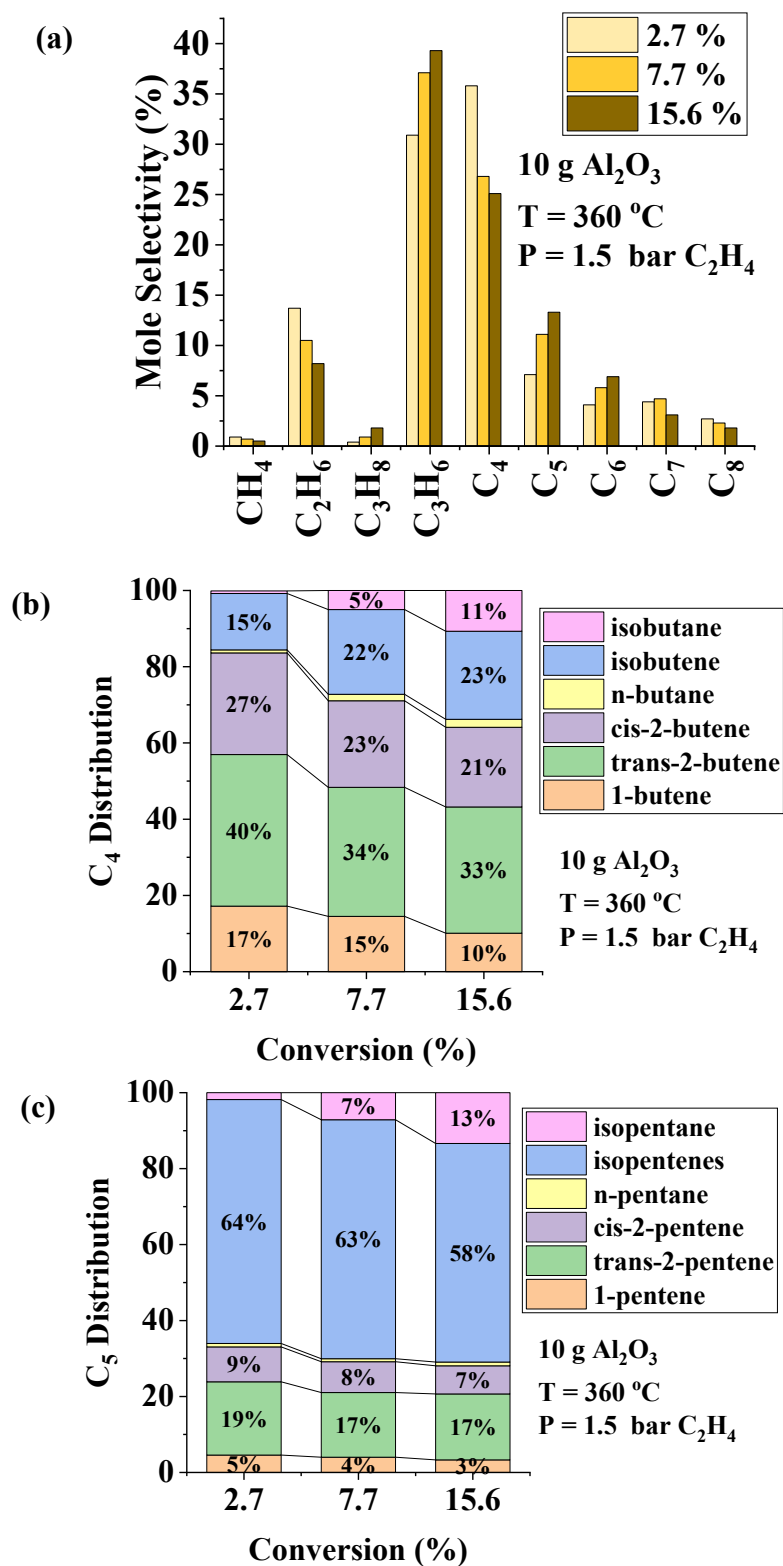


Figure 24. Products with Al_2O_3 versus conversion below 20 % at 1.5 bar C_2H_4 , 360 °C. (a) Carbon number distribution, (b) C_4 distribution, (c) C_5 distribution.

3.3.5 Selectivity versus Temperature

The reactions of ethylene with Al_2O_3 reveal a transition in product behavior above about 400 °C, shifting from higher MW products below 400 °C to decomposition products (methane, ethane, coke) above 400 °C. As seen in Figure B.2, the selectivity to methane increased from less than 1 % at 300 °C to 14 % at 470 °C. Likewise, the ethane selectivity increased from 8 to 47 %. The remaining products are mostly propylene and C_4 with less than 3 % each of C_5 to C_7 . The high selectivity to saturated products were accompanied by blackening of the Al_2O_3 at 470 °C, indicating coke deposition. At 300 °C, the Al_2O_3 remained white during the experiment.

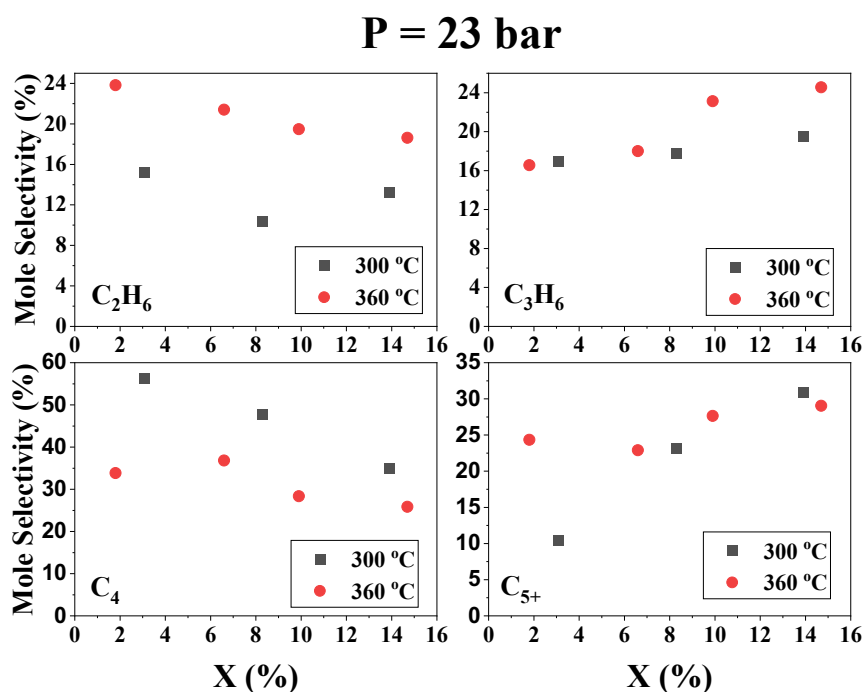


Figure 25. Selectivity of Major Products with Al_2O_3 at 300 vs 360 °C at 23 bar of C_2H_4 below 20 % conversion.

For temperatures below 400 °C, such as 300 compared to 360 °C at 23 bar, at higher temperature more ethane and less C_4 was formed at each conversion (see Figure 25). The propylene and C_{5+} showed more complex trends. For example, the propylene selectivity appears the same at both temperatures until about 8 % conversion; above 8 % conversion more propylene forms at 360 °C. Likewise, the C_{5+} selectivity is nearly the same at both temperatures above 8 % conversion but is clearly higher at 360 °C below 8 % conversion. As seen in Figure 22 above, as conversion increases, secondary reactions become important leading to changes in the product distributions.

Thus, these features as seen in Figure 25 highlight the complicated nature of interpreting product changes at different temperatures due to consecutive reactions in oligomerization chemistry.

Comparison of the MW and isomer distributions between 300 and 360 °C at 1.5 bar and a single conversion (~ 8 %), seen in Figure B.3, reveals similar features of higher ethane selectivity and lower C₄ selectivity at 360 compared to 300 °C. The 60 °C increase also lead to about twice as much isobutene formed (22 vs 11 % of C₄). The branched C₅ only slightly increased from 65 to 70 %; however, the ratio of isopentane to isopentenes decreased from 0.23 to 0.11 upon going from 300 to 360 °C. Thus, there are clear temperature effects on the products, both to the molecular-weight and amount of branched C₄.

3.3.6 Selectivity versus Pressure

The effects of pressure on the products at 1.5 vs. 23 bar at 360 °C below 20 % conversion is depicted by Figure 26. Propylene, C₄, C₅₊, and ethane are the main products. Ethane and propylene show the most straightforward pressure dependences. At 360 °C, the ethane selectivity at 23 bar is slightly less than twice the selectivity at 1.5 bar. On the contrary, about twice as much propylene is produced at 1.5 bar than 23 bar. Both the C₄ and C₅₊ products appear in comparable amounts at both pressures. Analogous to the effects of temperature in Figure 25, the products may show complex selectivity profiles due to the competing consecutive reactions.

Additionally, at 43 bar and about 8 % conversion, most of the same trends are evident, with propylene being 38 % at 1.5 bar but only 12 % at 43 bar (see Figure B.4). The C₄ was 27 % at 1.5 bar but comprised 40 % of the products at 43 bar. Similarly, there were almost twice as many C₆ products at 43 bar. Thus, a striking observation is that at the higher pressures the product distributions apparently embody earlier stages of the reaction where oligomerization is the main reaction (C₄, C₆, C₈, etc), before cracking results in significant non-oligomers. That is, the even carbon oligomers (C₄, C₆, and C₈) are more abundant than C₃, C₅, C₇, and C₉ non-oligomers, as opposed to the single-carbon growth pattern characteristic at higher reaction extents and lower pressures.

When comparing the effects of conversion, temperature, and pressure on the products, it was apparent that secondary reactions play an important role in the product distributions, especially as conversion increased beyond 20 %. Propylene, for example, increased to a maximum selectivity below 20 % conversion in Figure 20, and then steadily decreased up to 70 % conversion. It is

therefore insightful to evaluate the reactions of propylene with Al_2O_3 , to understand the difference in kinetics and product behavior to ethylene.

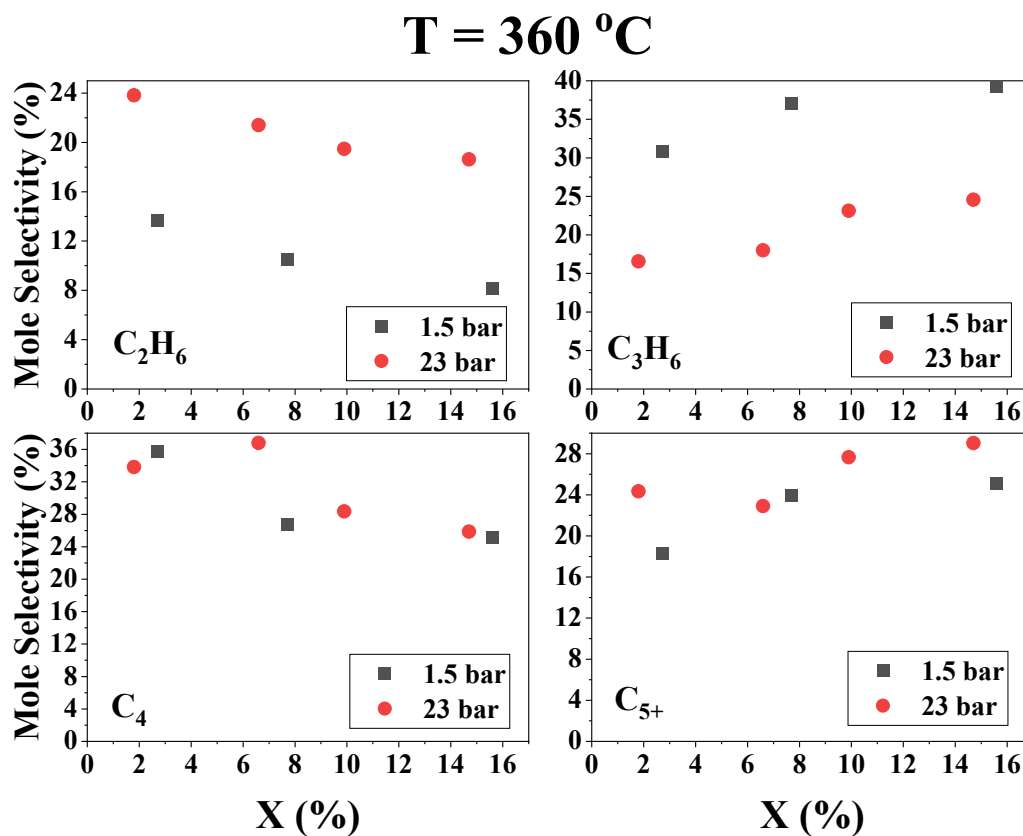


Figure 26. Selectivity of Major Products at 1.5 vs 23 bar of C_2H_4 at 360 °C below 20 % conversion.

3.3.7 Reaction of Propylene with Al_2O_3

The Arrhenius parameters for propylene with Al_2O_3 were measured from 260 to 300 °C at 1.5 bar, shown in Figure 27. Over this temperature range, the apparent activation energy was measured to be 55 kJ/mol, the same value as ethylene. The conversion of C_3H_6 at 300 °C and 1.5 bar was 7.4 % at a GHSV of 61 hr^{-1} . For comparison, at the same conditions, the C_2H_4 conversion was 0.85 % at a GHSV of 20 hr^{-1} . Thus, propylene reacts about an order of magnitude faster than ethylene at 300 °C and 1.5 bar, an important distinction since propylene is one of the main products early in the reaction (below 20 % conversion) and could result in more facile bond activation leading to increased ethylene consumption or higher MW products.

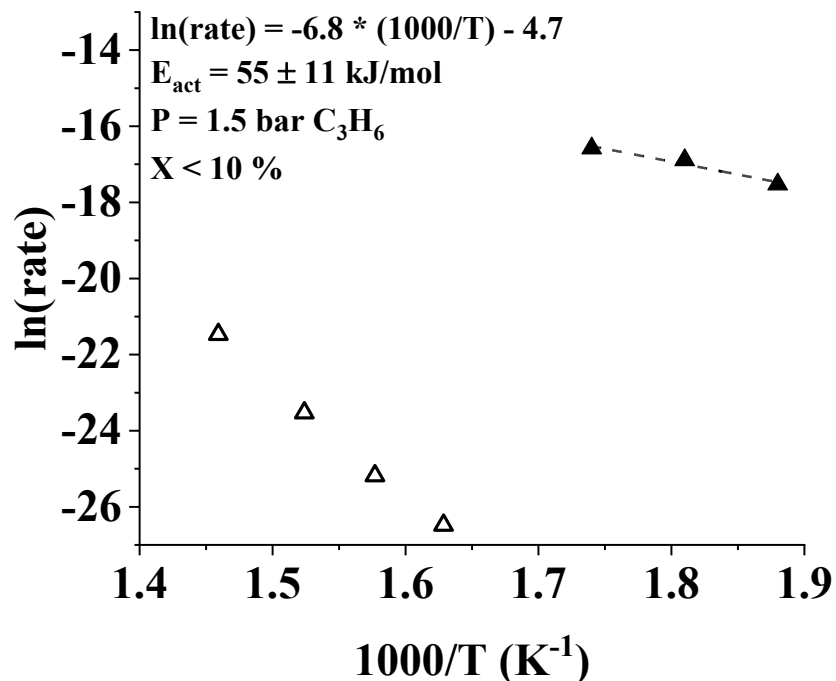


Figure 27. Kinetics of C_3H_6 reactions with Al_2O_3 . Arrhenius plot from 260 to 300 °C of 1.5 bar C_3H_6 . $X < 10 \%$ The thermal reaction of C_3H_6 from 400 to 500 °C are shown in open triangles for comparison.

When pure propylene was reacted over Al_2O_3 from 260 to 300 °C at 1.5 bar, the molecular weight distribution revealed a disproportionation had occurred, with ethylene and isobutene as the major products, forming in a 1:1 molar ratio at low conversion (2.0 % at 260 °C). The product distribution at 2.0 % conversion at 260 °C in Figure 28 shows that ethylene and isobutene are the main products, comprising 27 and 28 % of the products, respectively, followed by C_6 (23 %). Propane was about 4 %, and neither methane nor ethane were detected. Small amounts of n-butenes, C_5 , C_7 , and C_8 products were also formed (< 5 % each). The C_5 isomers, in contrast to the C_4 , were mostly linear. Of the C_5 , only about 10 % were isopentenes, and 81 % were 2-pentenes. The C_6 isomers, shown in Figure B.7, visibly consist of more than 20 distinct isomers. By comparing the GC data for C_3H_6 to C_2H_4 at roughly the same conditions, one can see that the chromatograms for the C_6 isomers are almost superimposable, indicating that the C_6 distributions are nearly identical for both C_2H_4 and C_3H_6 . Next, the effects of reaction temperature and conversion for propylene are illustrated.

The effects of increasing temperature from 260 to 300 °C, shown in Figure B.5, portray several notable shifts. Less ethylene and C_6 and more C_4 are formed at 300 °C compared to at 260 °C. The

C₄ reveal a gradual increase in n-butenes compared to isobutene at higher temperatures. Isobutene decreased from 78 to 73 % of C₄ while n-butenes increased from 16 to 20 % at 300 °C compared to 260 °C. The C₅ experienced a sharper change, with isopentenes increasing from 15 % of C₅ at 260 °C to 31 % at 300 °C.

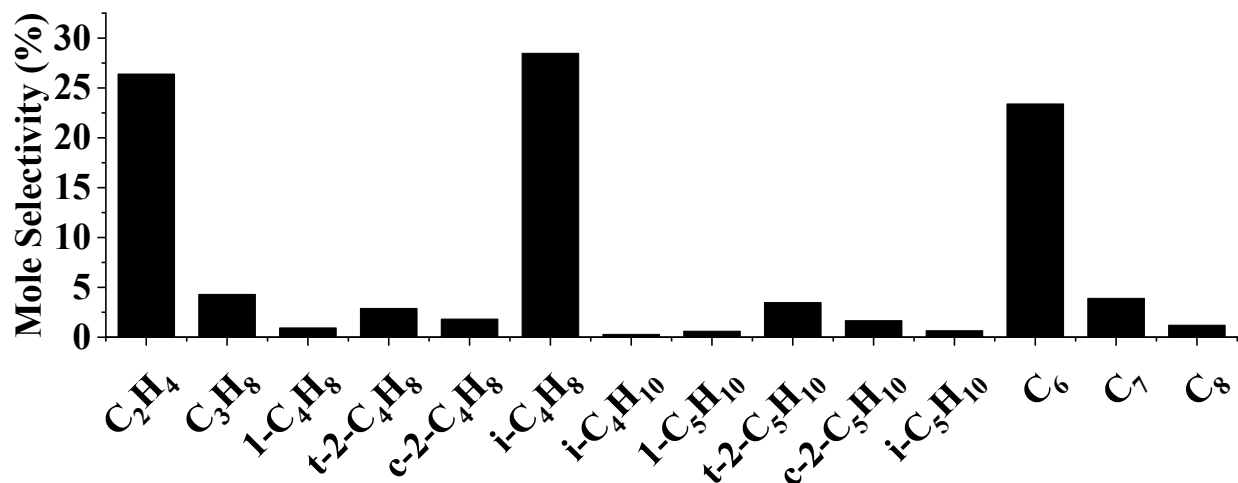


Figure 28. Products of C₃H₆ with Al₂O₃ at 2.0 % conversion 260 °C and 1.5 bar

Increasing the conversion from 7.4 to 25.2 % at 300 °C, depicted in Figure B.6, demonstrated clear shifts in selectivity, with ethylene and C₆ each decreasing from about 20 to 15 mole % while C₄, C₅, and C₇ increased. Ethylene and C₆ both decreased from around 20 to 15 mole %. The net increase in C₄ appears to be largely due to an increase in isobutane and n-butenes as opposed to the major product, isobutene. The isobutene to isobutane ratio decreased with increasing conversion, from 45 to 13. Likewise, the isopentene to isopentane ratio fell from 87 to 22. Both n-butane and n-pentane were less than 0.2 % of their respective carbon groups across the whole range of conversion. The isopentene selectivity increased from 25 % of C₅ at 7.4 % conversion to 36 % at 25.2 % conversion.

3.3.8 Reaction of 1-Hexene with Al₂O₃

When 1-hexene was flowed over Al₂O₃ at 260 °C, more than 90 % of it was converted (see Table 4). When no Al₂O₃ was present, no conversion of 1-hexene occurred at 260 °C. To obtain a comparable conversion in the empty reactor, a temperature of about 420 °C was required. Over 95 % of the products were other C₆ isomers. In fact, the major C₆ isomers formed appear by

alumina at 260 °C coincide almost identically with those in the thermal isomerization at 420 °C (see Figure B.9). The isomerization rate was 22×10^{-9} mol/cm³/s compared to a rate of cracking of 0.6×10^{-9} mol/cm/s, a factor of about 40x. It was of interest to compare the rates of isomerization and cracking at a relevant concentration to 1-hexene in the products of propylene, to determine if cracking of 1-hexene, or its isomerization products, contributes to the non-oligomer products formed. The selectivity to C₆ products at 2.0 % conversion was 23.4 mole %, such that the mole fraction at the reactor outlet was 0.0023, resulting in a partial pressure of about 0.3 kPa of C₆. Therefore, to a first-order approximation, the rate of 1-hexene cracking would be 3.2×10^{-11} mol/cm³/s, which is about 0.1 % of the rate of C₃H₆ conversion to products at the 260 °C and 1.5 bar. Thus, 1-hexene or its isomers do not contribute substantially to the observed non-oligomer products via cracking, for example, conversion of ethylene to propylene or conversion of propylene to ethylene and butenes.

Table 4. 1-C₆H₁₂ Conversion with Al₂O₃ and Thermally

Reactor Loading	Al₂O₃ (11 cm³)	Empty Quartz (11 cm³)	Empty Quartz (25 cm³)
Average Temperature (°C)	260	260	400
Flow of N ₂ feed (sccm)	5	5	20
1-Hexene Pressure (kPa)	5	5	20
Conversion (%)	92.9	Tr	86.0
Yield to C ₆ isomers (carbon %)	90.5		85.1
Number of C ₆ isomer peaks	> 8		> 12
Yield to non-C ₆ isomers (carbon %)	2.4		0.9
Rate of 1-hexene isomerization (mol/cm ³ /s) x 10 ⁹	22		51
Rate of 1-hexene cracking (mol/cm ³ /s) x 10 ⁹	0.6		0.5
Ratio of isomerization to cracking	40x		100x

C₆ isomers were about 97 % of the products on a carbon basis, whereas the cracking products comprised the remaining 3 %. The C₆ isomers are shown in Figure B.8, revealing the presence of 3 major isomers and at least 9 total isomers. The most abundant non-C₆, or cracking, products were propylene and C₄, followed by C₅, C₇, C₂H₄, and C₈ (see Figure 29). Methane and ethane were each less than 1 % of the non-C₆ products. The C₄ isomers were highly linear, with 4 % isobutene,

and the other 96 % mostly 2-butenes. 1-Butene comprised the remainder of C₄ (14 %). The C₅ isomers were also highly linear, with just 16 % selectivity to isopentenes. The n-pentenes, like n-butenes, showed preference for the 2-pentenes (75 %) over 1-pentene (8 %).

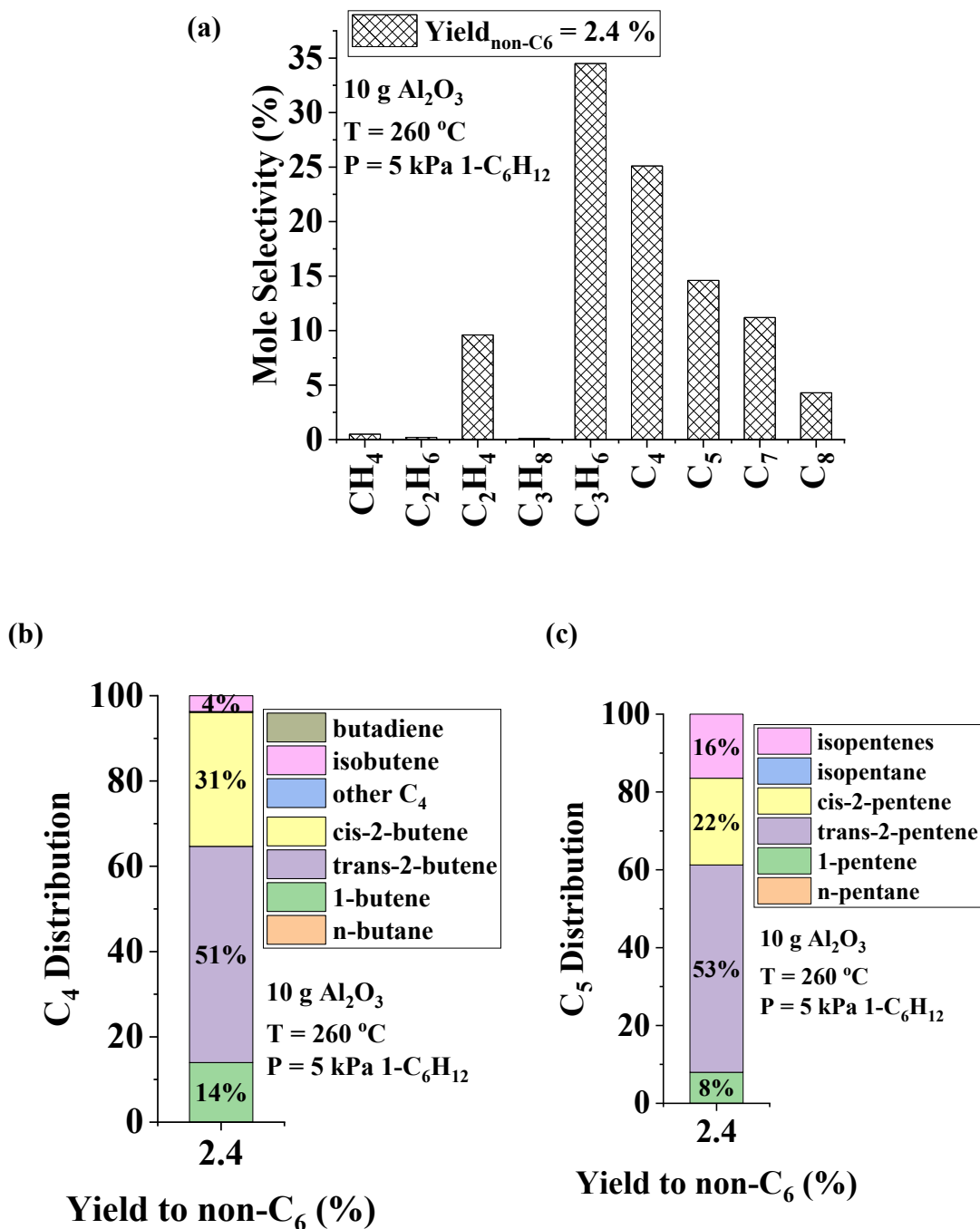


Figure 29. Products with Al₂O₃ with 5 kPa 1-hexene fed at 260 °C

3.4 Discussion

The thermal reactions of several olefins were recently investigated in depth, establishing the detailed product distributions and kinetics from 300 to 500 °C. Ethylene was found to be sensitive to pressure and temperature, with the rates being high above 35 bar and 450 °C. In fact, the reaction order was found to be 2nd. Therefore, in this study it was hypothesized that high surface area supports would increase the rate of the thermal reaction due to the higher effective olefin concentration adsorbed on the surface compared to the gas phase. In conjunction, we hypothesized that the supports might promote bond activation of the olefins, either by physical (e.g. van der Waals) or chemical interactions (e.g. Lewis acidity), conferring additional rate enhancement and/or alteration of the product distributions.

3.4.1 Effect of High Surface Area Supports on Rates, Kinetics, and Products

In this study, ethylene was converted at higher rates when the thermal volume was packed with a high surface area support. Silica and alumina were evaluated, and the results indicate that high surface area alone does not control the rate of ethylene conversion relative to the empty reactor. For example, the alumina was 270 times more active per m² than silica at 340 °C and 43 bar.

The gas phase radical oligomerization reaction consists of initiation, propagation, and termination steps. The overall rate of ethylene consumption is thus a consequence of the relative rates of propagation to initiation/termination. For example, in thermal ethane pyrolysis, the reaction chain length corresponds to roughly 100 propagation steps per initiation and corresponding termination step.⁹⁰ Increasing the rate of initiation or increasing the propagation rate could both give rise to higher overall ethylene conversion in the presence of the supports. Additionally, new initiation mechanisms could also occur due to physical or chemical interactions with the support surface, resulting in more facile bond breakage and/or surface stabilized reactive intermediates. At this point, however, no key initiation reactions or intermediates can be ascribed to the observed rates or changes in product distributions of silica and alumina, as rigorous energetic and kinetic modeling are needed to elucidate the complex reaction system.

Secondly, the sensitivity of the rate with respect to temperature and pressure were different for each support. Each had apparent activation energies and reaction orders less than the observed values for the gas phase reaction, which were 244 kJ/mol and 2nd order, respectively. At 1.5 bar

alumina had the lower activation energy (55 kJ/mol) but the higher rate. Silica, with the lower rate, had the higher activation energy (89 kJ/mol). At 43 bar, the alumina and silica demonstrated larger activation energies of 76 and 176 kJ/mol, respectively. These relative shifts in rate behavior coincide with different apparent reaction orders for silica (1.4) and alumina (1.1). The observed kinetic behaviors are accompanied by distinguished product distributions for each support, which can be correlated to the known surface chemistry for each (vide infra).

Silica

Silica gave rise to a similar product distribution to the empty reactor below 1 % conversion at 43 bar, aside from producing more 2-butenes. As mentioned above, the activation energy of 176 kJ/mol at 43 bar and reaction order of 1.4 are the closest to the values for the empty reactor of all the supports tested. Thus, an important connection is that the kinetics and products under the influence of silica are most like the gas phase reaction, suggesting that silica participates to a lesser extent than alumina.

Still, a rate enhancement of even 1 order of magnitude is significant (as in Figure 20-a), since packing the reactor with silica effectively removes much of the reactor volume which would otherwise host the gas phase reaction. This is not the case in ethane cracking, for example. Ethane thermal cracking was found previously to be more productive in empty reactors than with supports or even bimetallic Pt catalysts. This contrary behavior for ethylene versus ethane suggests that the support enhances the initiation and/or propagation reaction steps relative to the termination reaction steps, however the influence becomes less impactful at 43 bar compared to 1.5 bar. The lack of major product alterations is consistent with the absence of strong Brønsted acid sites on amorphous silica, which does not catalyze alkane dehydrogenation or cracking, for example.

Alumina

The kinetics observed using alumina were distinct from silica. The apparent reaction order (1.1) was lower than silica (1.4), and the apparent activation energy at 1.5 bar was also lower (55 kJ/mol). Akin to silica, the alumina experienced a moderate increase in activation energy at 43 bar (76 kJ/mol). In other words, the value becomes closer to that of the gas phase reaction at higher pressure, which indicates a shift in relative contributions between the gas phase and surface

reaction. The products with Al₂O₃ behave in some respects like the gas phase reaction, and in some regards like a catalytic, surface reaction, as explained in the next section.

3.4.2 Insights from the Products of C₂H₄ with Al₂O₃ versus Thermally

MW Distribution

Non-oligomers were present under all reaction conditions with Al₂O₃, analogous to the thermal reaction. However, dimerization was visibly favored at low conversion and higher pressure. The preference for dimerization was not observed at higher conversions and lower pressures. Instead, a MW distribution reminiscent of the gas phase thermal oligomerization, with an apparent one-carbon growth pattern, develops as early as 2.7 % conversion at 360 °C and 1.5 bar. The key differences to the purely thermal reaction present themselves in terms of C₄ and C₅ isomer distributions and the extent of hydrogen transfer reactions.

Isomerization of C₄, C₅, and C₆

Branched C₄ and C₅ were identified under all conditions, which were not major products thermally. At low conversions (0.1 %), isobutene was a minor C₄ isomer (about 4 %) but became significant (> 20 %) at higher conversions (> 5 %), suggesting that it forms because of secondary reactions of the primary products. Higher temperature was a factor leading to higher isobutene formation, too, with about twice as much branched C₄ at 360 °C compared to 300 °C at 1.5 bar and ca. 8 % conversion. This outcome is unsurprising since skeletal isomerization requires the cleavage of a C-C bond, which is endothermic, during some step of the reaction. In contrast, oligomerization (C-C forming) reaction steps are exothermic, which are less thermodynamically favored at higher temperatures. The isopentenes were substantial (> 50 % of C₅) at all conditions. In fact, in contrast to isobutene, the isopentenes were the principal C₅ at low conversion too. Accordingly, there were less drastic changes in branched C₅ as a function of conversion or temperature. Lastly, the number of C₆ isomers detected (nearly 20) indicates that C₆ are also highly branched.

It is not immediately obvious how isobutene should form in this system. The skeletal isomerization of linear butenes is believed to occur in Brønsted acid zeolites via sequential oligomerization, isomerization, and cracking reactions. Al₂O₃, though, is known to lack the high cracking activity that Brønsted acid catalysts possess and does not show spectroscopic evidence

of Brønsted acidity. Furthermore, the results of 1-hexene isomerization and cracking over alumina demonstrated a high preference for linear versus branched C₄ and C₅ isomers. Thus, the data do not provide any evidence that oligomer cracking would give rise to isobutene. One other possibility for skeletal isomerization is a unimolecular route involving a methyl shift; still, there are very few reports of Al₂O₃ catalyzing unimolecular skeletal isomerization of olefins.^{68,71} Nonetheless, alumina is known to catalyze double bond and cis/trans isomerization of olefins,^{58,59,63,66} which is consistent with the observation in this study that 1-butene and 1-pentene were minor isomers (< 20 %), unlike in the gas phase reaction.

H-Transfer

Another distinguishing feature of the reactions of ethylene with alumina compared to the gas phase was the production of modest amounts of ethane (ca. 5-20 mole %), which were very low (< 1 mole %) in the absence of alumina. This phenomenon was reported by Hindin et al. previously at low ethylene pressures in the absence of significant oligomerization, which was coined “self-hydrogenation” and ascribed to highly strained Lewis acid sites formed by dehydration of the surface.⁶⁰

As conversion increased and isobutene/isopentenes accumulated in the system, isobutane and isopentane became increasingly important, suggesting that the iso-olefins were converted to iso-paraffins as the reaction progressed. These shifts, along with increases in propane selectivity, happened concurrently with a decreasing selectivity to ethane. A reasonable explanation is that the sites responsible for hydrogenating ethylene into ethane also hydrogenate other olefins as their concentrations increase. Intriguingly, n-butane did not increase to the same extent even though n-butenes were produced at much higher amounts than isobutene early in the reaction. The cause of this is not clear, but one hypothesis could be that there is greater steric hindrance for H-transfer to 2-butenes, which have methyl substituents at each sp² carbon atom, compared to isobutene. A second hypothesis is that having a tertiary sp² carbon atom is kinetically preferred, which would be the case if a tertiary carbenium or radical intermediate is involved but would suggest that ethane formation should be unfavorable too.

The production of saturated products without cofeeding hydrogen requires unsaturation of another species. No C₂ to C₄ products with multiple degrees of unsaturation (e.g. acetylene, propadiene, butadiene) were detected below 400 °C. In addition, the catalyst did not appear to be

accumulating significant amounts of coke below 400 °C – the ethylene conversion rates were stable over several days of testing, and the alumina did not turn black below 400 °C. It did change to a light orange color at 360 °C, however, which is a sign of oligomeric surface adsorbates. Such species might serve as coke precursors. However, apparently these do not lead to significant loss of activity, even at 70 % conversion.

3.4.3 Insights from the Contrasting Products Formed by C₃H₆ versus C₂H₄ with Al₂O₃

MW Distribution

The products for the reactions of propylene provide several sharp contrasts to those of ethylene. In terms of MW distribution differences, the main products at low conversion are not simply dimer products (C₆) but appear to be disproportionation products (ethylene and isobutene). This outcome was the opposite of the thermal reaction of propylene in our previous study which showed that propylene tends to form mostly (> 70 %) dimeric C₆ products at 400 °C. Cracking to form non-oligomers was minimal (< 30 %) until the temperature increased to about 500 °C. With alumina, even at 260 °C the dimer is the minor product (ca. 25 %) compared to isobutene and ethylene and other non-C₆ products. In addition to the molecular-weight distribution differences, the branched-to-linear ratios of C₄ and C₅ isomers using alumina were reverse for propylene compared to ethylene. That is, ethylene produced relatively more linear C₄ and branched C₅, whereas propylene produced more branched C₄ and linear C₅. Finally, the extent of hydrogen transfer was also less with propylene.

Isomerization of C₄, C₅, and C₆

As noted above, propylene produces more than equilibrium amounts of isobutene with respect to n-butenes, whereas ethylene initially favors n-butenes, followed by a convergence towards equilibrium with the n-butenes above about 5 % conversion. Additionally, when propylene was reacted over alumina, the amount of isobutene formed at low conversion was close to the ethylene produced, which is unlike the reaction pathway catalyzed by Brønsted acid sites in H-ZSM-5, for example. H-ZSM-5 at 250 °C with a propylene feed, has been shown to produce C₄ and C₅ cracking products in stoichiometric amounts below 4 % conversion, which was ascribed to cracking of C₉

oligomers.⁹¹ Furthermore, no ethylene was reported with H-ZSM-5 at these conditions, highlighting again that alumina operates differently than Brønsted acid chemistry.

With propylene over alumina, the C₅ were highly linear, whereas ethylene produced mostly branched C₅ isomers. Moreover, unlike the opposing C₄ and C₅ isomer behavior for each, the C₆ composition appeared to be almost identical whether ethylene or propylene was the reactant. The comparable C₆ distributions seems to eliminate the possibility that the substantial variations in C₄ and C₅ isomers between ethylene and propylene are due to different higher oligomer structures. This is also supported by the 1-hexene isomerization/cracking experiments, which produced highly linear C₄ and C₅ that are not consistent with either ethylene or propylene feed reactions. Instead, this suggests that the different C₄ and C₅ isomer trends are due to the configurations with which each monomer adds to reactive intermediates present in each case. Thus, an intricate reaction pathway seems to be at play, which will require a more rigorous theoretical and modeling approach to elucidate further.

H-Transfer

Less saturates were produced by propylene than with an ethylene feed. For example, ethane was about 10 mole % from ethylene at about 5-10 % conversion, whereas propane was only about 5 mole % from propylene. Although ethylene was a major product, very little ethane (< 0.1 %) was detected with a propylene feed even at 25 % conversion at 300 °C. Lower selectivity to isobutane and isopentane was witnessed as well. This result is conflicting to the thermal reactions of ethylene and propylene, in which propylene produces more saturated products (methane, ethane, and propane), which was reconciled by its allylic C-H bond. Ethylene contains four strong, vinyl C-H bonds, whereas propylene possesses a much weaker allylic C-H. The fact that more hydrogen transfer occurs with ethylene suggests that the activation of the allyl C-H bond is not significant compared to vinyl C-H activation.

This behavior is in good agreement with the previous D₂ exchange experiments with Al₂O₃ compared to other solid oxide materials. For example, pure Al₂O₃ has been demonstrated to perform D₂ exchange with ethylene at room temperature at high rates.^{82,83} Furthermore, D₂ exchange with propylene at room temperature occurred preferentially at the unsubstituted sp² carbon atoms, followed by the substituted sp², compared to the allylic C-H.⁸⁴ Thus, in the context of H exchange preference, the results in this study for the relative amounts of H-transfer between

ethylene and propylene are consistent with the previous observations. It remains to be seen, however, if this ability to activate vinyl C-H bonds is connected to the peculiar C₄ to C₆ branching behavior of the reactions of ethylene and propylene over alumina. For example, C-C bonds are generally weaker than C-H bonds. Therefore, it would be reasonable that vinyl C-CH₃ bonds are also vulnerable to activation compared to vinyl C-H bonds. This would be supported by the fact that propylene was an order of magnitude more reactive than ethylene, even though the products did not indicate that the allyl C-H bond was involved. Additionally, aluminas also catalyze D₂ exchange with methane at room temperature, implying they form methyl surface intermediates, which would be expected if methyl scrambling of products is occurring from ethylene and propylene feeds.⁸¹

3.5 Conclusion

In this study, the interaction of high surface area silica and alumina supports with the thermal reactions of ethylene and propylene were investigated. Amorphous silica and γ -alumina each converted ethylene to products at higher rates than the gas phase, thermal oligomerization. However, the product behaviors and apparent kinetics were distinct for each. Silica was less impactful, with products and kinetics closer to the gas phase radical reaction. Alumina demonstrated the ability to produce high yields of C₅ to C₁₀ liquids at 23 bar and 360 °C, with more product branching than the thermal reaction, and there was minimal deactivation of the rate. The reaction chemistry appears to be related to the Lewis acidity of Al₂O₃ rather than Brønsted acid (carbenium ion) or transition metal (metal-alkyl) oligomerization. The explicit role of the radical reaction in the presence of alumina remains unclear, however, this study opens the door for future studies about possible catalytic reactions and surface intermediates using theory and/or modeling. Under these conditions, the rate with alumina was at least 100 times than the thermal reaction. The results of this study will also be beneficial to ongoing research focused on understanding the complex catalytic Lewis acid sites of aluminas.

3.6 References

- (1) Bell, A. T.; Alger, M. M.; Flytzani-Stephanopoulos, M.; Gunnoe, T. B.; Lercher, J. A.; Stevens, J.; Alper, J.; Tran, C. *The Changing Landscape of Hydrocarbon Feedstocks for Chemical Production: Implications for Catalysis: Proceedings of a Workshop*; 1344369; 2016; p 1344369. <https://doi.org/10.2172/1344369>.
- (2) Ridha, T.; Li, Y.; Gençer, E.; Siirola, J.; Miller, J.; Ribeiro, F.; Agrawal, R. Valorization of Shale Gas Condensate to Liquid Hydrocarbons through Catalytic Dehydrogenation and Oligomerization. *Processes* **2018**, *6* (9), 139. <https://doi.org/10.3390/pr6090139>.
- (3) Nalley, S.; LaRose, A. *Annual Energy Outlook 2021*; Press Release; Washington, D.C., 2021.
- (4) Pillai, S. M.; Ravindranathan, M.; Sivaram, S. Dimerization of Ethylene and Propylene Catalyzed by Transition-Metal Complexes. *Chem. Rev.* **1986**, *86* (2), 353–399. <https://doi.org/10.1021/cr00072a004>.
- (5) O'Connor, C. T.; Kojima, M. Alkene Oligomerization. *Catalysis Today* **1990**, *6* (3), 329–349. [https://doi.org/10.1016/0920-5861\(90\)85008-C](https://doi.org/10.1016/0920-5861(90)85008-C).
- (6) Skupinska, Jadwiga. Oligomerization of α -Olefins to Higher Oligomers. *Chem. Rev.* **1991**, *91* (4), 613–648. <https://doi.org/10.1021/cr00004a007>.
- (7) Al-Jarallah, A. M.; Anabtawi, J. A.; Siddiqui, M. A. B.; Aitani, A. M.; Al-Sa'doun, A. W. Ethylene Dimerization and Oligomerization to Butene-1 and Linear α -Olefins. *Catalysis Today* **1992**, *14* (1), 1–121. [https://doi.org/10.1016/0920-5861\(92\)80128-A](https://doi.org/10.1016/0920-5861(92)80128-A).
- (8) Forestière, A.; Olivier-Bourbigou, H.; Saussine, L. Oligomerization of Monoolefins by Homogeneous Catalysts. *Oil & Gas Science and Technology - Rev. IFP* **2009**, *64* (6), 649–667. <https://doi.org/10.2516/ogst/2009027>.
- (9) McGuinness, D. S. Olefin Oligomerization via Metallacycles: Dimerization, Trimerization, Tetramerization, and Beyond. *Chem. Rev.* **2011**, *111* (3), 2321–2341. <https://doi.org/10.1021/cr100217q>.
- (10) Sydora, O. L. Selective Ethylene Oligomerization. *Organometallics* **2019**, *38* (5), 997–1010. <https://doi.org/10.1021/acs.organomet.8b00799>.
- (11) Olivier-Bourbigou, H.; Breuil, P. A. R.; Magna, L.; Michel, T.; Espada Pastor, M. F.; Delcroix, D. Nickel Catalyzed Olefin Oligomerization and Dimerization. *Chem. Rev.* **2020**, *120* (15), 7919–7983. <https://doi.org/10.1021/acs.chemrev.0c00076>.
- (12) Finiels, A.; Fajula, F.; Hulea, V. Nickel-Based Solid Catalysts for Ethylene Oligomerization – a Review. *Catal. Sci. Technol.* **2014**, *4* (8), 2412–2426. <https://doi.org/10.1039/C4CY00305E>.
- (13) Nicholas, C. P. Applications of Light Olefin Oligomerization to the Production of Fuels and Chemicals. *Applied Catalysis A: General* **2017**, *543*, 82–97. <https://doi.org/10.1016/j.apcata.2017.06.011>.
- (14) Ghashghaee, M. Heterogeneous Catalysts for Gas-Phase Conversion of Ethylene to Higher Olefins. *Reviews in Chemical Engineering* **2018**, *34* (5), 595–655. <https://doi.org/10.1515/revce-2017-0003>.
- (15) Schmerling, L.; Ipatieff, V. N. The Mechanism of the Polymerization of Alkenes. In *Advances in Catalysis*; Elsevier, 1950; Vol. 2, pp 21–80. [https://doi.org/10.1016/S0360-0564\(08\)60374-0](https://doi.org/10.1016/S0360-0564(08)60374-0).

- (16) Jones, E. K. Polymerization of Olefins from Cracked Gases. In *Advances in Catalysis*; Elsevier, 1956; Vol. 8, pp 219–238. [https://doi.org/10.1016/S0360-0564\(08\)60541-6](https://doi.org/10.1016/S0360-0564(08)60541-6).
- (17) Oblad, A. G.; Mills, G. A.; Heinemann, H. Polymerization of Olefins (to Liquid Polymers). In *Catalysis*; Reinhold Publishing Corporation, 1958; Vol. 6.
- (18) Corma, A.; Iborra, S. Oligomerization of Alkenes. In *Catalysts for Fine Chemical Synthesis*; Derouane, E. G., Ed.; John Wiley & Sons, Ltd: Chichester, UK, 2006; pp 125–140. <https://doi.org/10.1002/0470094214.ch6>.
- (19) Sanati, M.; Hörnell, C.; Järäs, S. G. The Oligomerization of Alkenes by Heterogeneous Catalysts. In *Catalysis*; Spivey, J. J., Ed.; Royal Society of Chemistry: Cambridge, 2007; Vol. 14, pp 236–288. <https://doi.org/10.1039/9781847553263-00236>.
- (20) Mehlberg, R. L.; Pujadó, P. R.; Ward, D. J. Olefin Condensation. In *Handbook of Petroleum Processing*; Treese, S. A., Pujadó, P. R., Jones, D. S. J., Eds.; Springer International Publishing: Cham, 2015; pp 457–478. https://doi.org/10.1007/978-3-319-14529-7_6.
- (21) Antunes, B. M.; Rodrigues, A. E.; Lin, Z.; Portugal, I.; Silva, C. M. Alkenes Oligomerization with Resin Catalysts. *Fuel Processing Technology* **2015**, *138*, 86–99. <https://doi.org/10.1016/j.fuproc.2015.04.031>.
- (22) Dunstan, A. E. Fluid Fuels To-Day and to-Morrow. Second Jubilee Memorial Lecture. *J. Soc. Chem. Ind.* **1932**, *51* (41), 822–842. <https://doi.org/10.1002/jctb.5000514102>.
- (23) Dunstan, A. E.; Hague, E. N.; Wheeler, R. V. Symposium on Hydrocarbon Decomposition Thermal Treatment of Gaseous Hydrocarbons I. Laboratory Scale Operation. *Ind. Eng. Chem.* **1934**, *26* (3), 307–314. <https://doi.org/10.1021/ie50291a019>.
- (24) Dunstan, A. E.; Hague, E. N.; Wheeler, R. V. The Heat Treatment of Hydrocarbons with Special Reference to the Gaseous Hydrocarbons. Part II. *J. Soc. Chem. Ind.* **1932**, *51* (18), 131T-140T. <https://doi.org/10.1002/jctb.5000511807>.
- (25) Frolich, P. K.; Wiezevich, P. J. Symposium on the Chemistry of Gaseous Hydrocarbons Cracking and Polymerization of Low Molecular Weight Hydrocarbons. *Ind. Eng. Chem.* **1935**, *27* (9), 1055–1062. <https://doi.org/10.1021/ie50309a022>.
- (26) Wagner, C. R. Production of Gasoline by Polymerization of Olefins. *Ind. Eng. Chem.* **1935**, *27* (8), 933–936. <https://doi.org/10.1021/ie50308a018>.
- (27) Maschwitz, P. A.; Henderson, L. M. Polymerization of Hydrocarbon Gases to Motor Fuels. *PROGRESS IN PETROLEUM TECHNOLOGY* **1951**, *5*. <https://doi.org/10.1021/ba-1951-0005>.
- (28) Asinger, F. THE WORKING UP OF LOWER, NORMALLY GASEOUS PARAFFINS AND MONO-OLEFINS TO GIVE CARBURETTOR FUELS. In *Mono-Olefins*; Elsevier, 1968; pp 414–505. <https://doi.org/10.1016/B978-0-08-011547-4.50008-2>.
- (29) Egloff, G.; Schaad, R. E.; Lowry, C. D. Decomposition and Polymerization of the Olefinic Hydrocarbons. *J. Phys. Chem.* **1931**, *35* (7), 1825–1903. <https://doi.org/10.1021/j150325a001>.
- (30) Stanley, H. M. The Polymerisation Reactions of Ethylene. *J. Soc. Chem. Ind.* **1930**, *49* (34), T349–T354. <https://doi.org/10.1002/jctb.5000493415>.
- (31) Yamada, B.; Zetterlund, P. B. General Chemistry of Radical Polymerization. In *Handbook of Radical Polymerization*; Matyjaszewski, K., Davis, T. P., Eds.; John Wiley & Sons, Inc.: Hoboken, NJ, USA, 2002; pp 117–186. <https://doi.org/10.1002/0471220450.ch3>.

- (32) Elias, H.-G. Free-Radical Polymerization. In *Macromolecules*; Wiley-VCH Verlag GmbH: D-69451 Weinheim, Germany, 2014; pp 309–367. <https://doi.org/10.1002/9783527627219.ch10>.
- (33) Peuckert, M.; Keim, W. A New Nickel Complex for the Oligomerization of Ethylene. *Organometallics* **1983**, *2* (5), 594–597. <https://doi.org/10.1021/om00077a004>.
- (34) Lutz, E. F. Shell Higher Olefins Process. *J. Chem. Educ.* **1986**, *63* (3), 202. <https://doi.org/10.1021/ed063p202>.
- (35) Keim, W. Nickel: An Element with Wide Application in Industrial Homogeneous Catalysis. *Angew. Chem. Int. Ed. Engl.* **1990**, *29* (3), 235–244. <https://doi.org/10.1002/anie.199002351>.
- (36) Freitas, E. R.; Gum, C. R. CEP SHOP Process 1979.Pdf. *Chemical Engineering Progress*. 1979, pp 73–76.
- (37) Andrews, J.; Bonnifay, P. The IFP Dimersol Process for Dimerization of Propylene into Isohexenes. In *ACS Symposium Series*; AMERICAN CHEMICAL SOCIETY, 1977; pp 328–340.
- (38) Al-Sherehy, F. A. IFP-SABIC Process for the Selective Ethylene Dimerization to Butene-1. In *Studies in Surface Science and Catalysis*; Elsevier, 1996; Vol. 100, pp 515–523. [https://doi.org/10.1016/S0167-2991\(96\)80052-8](https://doi.org/10.1016/S0167-2991(96)80052-8).
- (39) Manyik, R. A Soluble Chromium-Based Catalyst for Ethylene Trimerization and Polymerization. *Journal of Catalysis* **1977**, *47* (2), 197–209. [https://doi.org/10.1016/0021-9517\(77\)90167-1](https://doi.org/10.1016/0021-9517(77)90167-1).
- (40) McGuinness, D. S.; Wasserscheid, P.; Keim, W.; Hu, C.; Englert, U.; Dixon, J. T.; Grove, C. Novel Cr-PNP Complexes as Catalysts for the Trimerisation of Ethylene. *Chem. Commun.* **2003**, No. 3, 334–335. <https://doi.org/10.1039/b210878j>.
- (41) Ziegler, K. Aluminium-organische Synthese im Bereich olefinischer Kohlenwasserstoffe. *Angew. Chem.* **1952**, *64* (12), 323–329. <https://doi.org/10.1002/ange.19520641202>.
- (42) Shiraki, Y.; Kawano, S.; Takeuchi, K. Process For Preparing Linear A-Olefins. 4783573, November 8, 1988.
- (43) Sullivan, F. W.; Ruthruff, R. F.; Kuentzel, W. E. Pyrolysis and Polymerization of Gaseous Paraffins and Olefins. *Ind. Eng. Chem.* **1935**, *27* (9), 1072–1077. <https://doi.org/10.1021/ie50309a026>.
- (44) Egloff, G. POLYMER GASOLINE. *INDUSTRIAL AND ENGINEERING CHEMISTRY* **1936**, *28* (12), 7.
- (45) Lewis, W. K.; Gilliland, E. R.; Chertow, B.; Cadogan, W. P. Pure Gas Isotherms. *Ind. Eng. Chem.* **1950**, *42* (7), 1326–1332. <https://doi.org/10.1021/ie50487a023>.
- (46) Casquero Ruiz, J. de D.; Guil Pinto, J. M.; Pérez Masiá, A.; Ruiz Paniego, A. Thermodynamics of the Adsorption of Hydrocarbons on Alumina. *The Journal of Chemical Thermodynamics* **1986**, *18* (10), 903–914. [https://doi.org/10.1016/0021-9614\(86\)90148-5](https://doi.org/10.1016/0021-9614(86)90148-5).
- (47) Olivier, M.-G.; Jadot, R. Adsorption of Light Hydrocarbons and Carbon Dioxide on Silica Gel. *J. Chem. Eng. Data* **1997**, *42* (2), 230–233. <https://doi.org/10.1021/je960200j>.
- (48) Knözinger, H.; Ratnasamy, P. Catalytic Aluminas: Surface Models and Characterization of Surface Sites. *Catalysis Reviews* **1978**, *17* (1), 31–70. <https://doi.org/10.1080/03602457808080878>.

- (49) Liu, L.; Zhu, Y.-P.; Su, M.; Yuan, Z.-Y. Metal-Free Carbonaceous Materials as Promising Heterogeneous Catalysts. *ChemCatChem* **2015**, *7* (18), 2765–2787. <https://doi.org/10.1002/cctc.201500350>.
- (50) Liu, L.; Deng, Q.-F.; Agula, B.; Zhao, X.; Ren, T.-Z.; Yuan, Z.-Y. Ordered Mesoporous Carbon Catalyst for Dehydrogenation of Propane to Propylene. *Chem. Commun.* **2011**, 47 (29), 8334. <https://doi.org/10.1039/c1cc12806j>.
- (51) Ukpong, A. M. *Ab Initio* Studies of Propane Dehydrogenation to Propene with Graphene. *Molecular Physics* **2020**, *118* (24), e1798527. <https://doi.org/10.1080/00268976.2020.1798527>.
- (52) Knyazheva, O. A.; Baklanova, O. N.; Lavrenov, A. V. Catalytic Dehydrogenation on Carbon. *Solid Fuel Chem.* **2020**, *54* (6), 345–353. <https://doi.org/10.3103/S0361521920060051>.
- (53) Hu, Z.-P.; Chen, C.; Ren, J.-T.; Yuan, Z.-Y. Direct Dehydrogenation of Propane to Propylene on Surface-Oxidized Multiwall Carbon Nanotubes. *Applied Catalysis A: General* **2018**, *559*, 85–93. <https://doi.org/10.1016/j.apcata.2018.04.017>.
- (54) Greensfelder, B. S.; Voge, H. H.; Good, G. M. Catalytic and Thermal Cracking of Pure Hydrocarbons: Mechanisms of Reaction. *Ind. Eng. Chem.* **1949**, *41* (11), 2573–2584. <https://doi.org/10.1021/ie50479a043>.
- (55) Ipatieff, V. N. Katalytische Reaktionen bei hohen Temperaturen und Drucken. X. Mitteilung: Einfluß des Druckes auf den Gang der Katalyse. *Chem. Central-Blatt* **1906**, *II*, 86.
- (56) Ipatieff, V. N. Каталитическая реакция при высоких давлениях и температурах влияние давления на ходъ катализа. *Zh. Russ. Fiz. Khim.* **1906**, 63–75.
- (57) Brey, W. S.; Krieger, K. A. The Surface Area and Catalytic Activity of Aluminum Oxide. *J. Am. Chem. Soc.* **1949**, *71* (11), 3637–3641. <https://doi.org/10.1021/ja01179a016>.
- (58) Oblad, A. G.; Messenger, J. U.; Brown, H. T. Isomerization of 1- and 2-Pentenes. *Ind. Eng. Chem.* **1947**, *39* (11), 1462–1466. <https://doi.org/10.1021/ie50455a015>.
- (59) Naragon, E. A. Catalytic Isomerization of 1-Hexene. *Ind. Eng. Chem.* **1950**, *42* (12), 2490–2493. <https://doi.org/10.1021/ie50492a028>.
- (60) Hindin, S. G.; Weller, S. W. The Effect of Pretreatment on the Activity of Gamma-Alumina. I. Ethylene Hydrogenation. *J. Phys. Chem.* **1956**, *60* (11), 1501–1506. <https://doi.org/10.1021/j150545a008>.
- (61) Hindin, S. G.; Weller, S. W. 10 Catalysis of Ethylene Hydrogenation and Hydrogen-Deuterium Exchange by Dehydrated Alumina. In *Advances in Catalysis*; Elsevier, 1957; Vol. 9, pp 70–75. [https://doi.org/10.1016/S0360-0564\(08\)60155-8](https://doi.org/10.1016/S0360-0564(08)60155-8).
- (62) Pines, H.; Haag, W. O. Alumina: Catalyst and Support. I. Alumina, Its Intrinsic Acidity and Catalytic Activity ¹. *J. Am. Chem. Soc.* **1960**, *82* (10), 2471–2483. <https://doi.org/10.1021/ja01495a021>.
- (63) Brouwer, D. The Mechanism of Double-Bond Isomerization of Olefins on Solid Acids. *Journal of Catalysis* **1962**, *1* (1), 22–31. [https://doi.org/10.1016/0021-9517\(62\)90005-2](https://doi.org/10.1016/0021-9517(62)90005-2).
- (64) Sinfelt, J. H. Kinetics of Ethylene Hydrogenation over Alumina. *J. Phys. Chem.* **1964**, *68* (2), 232–237. <https://doi.org/10.1021/j100784a003>.
- (65) Corado, A. Catalytic Isomerization of Olefins on Alumina *III. Catalyst Deactivation and Its Effects on the Mechanism. *Journal of Catalysis* **1975**, *37* (1), 68–80. [https://doi.org/10.1016/0021-9517\(75\)90134-7](https://doi.org/10.1016/0021-9517(75)90134-7).

- (66) Medema, J. Isomerization of Butene over Alumina*1. *Journal of Catalysis* **1975**, *37* (1), 91–100. [https://doi.org/10.1016/0021-9517\(75\)90136-0](https://doi.org/10.1016/0021-9517(75)90136-0).
- (67) Butler, A. C.; Nicolaidis, C. P. Catalytic Skeletal Isomerization of Linear Butenes to Isobutene. *Catalysis Today* **1993**, *18* (4), 443–471. [https://doi.org/10.1016/0920-5861\(93\)80063-7](https://doi.org/10.1016/0920-5861(93)80063-7).
- (68) Rodemerck, U.; Kondratenko, E. V.; Otroshchenko, T.; Linke, D. Unexpectedly High Activity of Bare Alumina for Non-Oxidative Isobutane Dehydrogenation. *Chem. Commun.* **2016**, *52* (82), 12222–12225. <https://doi.org/10.1039/C6CC06442F>.
- (69) Zhao, D.; Lund, H.; Rodemerck, U.; Linke, D.; Jiang, G.; Kondratenko, E. V. Revealing Fundamentals Affecting Activity and Product Selectivity in Non-Oxidative Propane Dehydrogenation over Bare Al₂O₃. *Catal. Sci. Technol.* **2021**, *11* (4), 1386–1394. <https://doi.org/10.1039/D0CY01980A>.
- (70) Wang, P.; Xu, Z.; Wang, T.; Yue, Y.; Bao, X.; Zhu, H. Unmodified Bulk Alumina as an Efficient Catalyst for Propane Dehydrogenation. *Catal. Sci. Technol.* **2020**, *10* (11), 3537–3541. <https://doi.org/10.1039/D0CY00779J>.
- (71) Rodemerck, U.; Sokolov, S.; Stoyanova, M.; Bentrup, U.; Linke, D.; Kondratenko, E. V. Influence of Support and Kind of VO Species on Isobutene Selectivity and Coke Deposition in Non-Oxidative Dehydrogenation of Isobutane. *Journal of Catalysis* **2016**, *338*, 174–183. <https://doi.org/10.1016/j.jcat.2016.03.003>.
- (72) Busca, G. Spectroscopic Characterization of the Acid Properties of Metal Oxide Catalysts. *Catalysis Today* **1998**, *41* (1–3), 191–206. [https://doi.org/10.1016/S0920-5861\(98\)00049-2](https://doi.org/10.1016/S0920-5861(98)00049-2).
- (73) Knozinger, H. A Test for the Development of Protonic Acidity in Alumina at Elevated Temperatures. *Journal of Catalysis* **1972**, *25* (3), 436–438. [https://doi.org/10.1016/0021-9517\(72\)90246-1](https://doi.org/10.1016/0021-9517(72)90246-1).
- (74) Holm, V. C. F.; Clark, A. Catalytic Properties of Fluorine-Promoted Alumina. *I&EC Product Research and Development* **1963**, *2* (1), 38–39. <https://doi.org/10.1021/i360005a009>.
- (75) Choudhary, V. R. Fluorine Promoted Catalysts: Activity and Surface Properties. *Product R&D* **1977**, *16* (1), 12–22. <https://doi.org/10.1021/i360061a003>.
- (76) Cheng, Z.; Ponec, V. Fluorinated Alumina as a Catalyst for Skeletal Isomerization of *n*-Butene. *Applied Catalysis A: General* **1994**, *118* (2), 127–138. [https://doi.org/10.1016/0926-860X\(94\)80308-0](https://doi.org/10.1016/0926-860X(94)80308-0).
- (77) Gayubo, A. G.; Llorens, F. J.; Cepeda, E. A.; Bilbao, J. Deactivation and Regeneration of a Chlorinated Alumina Catalyst Used in the Skeletal Isomerization of *n*-Butenes. *Ind. Eng. Chem. Res.* **1997**, *36* (12), 5189–5195. <https://doi.org/10.1021/ie9702385>.
- (78) Bondt; Deiman; van Troostwyk; Lauwerenburg. Sur trois espèces différentes de Gaz hydrogène carboné, retirées de l'éther et de l'alcool par différents procédés. *Ann. Chim. Phys.* **1797**, *21*, 48–71.
- (79) Knözinger, H. Dehydration of Alcohols on Aluminum Oxide. *Angew. Chem. Int. Ed. Engl.* **1968**, *7* (10), 791–805. <https://doi.org/10.1002/anie.196807911>.
- (80) Holm, C. V. C. F.; Blue, R. W. Hydrogen-Deuterium Exchange Activity of Silica-Alumina. *Ind. Eng. Chem.* **1951**, *43* (2), 501–505. <https://doi.org/10.1021/ie50494a052>.
- (81) Larson, J. G.; Hall, W. K. Studies of the Hydrogen Held by Solids. VII. The Exchange of the Hydroxyl Groups of Alumina and Silica-Alumina Catalysts with Deuterated Methane. *J. Phys. Chem.* **1965**, *69* (9), 3080–3089. <https://doi.org/10.1021/j100893a044>.

- (82) Larson, J. G.; Hightower, J. W.; Hall, W. K. Tracer Studies of Acid-Catalyzed Reactions. III. Preparation of Perdeuterio Olefins and Cyclopropane by Reaction with Deuterium over Alumina. *J. Org. Chem.* **1966**, *31* (4), 1225–1227. <https://doi.org/10.1021/jo01342a058>.
- (83) Hightower, J. Tracer Studies of Acid-Catalyzed Reactions IX. Exchange of D₂ with Noncyclic Olefins over Alumina. *Journal of Catalysis* **1969**, *13* (2), 161–168. [https://doi.org/10.1016/0021-9517\(69\)90388-1](https://doi.org/10.1016/0021-9517(69)90388-1).
- (84) Hughes, B. T.; Kemball, C.; Tyler, J. K. Exchange Reactions of Propene on Oxide Catalysts Investigated by Microwave Spectroscopy. *J. Chem. Soc., Faraday Trans. 1* **1975**, *71* (0), 1285. <https://doi.org/10.1039/f19757101285>.
- (85) Lucchesi, P. J.; Carter, J. L.; Yates, D. J. C. AN INFRARED STUDY OF THE CHEMISORPTION OF ETHYLENE ON ALUMINUM OXIDE. *J. Phys. Chem.* **1962**, *66* (8), 1451–1456. <https://doi.org/10.1021/j100814a018>.
- (86) Yates, D. J. C.; Lucchesi, P. J. Effects of γ -Radiation on the Surface Properties of Silica as Studied by the Infrared Spectra of Adsorbed Molecules. *J. Am. Chem. Soc.* **1964**, *86* (20), 4258–4265. <https://doi.org/10.1021/ja01074a007>.
- (87) Pease, R. N. THE NON-CATALYTIC POLYMERIZATION AND HYDROGENATION OF ETHYLENE. *J. Am. Chem. Soc.* **1930**, *52* (3), 1158–1164. <https://doi.org/10.1021/ja01366a052>.
- (88) Halstead, M. P.; Quinn, C. P. Pyrolysis of Ethylene. *Trans. Faraday Soc.* **1968**, *64*, 103. <https://doi.org/10.1039/tf9686400103>.
- (89) Boyd, M. L.; Wu, T.-M.; Back, M. H. Kinetics of the Thermal Reactions of Ethylene. Part I. *Can. J. Chem.* **1968**, *46* (14), 2415–2426. <https://doi.org/10.1139/v68-394>.
- (90) Quinn, C. P. The Thermal Dissociation and Pyrolysis of Ethane. *Proc. R. Soc. Lond. A* **1963**, *275* (1361), 190–199. <https://doi.org/10.1098/rspa.1963.0163>.
- (91) Vernuccio, S.; Bickel, E. E.; Gounder, R.; Broadbelt, L. J. Microkinetic Model of Propylene Oligomerization on Brønsted Acidic Zeolites at Low Conversion. *ACS Catal.* **2019**, *9* (10), 8996–9008. <https://doi.org/10.1021/acscatal.9b02066>.

4. FUTURE DIRECTIONS

The work comprised in this thesis advances the understanding of the chemistry of thermal ethylene reactions on two major fronts:

- (1) New insights into the purely thermal initiation pathway, detailed product behaviors, and kinetic analysis.
- (2) The development of a baseline understanding of the influence of bare catalyst supports such as silica or γ -alumina on the thermal oligomerization of ethylene, in terms of both rate enhancement and changes to the product distribution.

Pertaining to point (1), this thesis has demonstrated that ethylene radical oligomerization can initiate purely thermally despite the lack of allylic C-H bonds. DFT calculations support a two-phase initiation process, highlighted by the formation of diradicals, eventually leading to the generation of free radicals which can contribute to growing alkyl chains. Following initiation and the formation of free radicals, a family of propagation reactions take place, the result of which is embodied by the dynamic product distribution trends with respect to temperature, pressure, and conversion in Chapter 2. Thus, the first impact from this work is the generation of reaction pathway data (i.e. product selectivity vs conversion) which can be input into a microkinetic model, which is currently being pursued by collaborators in Linda Broadbelt's group at Northwestern University. A rigorous modeling approach will elucidate the rate controlling reactions and potentially provide predictions as to the optimum temperature and pressure conditions given a desired activity or product composition.

In the second area of broader impact, this thesis has provided an elementary account of the reaction kinetics and product trends when using a high-surface area support such as alumina to influence the thermal reaction. The reaction chemistry using alumina as an oligomerization catalyst aligns more closely with a Lewis acid function in contrast to Brønsted or transition metal catalysis. The impact is that this is an unprecedented type of oligomerization catalysis, which opens the door for many related studies with other high surface area supports and catalysts.

In terms of high-surface area supports, one could envision studies using other oxides such as magnesia, titania, ceria, etc. as well as activated carbons or non-acidic zeolites. These materials do

not contain traditional strong acid sites but may contain Lewis acidity which could be key to unlocking further rate enhancements or steering of the products towards a desired fuel grade.

The second facet of searching for other active materials involves single-site metal ions deposited on the surface of any of these high surface area supports. In our group, we have previously synthesized Zn^{2+} , Ga^{3+} , and Co^{2+} single site catalysts supported on Al_2O_3 for propane dehydrogenation and propylene hydrogenation. Unlike Ni^{2+} single sites, each is quite stable even up to 550 °C in H_2 treatment, an important feature for potential high temperature oligomerization catalysts. Thus a 2nd major impact for future research is the comparison of these single site $\text{M}/\text{Al}_2\text{O}_3$ catalysts with the unmodified Al_2O_3 in terms of rate enhancement and product distribution. While it is not yet clear what the active site of the unmodified Al_2O_3 is for these reactions, developing an understanding of which single site metal ions provide the best enhancement, if any, could reveal useful information about the active site, for example Lewis acid or Lewis base sites.

APPENDIX A. SUPPORTING INFORMATION FOR CHAPTER 2

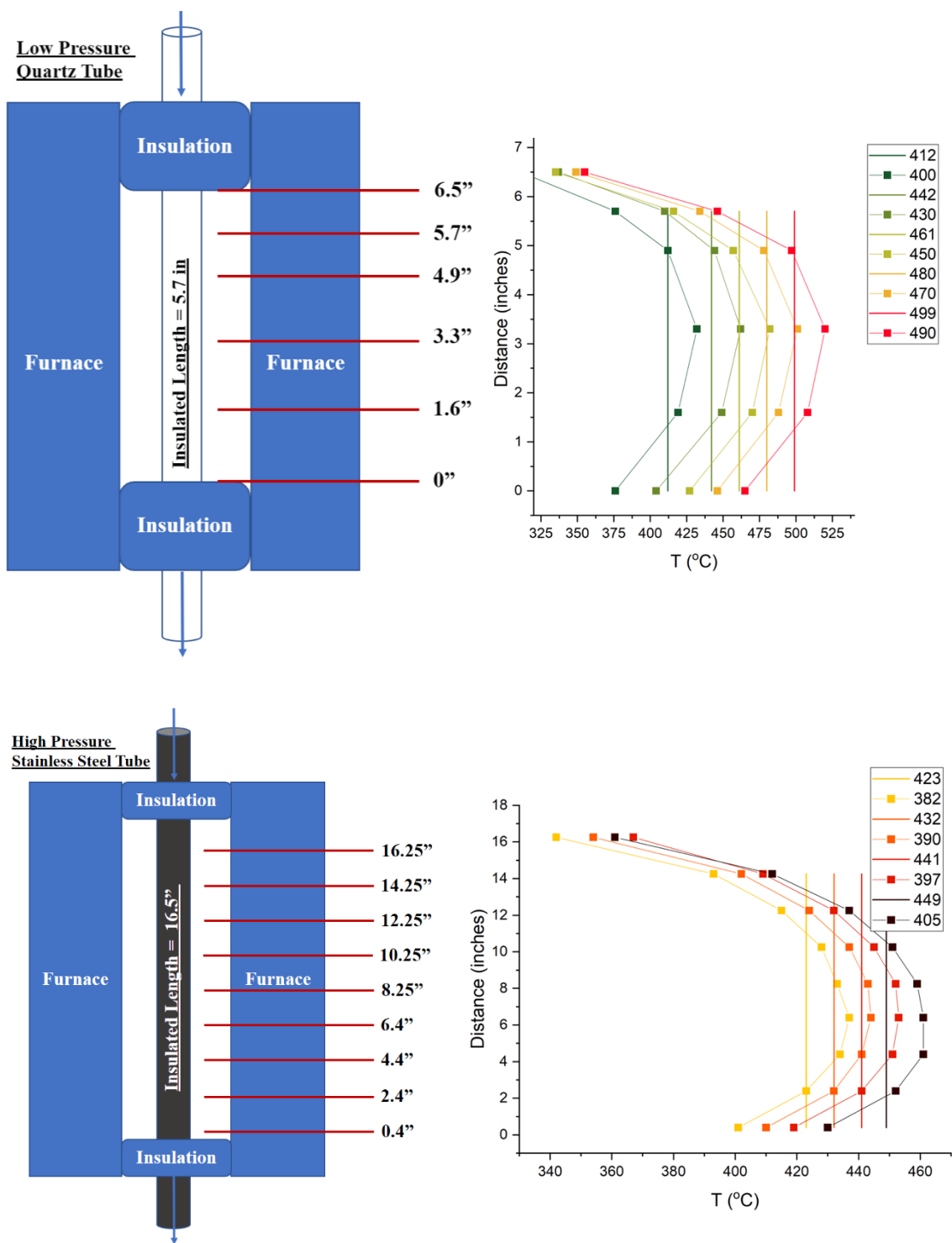


Figure A.1. Top: Quartz reactor tube temperature profiles from Setpoint 400 °C to 490 °C. Solid vertical lines are the averaged values reported. Bottom: Stainless steel reactor used for high pressure experiments from Setpoint 382 °C to 405 °C.

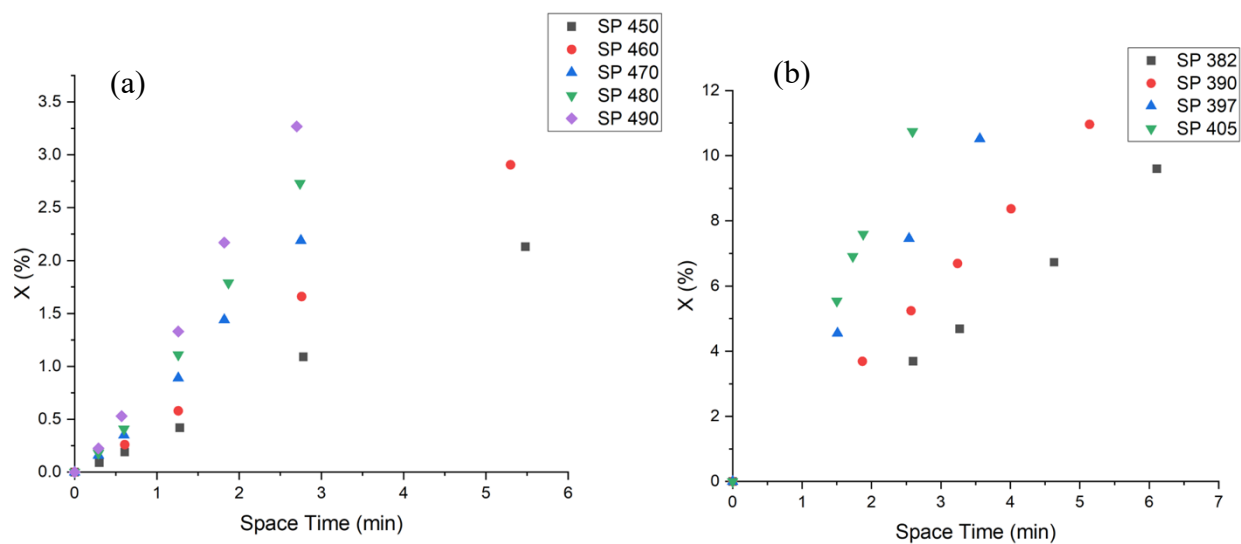


Figure A.2. Conversion measured versus space time. (a): 1.5 bar C_2H_4 . (b): 21.0 bar C_2H_4

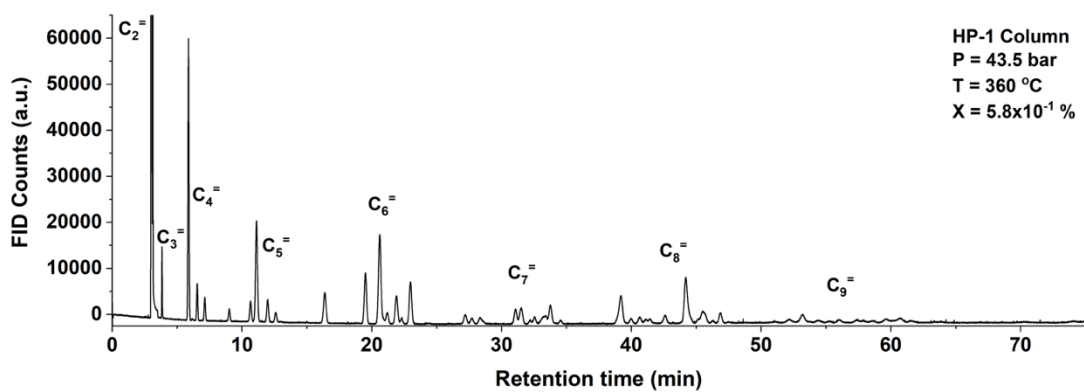


Figure A.3. Product distributions for ethylene feed below 400 °C at low conversion. Raw GC chromatogram at 43.5 bar and 360 °C and 5.8×10^{-1} % conversion using HP-1 column.

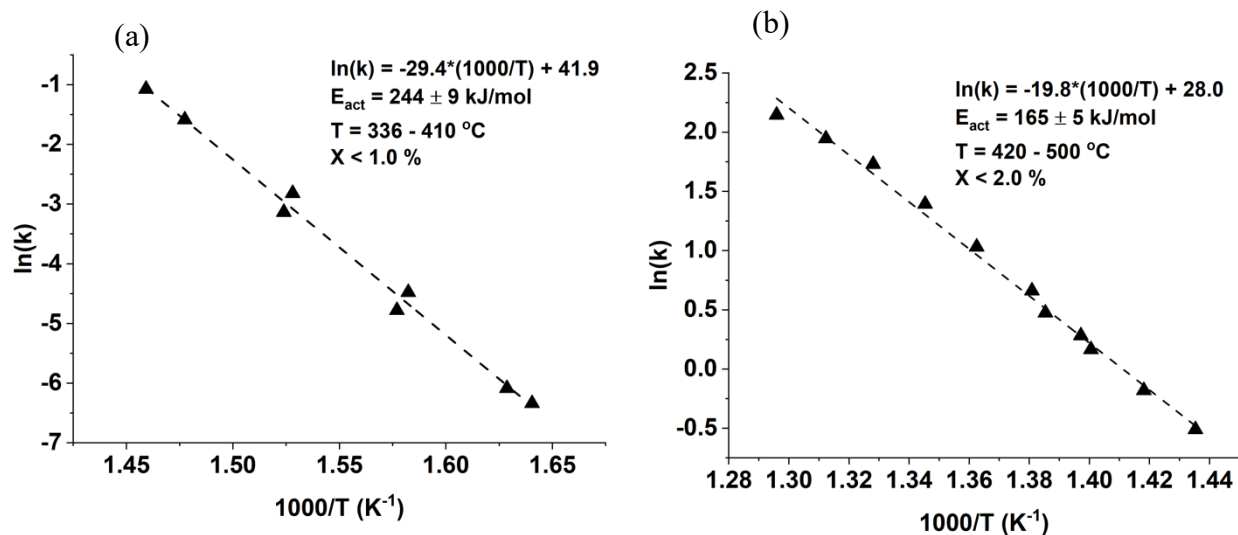


Figure A.4. (a) The activation energy analysis from 336 to 410 °C, rates were measured with conversions below 1.0 %. (b) The activation energy analysis from 420 to 500 °C at 1.5 and 21.0 bar, rates were measured with conversions below 5.0 %

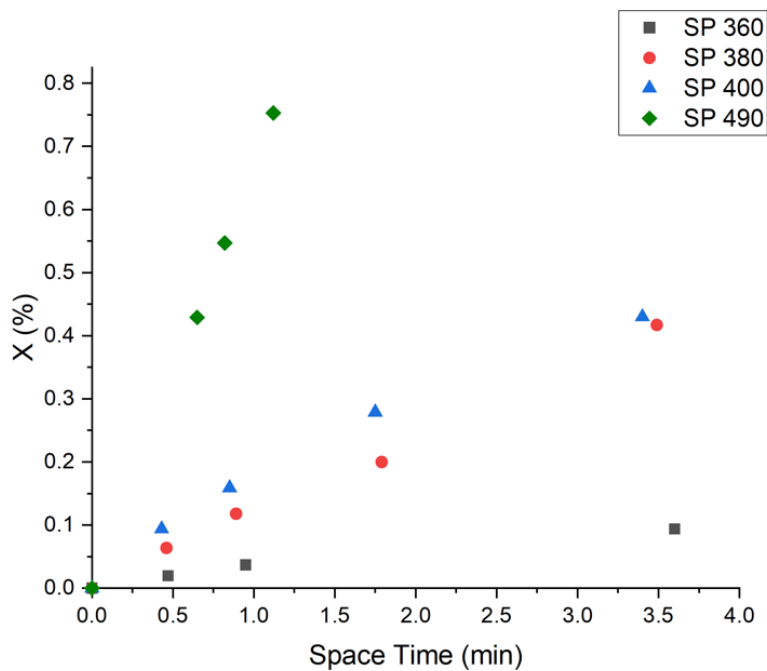


Figure A.5. Conversion measured versus space time. 1.5 bar C_3H_6 , Average temperature from 380 to 500 °C.

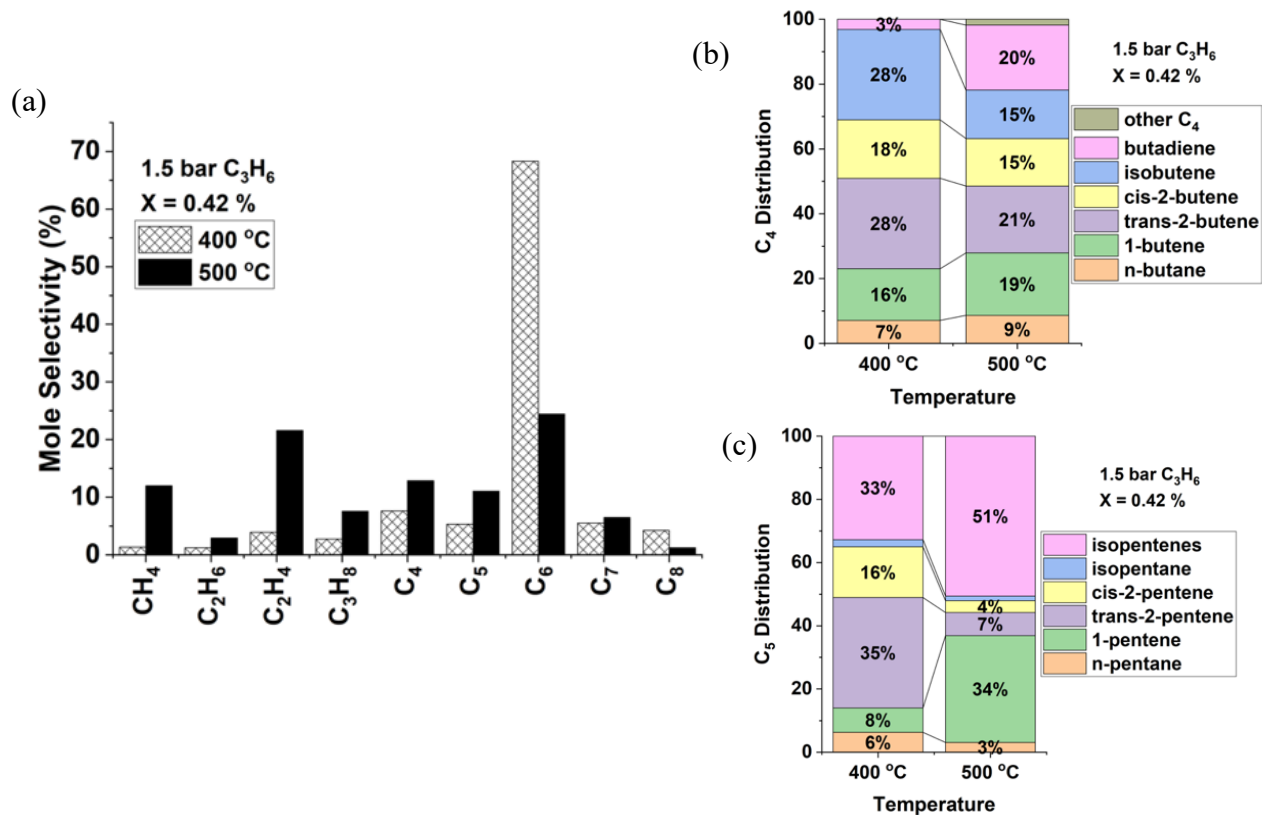


Figure A.6: Product distribution versus temperature at 0.42 % conversion of pure propylene reacted at 1.5 bar, temperature was either 400 or 500 °C. (a) Bv carbon number. (b) C₄ distribution. (c) C₅ distribution.

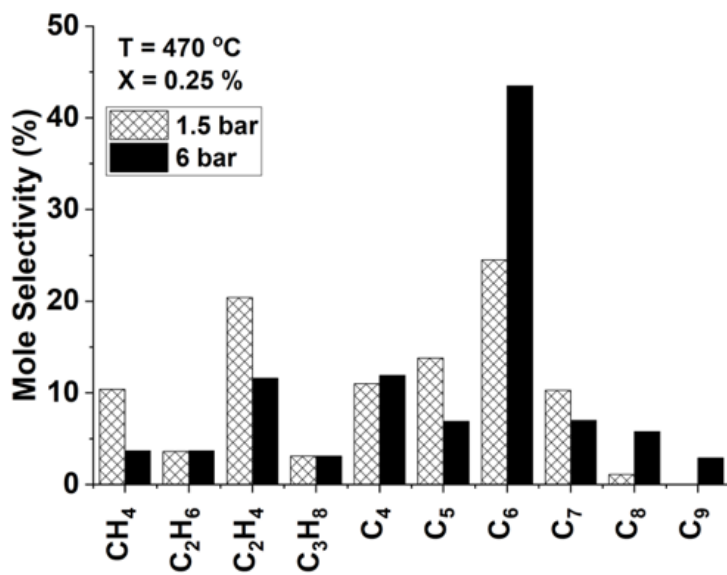


Figure A.7: Product distribution at 0.42 % conversion of pure propylene reacted at 1.5 bar and 400 °C.

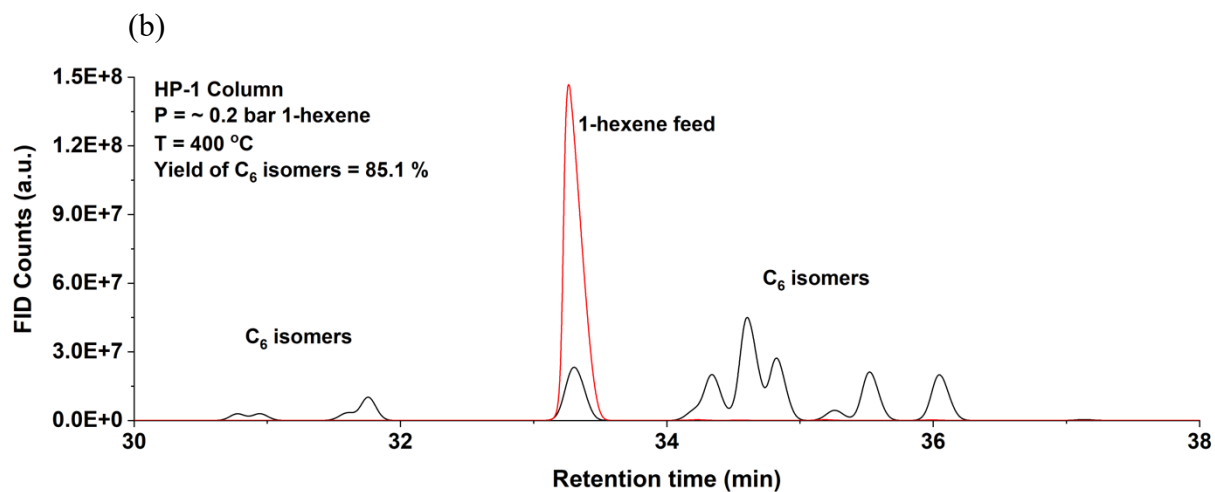
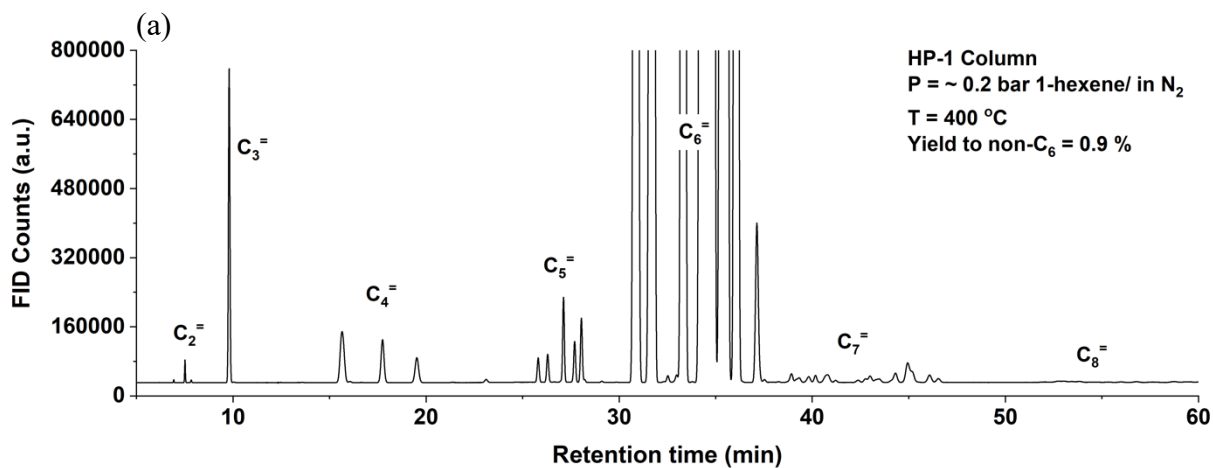


Figure A.8. Raw GC chromatogram of approximately 20 % 1-hexene feed at 1.0 bar and 400 °C, using HP-1 column. 1-hexene total conversion was 86.0 %. The red curve shows the 1-hexene feed through the reactor at room temperature. (a) The entire chromatogram scaled to show non-C₆ by carbon number. (b) The C₆ isomer products from 30 to 38 minutes of retention time.

Table A.1. Comparison of Relative Olefin Conversion Rates at 1.5 bar				
Feed Olefin	C ₂ H ₄		C ₃ H ₆	
Temperature (°C)	400	500	400	500
Conversion Rate (mol/cm ³ /s)	2.1 x 10 ⁻¹⁰	1.2 x 10 ⁻⁸	6.0 x 10 ⁻¹⁰	6.8 x 10 ⁻⁹
Mole fraction of C ₆ at 0.1 % conversion ^a	0.000039		0.00024	
Partial Pressure of C ₆ (kPa)	0.0059		0.036	
Rate of C ₆ Cracking (mol/cm ³ /s) ^b	8.3 x 10 ⁻¹³		5.0 x 10 ⁻¹²	
C ₆ Cracking/Conversion Rate	0.4 %		0.8 %	
C ₆ Isom./Conversion Rate ^c	40 - 180 %		80 - 370 %	
^a Mole fraction of C ₆ at 0.1 % conversion estimated using the experimentally observed selectivity to C ₆ ^b Extrapolated rate using 1 st order rate constant at 1 kPa ^c The relative isomerization to olefin conversion rate is presented as a range, estimated using the lowest and highest isomerization to cracking ratios observed, 100 and 460x, respectively.				

APPENDIX B. SUPPORTING INFORMATION FOR CHAPTER 3

Table B.1. Comparison of Ethylene Conversion Rates Normalized by Surface Area at 340 °C and 42.0 – 43.5 bar C₂H₄

	Rate per Volume (Molec _{C₂H₄} s ⁻¹ cm ⁻³)	Mass ^a (g)	Specific Surface Area ^b (m ² /g)	Surface Area (m ²)	Rate per Area (Molec _{C₂H₄} s ⁻¹ m ⁻²)	Rate per Area vs SiO ₂	Rate per Volume vs Empty Reactor ^c
Gas Phase	2.9x10-9	0	0	0	-	-	-
SiO ₂	7.5x10-9	11.6	480	5,600	4.0x10-11	-	2.6
Al ₂ O ₃	1600x10-9	2.4	200	480	1.1x10-8	270	550

^aBulk volume of each solid was 29 cm³ for SiO₂ and Carbon, based on particle and pellet sizes. For Al₂O₃, the volume was about 3 cm³ to limit the conversion below 10 % to obtain differential kinetics

^bAs reported by supplier of each support (see Methods Section)

^cThermal reaction rate was 2.9E-9 mol/cm³/s at 340 °C and 43.5 bar C₂H₄

Table B.2. Apparent Kinetic Parameters for Ethylene Reactions with and without High Surface Area Supports

	Reaction Order (1.5 to 43.0 bar) at 340 °C	E _{act} at 1.5 bar	E _{act} at 43.0 bar
Empty Reactor	1.9	244	
SiO ₂	1.4	89	176
Al ₂ O ₃	1.1	55	76

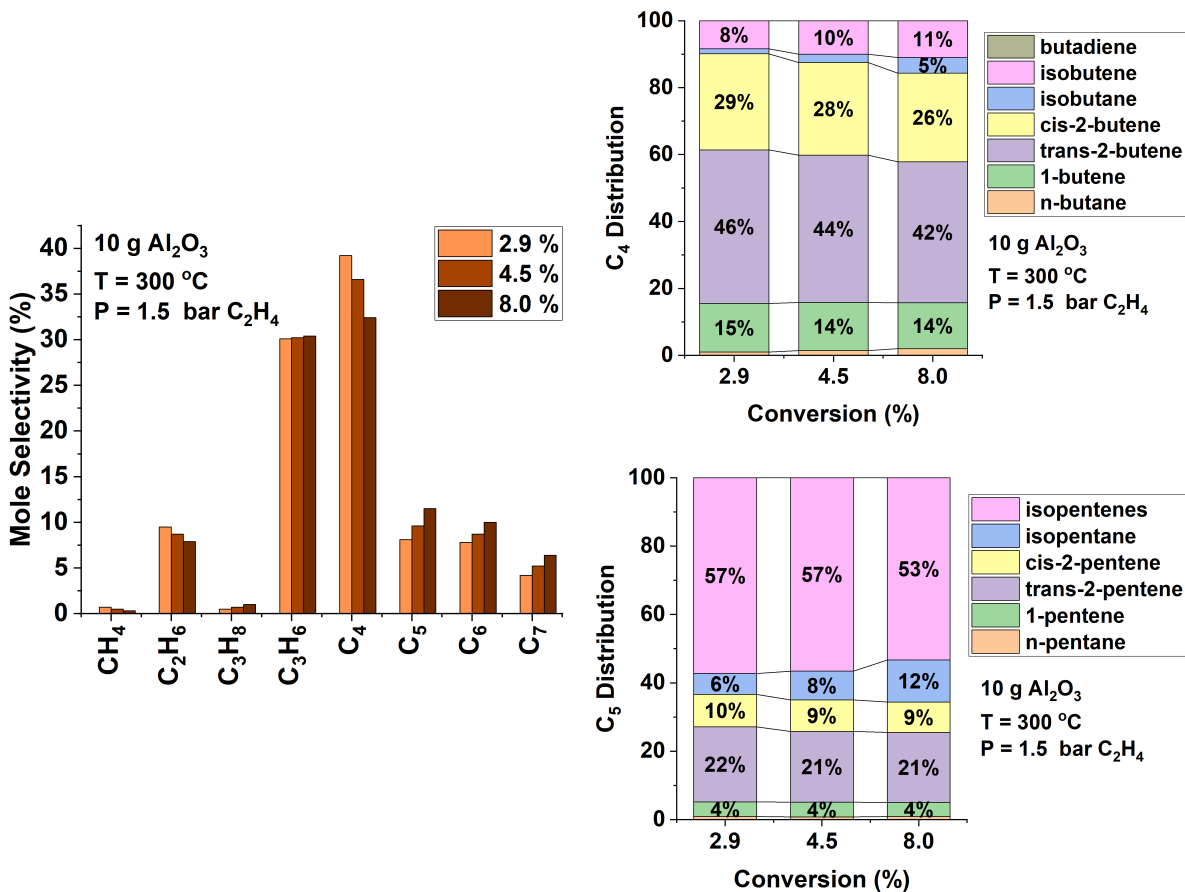


Figure B.1. Products with Al₂O₃ versus conversion below 10 % at 1.5 bar C₂H₄, 300 °C

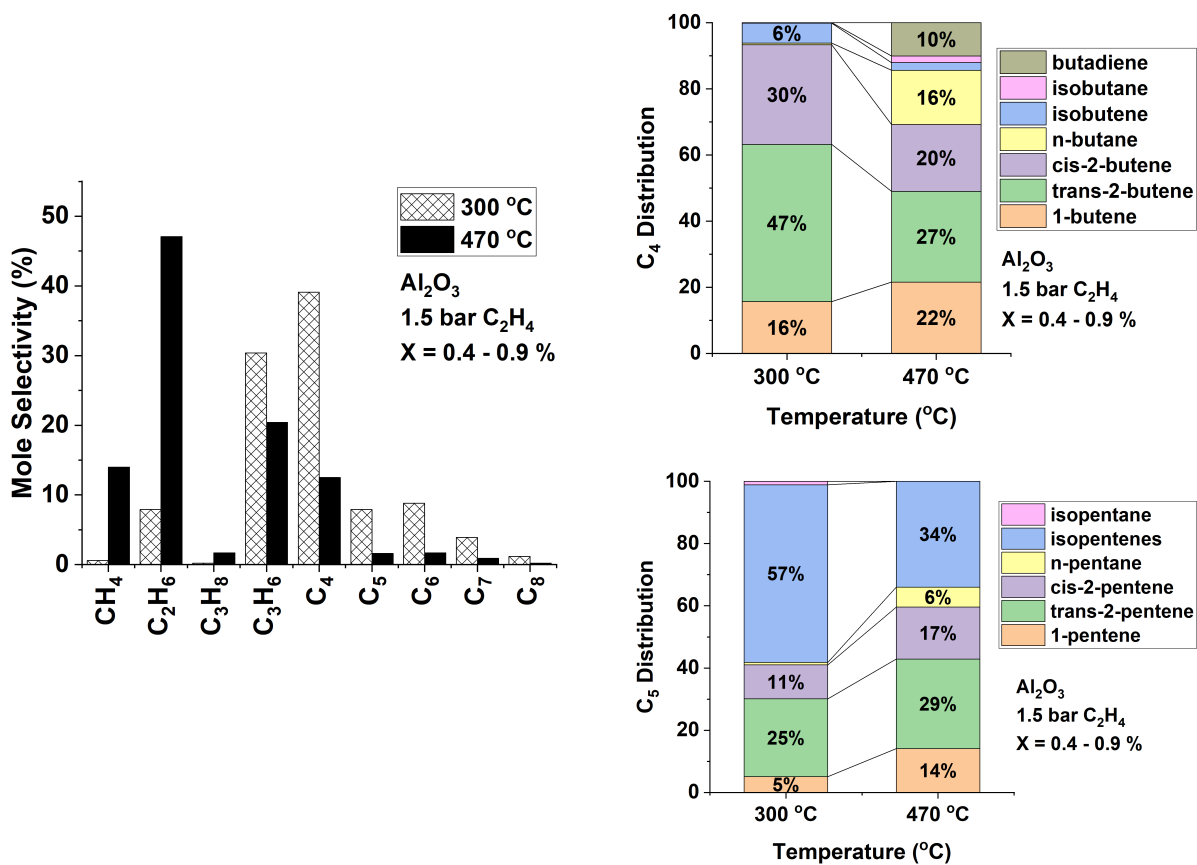


Figure B.2. Products with Al₂O₃ at 300 vs 470 °C at 0.4-0.9 % conversion and 1.5 bar C₂H₄

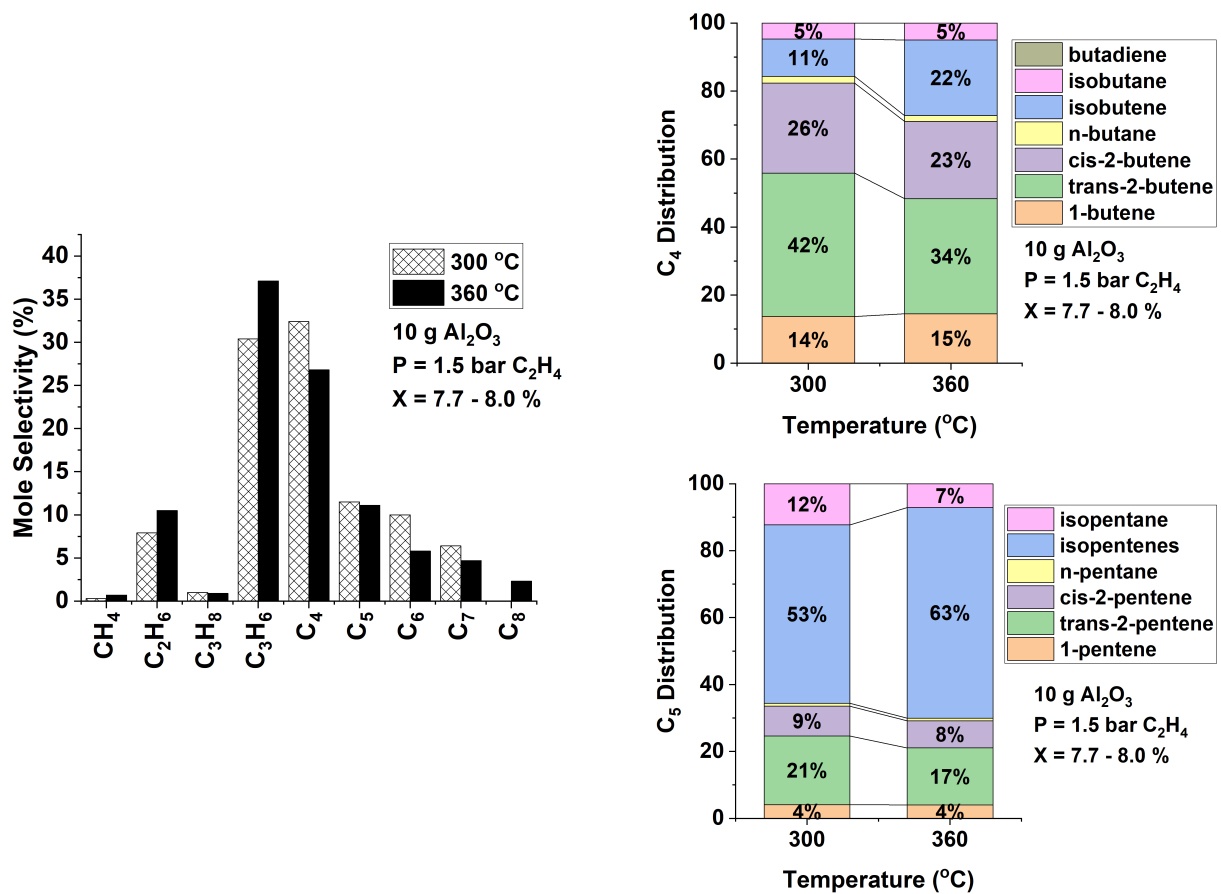


Figure B.3. Products with Al₂O₃ at 300 vs 360 °C at 7.7-8.0 % conversion and 1.5 bar C₂H₄

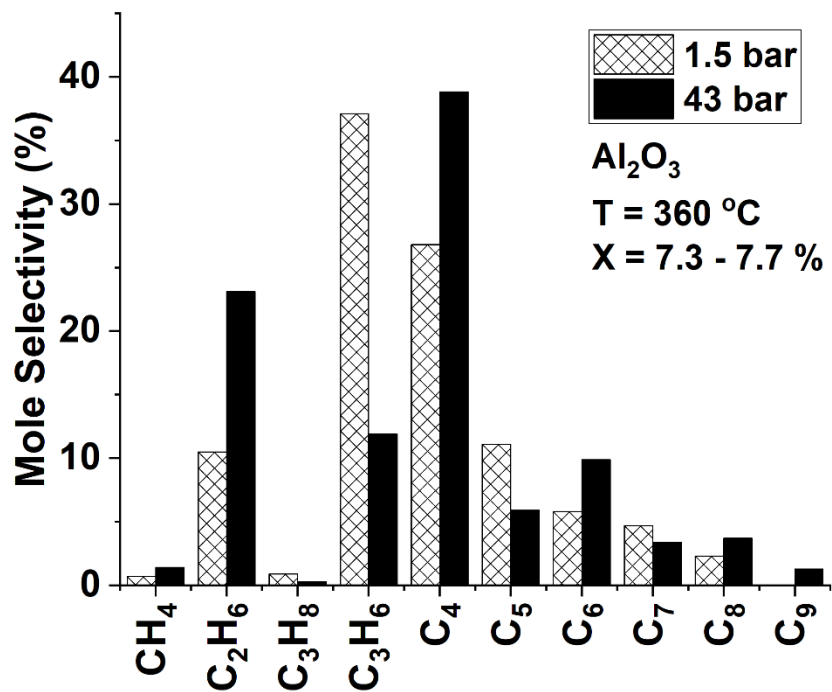


Figure B.4. Products with Al₂O₃ at 1.5 vs 43.0 bar and 360 °C at 7.3-7.7 % conversion

Table B.3. Ethylene Conversion Rates at Several Temperatures and Pressures with and without Al₂O₃.

P (bar)	T (°C)	Mass Al₂O₃ (g) Vol in () in cm³	Rate (mol/cm³/s) x 10⁹	Rate vs empty reactor
1.5	340	8.1 (11)	46	10,000x
1.5	340	0 (11)	0.0046	
1.5	360	8.1 (11)	63	4,000x
1.5	360	0 (11)	0.016	
43.0	340	2.4 (3)	1,600	550x
43.5	340	0 (29)	2.9	
43.0	360	2.4 (3)	2,700	140x
43.5	360	0 (29)	19	

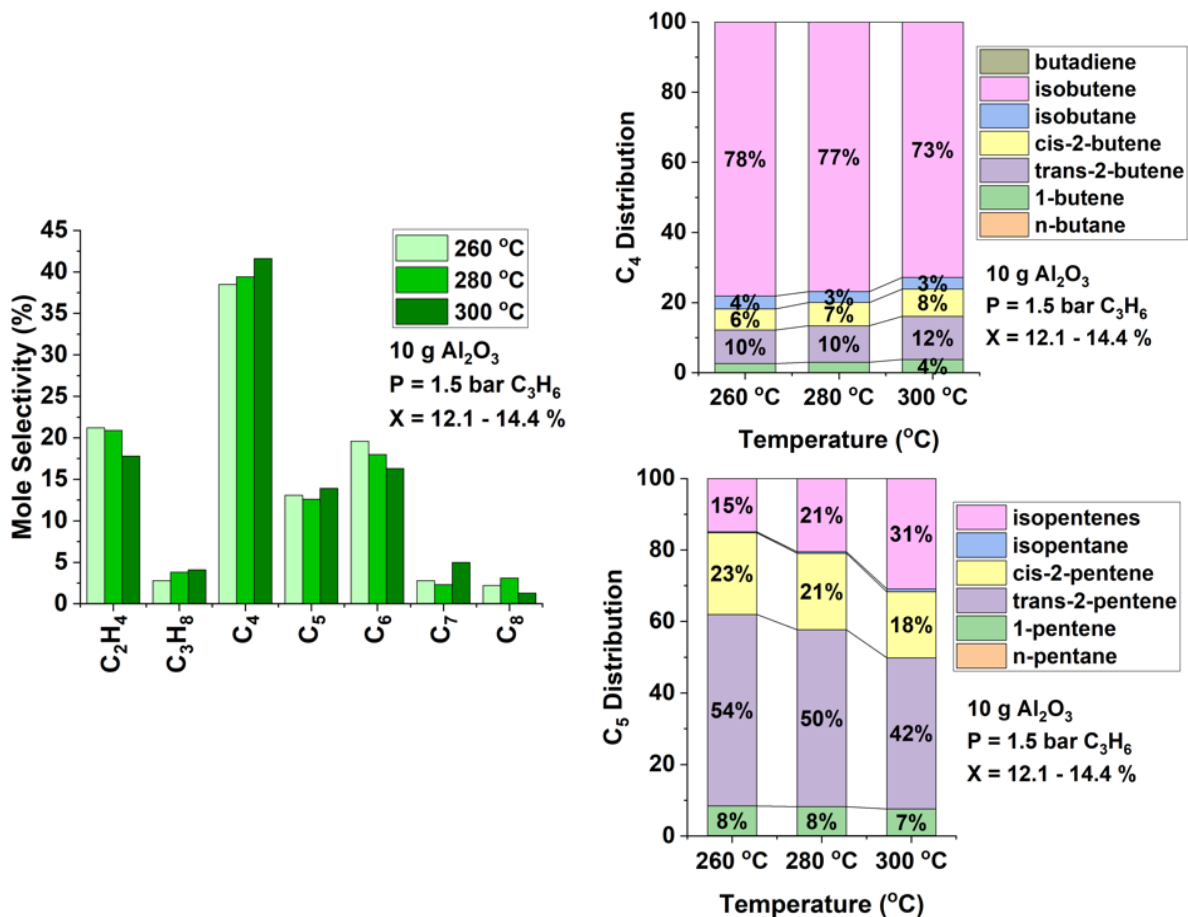


Figure B.5. Products with Al₂O₃ versus temperature from 260 to 300 °C at 12.1-14.4% conversion at 1.5 bar C₃H₆

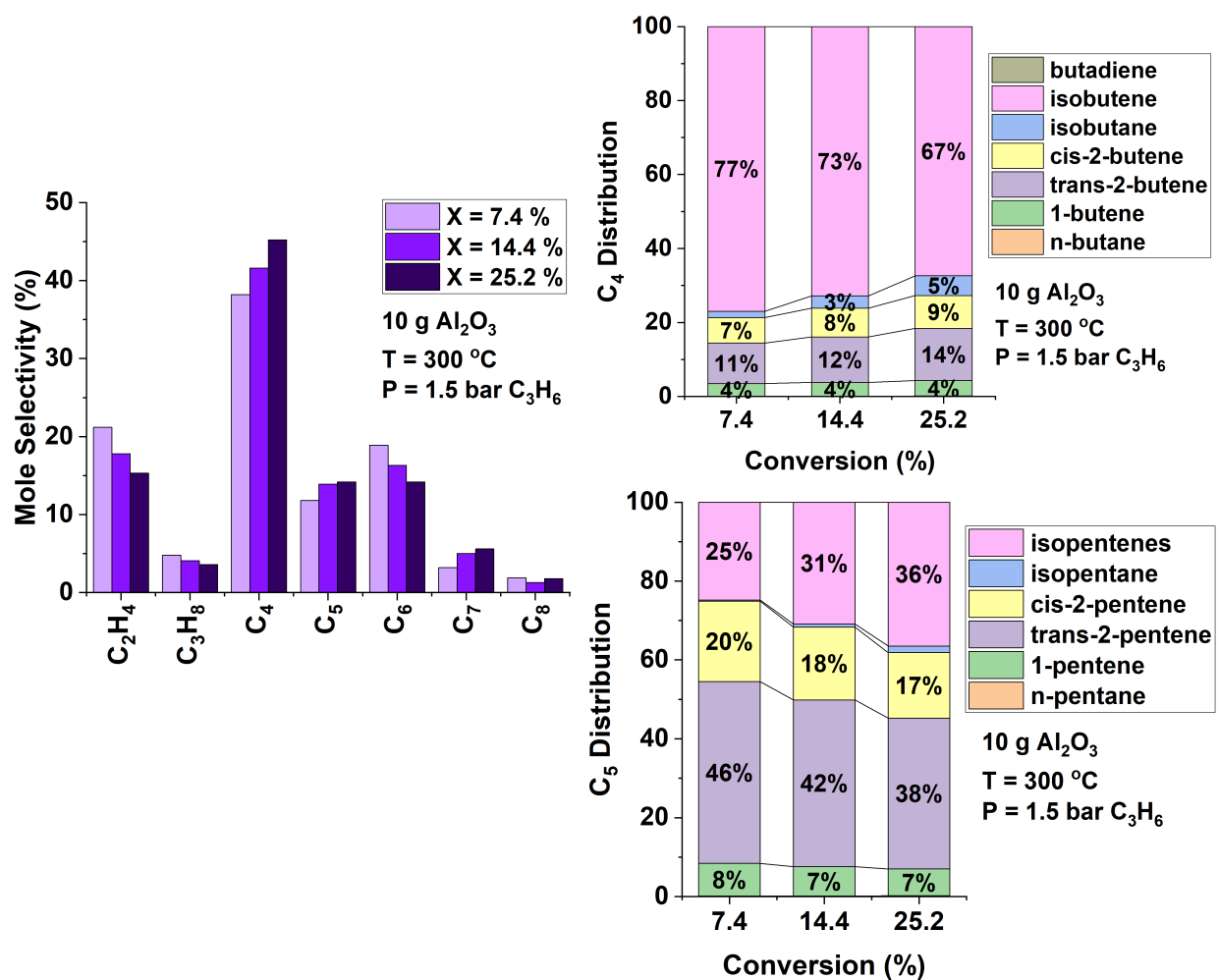


Figure B.6. Products with Al₂O₃ versus conversion from 7.4 to 25.2 % at 300 °C and 1.5 bar C₃H₆

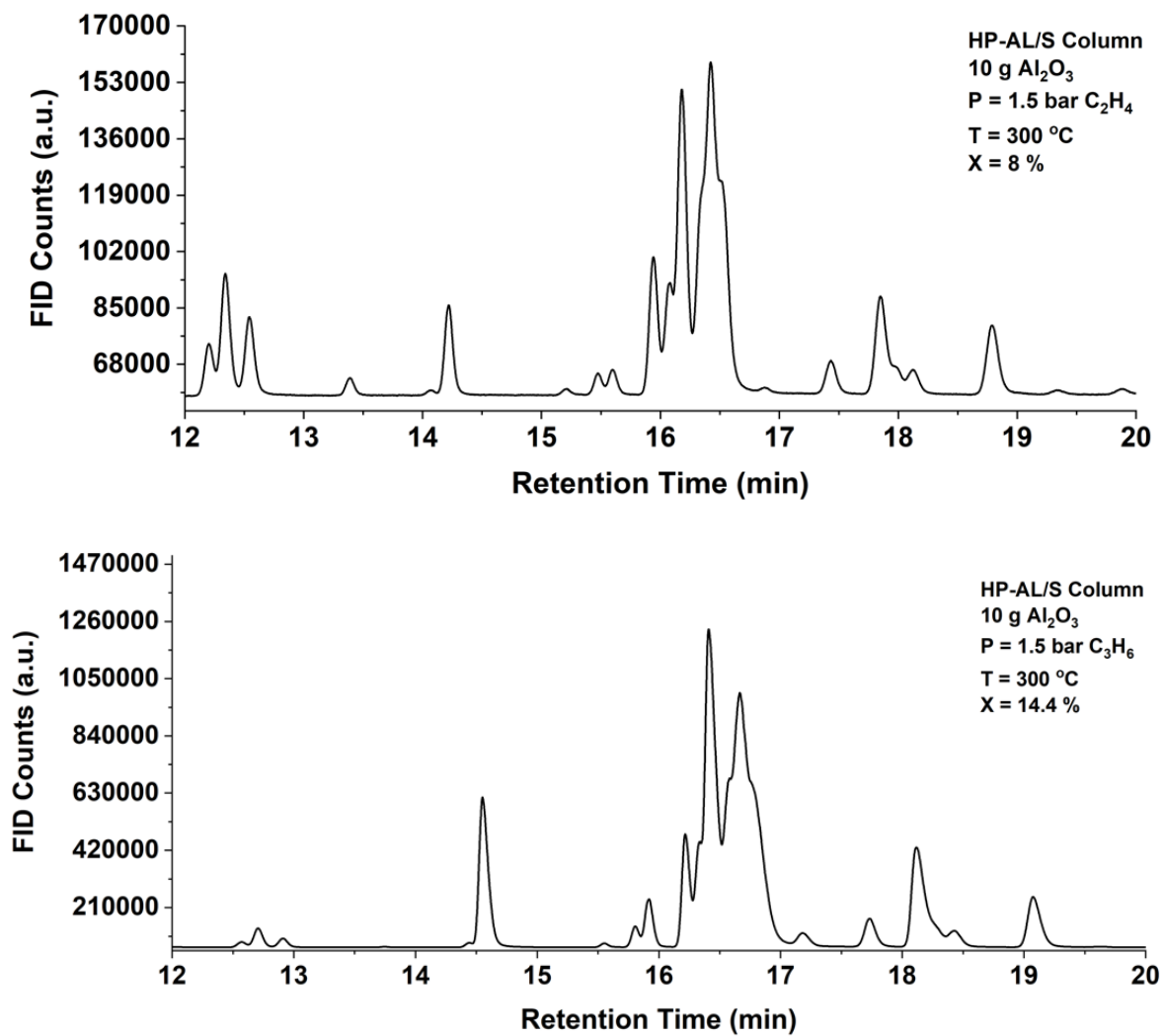


Figure B.7. The GC signal for retention times corresponding to C₆ products formed by Al₂O₃. (a) C₂H₄ feed at 1.5 bar and 300 °C, X = 8.0 %. (b) C₃H₆ feed at 1.5 bar and 300 °C, X = 14.4 %

Table B.4. Products of propylene reactions at 1.5 bar and 260 °C from 2.0 to 13.3 % conversion

	X (%)	2.0	6.1	13.3
	CH ₄	0.0	0.0	0.0
	C ₂ H ₆	0.0	0.0	0.0
	C ₂ H ₄	26.4	24.4	21.2
	C ₃ H ₈	4.3	3.4	2.8
	C ₄	34.4	36.3	38.5
	C ₅	6.4	9.8	13.1
	C ₆	23.4	21.7	19.6
	C ₇	3.9	3.1	2.8
	C ₈	1.2	1.3	2.2
C₄	n-C ₄	0.0	0.0	0.0
	1-C ₄	0.9	0.9	1.0
	t-2-C ₄	2.9	3.3	3.7
	c-2-C ₄	1.8	2.0	2.3
	i-C ₄	0.3	0.7	1.4
	i-C ₄ ⁼	28.5	29.3	30.0
	C ₄ ^{=,=}	0.0	0.0	0.0
C₅	n-C ₅	0.0	0.0	0.0
	1-C ₅ ⁼	0.6	0.9	1.1
	t-2-C ₅	3.5	5.4	7.0
	c-2-C ₅	1.7	2.4	3.0
	i-C ₅	0.0	0.0	0.0
	i-C ₅ ⁼	0.6	1.2	1.9

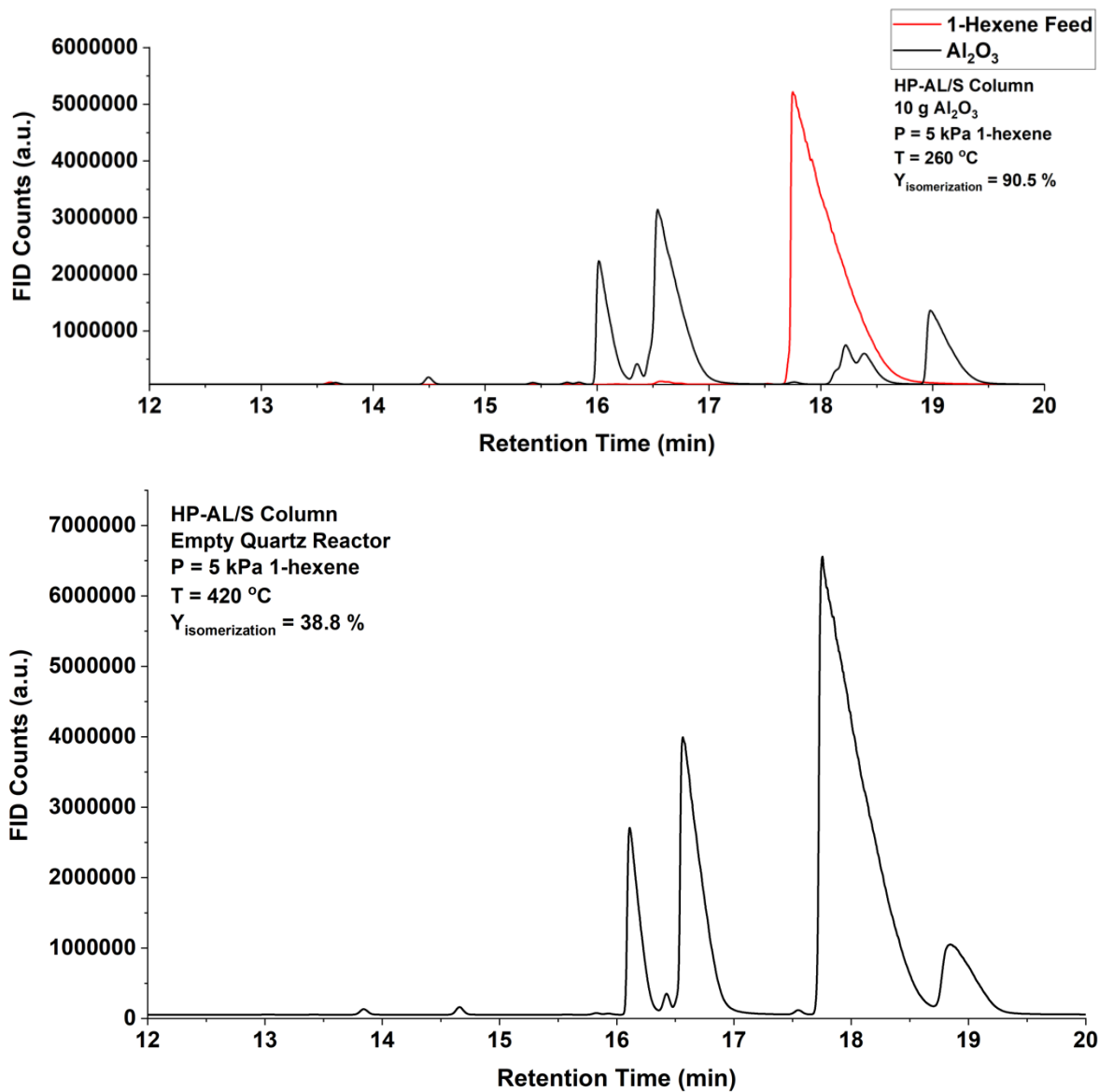


Figure B.8. The GC signal for retention times corresponding to C₆ isomers. (a) 5 kPa 1-C₆H₁₂ feed at 260 °C in the presence of Al₂O₃. (b) 5 kPa 1-C₆H₁₂ feed 420 °C in the empty quartz reactor

PUBLICATIONS

Miller, J.T., Libretto, N., **Conrad, M.A.**, Russell, C.K., “Zinc(II) and Gallium(III) Catalysts for Olefin Reactions” U.S. 2021/0162373 A1

Miller J.T., **Conrad, M.A.**, DeLine, J.E. “Methods for the Thermal Oligomerization to Liquid Fuel Range Products” *Provisional Patent Application Filed, 2021*

Qi, L., Zhang, Y., **Conrad, M.A.**, Russell, C.K., Miller J.T., Bell, A.T. “Ethanol Conversion to Butadiene over Isolated Zinc and Yttrium Sites Grafted onto Dealuminated Beta Zeolite,” *J. Am. Chem. Soc.*, 2020, 142, 34, 14674-14687.

Conrad, M.A., Shaw, A., Marsden, G., Broadbelt, L., Miller, J.T. “Insights into the Chemistry of the Homogeneous Thermal Oligomerization of Ethylene to Liquid-Fuel Range Hydrocarbons”, *Submitted to Ind. Engr. Chem. Res.*

Conrad, M.A., DeLine, J.E., Miller, J.T., “High Temperature Conversion of Ethylene to Liquid Hydrocarbons using γ -Alumina”, *Manuscript in preparation*